A STUDY OF ATMOSPHERIC OSCILLATIONS IN THE METEOR REGION ABOVE GRAHAMSTOWN

THESIS
Submitted in fulfilment of the
requirements for the Degree of
MASTER OF SCIENCE
at
RHODES UNIVERSITY
(Department of Physics and Electronics)

by

SANDILE B. MALINGA B.Sc. (HONS)

January 1995

ABSTRACT

The dynamics of the atmospheric meteor region have been studied using the data obtained with the Grahamstown (33°16'S, 26°30'E) meteor radar between the years 1987 and 1993 inclusive. Harmonic analysis and the maximum entropy method (MEM) were used for the spectral characterization of the wind above Grahamstown. The prevailing wind, tidal (periods 12- and 24-h) and other (periods 8- and 6-h) oscillations were extracted from the data using the guidelines agreed upon by the ATMAP community. Above Grahamstown the zonal and meridional prevailing winds were found to be predominantly eastward and equatorward respectively. Tidal amplitudes are comparable to the magnitude of the prevailing wind vector, with the diurnal tide being stronger than the semidiurnal tide. The phase differences between the zonal and meridional components of the semidiurnal and diurnal tides are - 2 h and - 5 h respectively, which is in reasonable agreement with the corresponding expected values of 3 h and 6 h. The tidal wind vectors are on average elliptically polarized with anticlockwise rotation. Longitudinal and day-to-day tidal variations were studied. From the longitudinal study, the semidiumal tide was found to be dominated by migrating modes, while the diurnal tidal behaviour suggests the presence of non-migrating modes with zonal wavenumber s = 4. Tides were found to be variable from day to day with little apparent correlation between the zonal and meridional components of the respective tides.

ACKNOWLEDGEMENTS

The completion of this thesis would not have been possible without the help and support of first and foremost God the Father, the Son and the Holy Spirit, as well as that of a number of people.

First, I wou Id like to thank my parents for the support they have given me ever since my education started. Without them I would not have reached this stage. On the practical side, I am greatly indebted especially to two people. The first is my supervisor, Prof. L. M. G. Poole, for his valuable help, guidance and support. I appreciate the fact that he was available to me and my work even after hours and during weekends and holidays. Secondly, my gratitude goes to Mrs. Linda Henderson for the typing, organizing and printing of my thesis. Not only that, but she also gave me much valuable advice from the initial stages of the typing, and saw to my day to day needs such as food and transport. Special thanks also goes to Sharon Way-Jones for doing most of the typing, Ian Dore who helped me with the printing of some of the graphs, and Justin Jonas for fixing RUCHEM now and then.

I would also like to thank all those who supported me in prayer, spiritually, emotionally, financially and in many other ways. These include my girlfriend Sayinile, "Aunt Meg" Hutchinson, Dierdre Jacobs and the "Power Hour" group.

Thank you to Deutscher Akademischer Austauschdienst (DAAD) for sponsoring me for the last four years, thus making this study possible.

Finally and most important of all, I would like to thank God, without whom I could not have completed this thesis. When things seemed dark, He was always by my side.

CONTENTS

CHAPTER 1

INTRODUCTION

1.1 INTRODUCTION

The atmosphere is a gaseous fluid surrounding the Earth, held by the Earth's gravitational attraction and strongly influenced by the Sun, the Earth's rotation, as well as a number of interrelated physical and chemical processes. The atmospheric motions that result from these processes (winds) play an important role in the transportation of chemical species, heat and momentum.

In this thesis, I am going to concentrate on the dynamics of the mesospheric and lower thermospheric region (85 - 105 km) using data obtained with the Grahamstown (33°19'S, 26°30'E) meteor radar which started operating in 1986. The radar is used to obtain echo data in the above height range, which is then processed to yield among other variables, the wind velocity (assumed to be horizontal) in the region as a function of time. Several data techniques are then applied to decompose the motion into its important components, namely, a prevailing wind and oscillatory components.

In the remaining sections of this chapter, I will briefly describe the Earth's atmosphere and some important aspects of the motion in the mesosphere and lower thermosphere.

1.2 THE ATMOSPHERE

The bulk of the atmospheric mass is found at the lower levels with 90% found below -20 km and 99.9% below -50 km (Iribarne and Cho, 1980). The atmosphere becomes thinner with height and eventually becomes indistinguishable from interplanetary gas. Consequently it has a distinct lower boundary and an indistinct upper boundary at which neutral gas escape becomes important. It is

divided into subspheres: the *troposphere,* which is bounded by the *tropopause* (13 5 km); the *stratosphere* which is bounded by the *stratopause* (50* 5 kin); the *mesosphere* which is bounded by the *mesopause* (85 * 5 km), the *thermosphere* which is bounded by the *thermopause,* which is the level at which the isothermal region begins (Odishaw, i 964). Above the therniopause is the *exosphere* which does not have a distinct upper boundary. The above boundaries depend on latitude and season (Beer, 1976). These subspheres are characterized by solar radiation absorbed, temperature structure, pressure, density, composition, degree of ionization and dynamics. Of interest to us is the "meteor region" which is 'the height range (- 80 - 110 km) from which most meteor echoes are received at decametric radio frequencies' (Poole, 1990).

1.2.1 SOLAR RADIATION

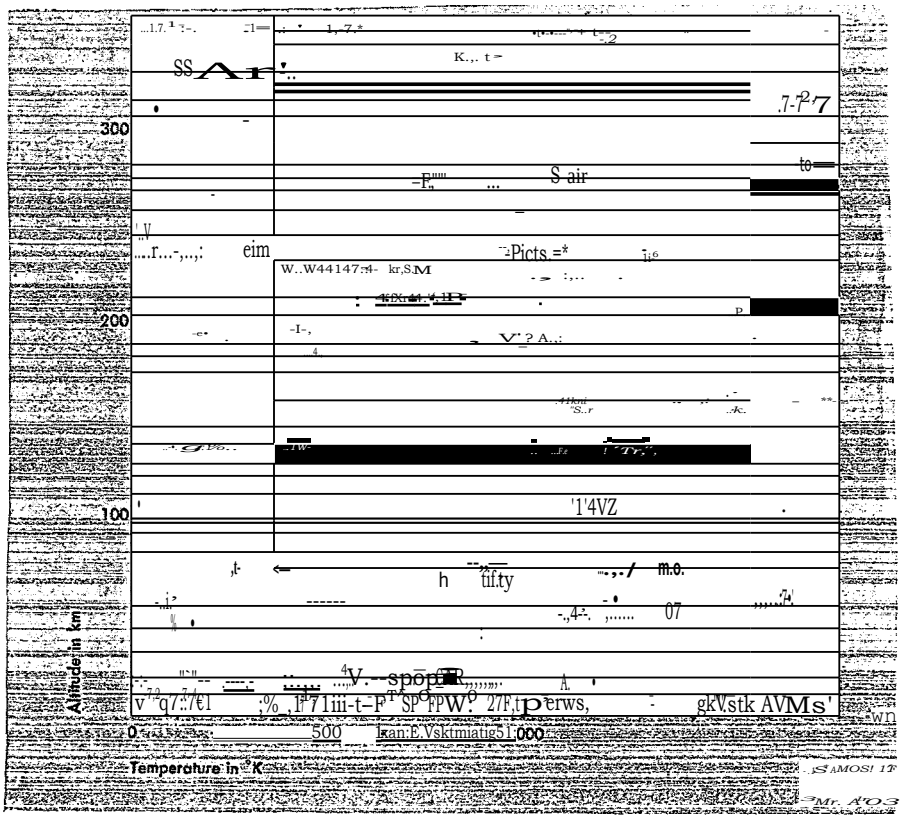

FIGURE 1.1. The atmospheric temperature structure at midlatitudes (after Goody and Walker, 1972)

As the incident solar radiation penetrates the atmosphere it is absorbed by different atmospheric constituents at different levels. As shown in Fig 1.1, more energetic radiation which consists of

short wavelength photons is absorbed higher up in the atmosphere, while the less energetic radiation (long wavelengths) penetrates deeper until it reaches dense gaseous species which can absorb it.

There is little absorption of visible radiation (-5000A) in the atmosphere except some absorption by ozone (0_3) and the weak excitation of molecular oxygen (0_2). Hence, most of the visible radiation reaches the ground. On the other hand, ultraviolet radiation (-3000A) suffers significant absorption in the atmosphere and is much reduced before reaching the ground. There are a number of absorbents, for example, 0_a N and H_2, but of importance to tidal excitation are 0_S and water vapour (H_20). The diurnal and semidiurnal tides, to be discussed later (see Section 1.3), are primarily excited as a result of insolation absorption by ozone and water vapour. The semidiurnal tide is excited mainly due to insolation absorption by ozone in the upper stratospheric and lower mesospheric regions, while the diurnal tide excitation is mainly due to insolation absorption by water vapour in the troposphere, and, to a lesser extent, ozone in the stratosphere and mesosphere (Harris, 1993)

1.2,2 ATMOSPHERIC TEMPERATURE, PRESSURE, DENSITY AND SCALE HEIGHT

The atmospheric temperature structure (Fig.1.1) is determined by the absorption of solar radiation. The tropospheric temperature is determined by both the incident solar radiation (visible and infrared) and the re-radiated infrared radiation. Water and carbon dioxide are the major absorbents in this region and the concentration of these decreases with height such that the troposphere is characterized by a negative temperature gradient starting at 273 ± 20 °K at the ground, to a local minimum (210 ± 20 °K) at the tropopause. Above the tropopause, 0_3 absorbs ultraviolet radiation resulting in a positive temperature gradient which ends at the stratopause with a local maximum temperature of 273 ± 20 °K. In the mesosphere loss processes become more important than absorption processes (Odishaw, 1964), and hence this region is characterized by a negative gradient bounded by a local minimum (190 ± 25 °K) at the mesopause. In the thermosphere, atomic oxygen (0) efficiently absorbs extreme ultraviolet (EUV) radiation (Goody and Walker, 1972), resulting in a positive temperature gradient bounded by a maximum temperature (_1000 °K) at the thermopause. In the exosphere the atmospheric thermal conductivity is very high such that most of the absorbed heat is conducted downwards such that

this region has an isothermal temperature structure (Beer, 1976).

Atmospheric temperature is related to pressure *(p)* and density (p) by the equation of state

$$P = \frac{pRT}{M}$$

where R is the gas constant and M is the molar mass. Pressure and density are related by the hydrostatic equation

$$\frac{dp}{dz} = -\rho g \qquad (1.2)$$

By eliminating p between (1.1) and (1.2) and assuming M, g, and T to be constant, we get p (by integration) to be

$$p = p_o \exp\left(-\frac{z}{H}\right) \qquad (1.3)$$

where the scale height $H\ (= RT/Mg)$ is the height range over which the pressure decreases by a factor of e.

1.2.3. ATMOSPHERIC DISSIPATION

Tidal oscillations (Chapter 2) are generally subject to damping due to momentum transfer as a result of viscous forces and heat transfer by thermal conduction and radiation. Before discussing the dissipative processes, it is appropriate to discuss the atmospheric mechanisms that result in momentum and heat transport, namely, *molecular* and *turbulent diffusion.*

1.2.3.1 ATMOSPHERIC TRANSPORT MECHANISMS

Molecular diffusion involves the microscopic transfer of momentum, heat and mass through the motion of molecules. The corresponding momentum, heat and mass transfer rates are of the form (Knudsen and Katz, 1958)

$$K = C\frac{dq}{dy} \qquad (1.5)$$

where q in the gradient term can be velocity, temperature or concentration. The corresponding constants *(C)* of proportionality are viscosity, thermal conductivity and diffusion coefficient, respectively.

Fluid motion in which all the fluid elements move in the direction of the average flow is called *laminar (or streamline) flow.* However, if *eddies'* depart from the direction of mean flow, the flow is *turbulent.* The transition between these two types of flow is determined by the Reynolds number (Houghton, 1977)

$$R = \frac{LU}{} \tag{1.6}$$

where v is the kinematic viscosity, Uis the velocity of the fluid and L is the typical length scale of the flow. If $R_e > 6000$ the flow becomes turbulent and this is the case for typical atmospheric parameters.

1.23.2 ATMOSPHERIC DISSIPATIVE PROCESSES

1.23.2.1 MOLECULAR AND EDDY DISSIPATION OF MOMENTUM.

The atmosphere is a viscous fluid and its viscous properties are both microscopic (molecular) and macroscopic (elemental). Molecules moving from one atmospheric layer to another will act as a driver or drag to the molecules in that layer depending on the relative velocities of the molecules in the two layers (Knudsen and Katz, 1958). This is accompanied by momentum transfer and hence mechanical damping in the layer from which momentum is transferred. This process is called *molecular dissipation* of momentum. Macroscopically, the eddies resemble molecules, and hence their movement from one layer to another also results in frictional drag which converts the translational motion of the eddies into irregular, thermal molecular motion. This process, known as *eddy (turbulent) dissipation* of momentum, thus has a mechanical damping effect.

An *eddy* is a mass of fluid that is capable of moving as a separate entity within its environment and still maintain its individuality.

1.2.3.2.2 MOLECULAR AND EDDY DIFFUSION OF HEAT.

As molecules move from one level to another collisions between the molecules occur, resulting in direct heat transfer by molecular conductivity. Effectively, there is a movement of thermal energy from one region to another therefore the thermal damping of tides.

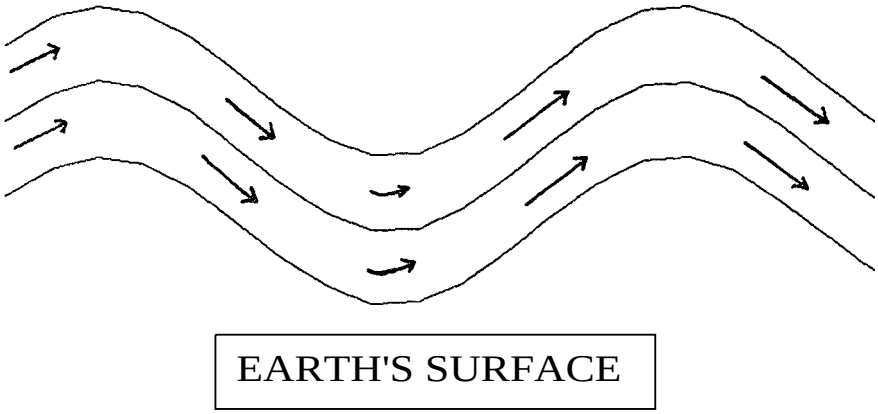

FIGURE 1.2. Eddy motion and heat transfer.

To understand *eddy conductivity* we consider Fig.1.2. If, for instance, the air near the troughs is heated by the warmer Earths surface while the air near the ridges loses thermal energy through radiation, the air on the left of the ridge will be warmer than that on the right. Effectively there is an upward transportation of thermal energy (Iribame and Cho, 1980) resulting in the thermal damping of tides.

1.2.3.2.3. ION DRAG

Similar to molecular viscosity and eddy viscosity, a difference in the magnitude of ion drift velocity and neutral wind velocity results in frictional drag (Rees, 1989) hence a dissipation of momentum. However, ion-neutral interactions become significant above 100 km (Chapman and Lindzen, 1970, hereafter CL) and therefore the dissipative effects of ion drag are not expected to significantly affect the meteor region.

1.2.3.2.4. INFRARED COOLING.

If there is a balance between infrared flux divergence and other heat transfer processes, a temperature perturbation would result in an increase or decrease in infrared cooling accompanied by the restoration of the original temperature (CL). Consequently the temperature component of the tide, and therefore the tide as a whole, will be damped. Though infrared cooling reaches its maximum around 50 km it does not significantly damp the semidiurnal tide, but has some effect on the diurnal tide in the meteor region (CL).

1.3 ATMOSPHERIC DYNAMICS

1.3.1 GENERAL

As mentioned earlier, atmospheric motions have an important influence on atmospheric processes. The motion in the meteor region is a superposition of three main components: *prevailing wind, waves* and *turbulence.* The prevailing wind changes over long periods (>1 month) while the other components are of a shorter duration. Atmospheric waves can conveniently be divided into three categories: *gravity waves*, *tides* and *planetary waves.* Gravity waves have periods of 10 min 10 hr (Glass and Spizzichino, 1974) and have great variability in time and space. Due to their small scale variation these can be studied at a single station. Tides have periods of 12- and 24-hour and will be studied in detail in this thesis. Planetary waves, on the other hand, have periods of > 1 day and are largely associated with tropospheric weather systems. Tides and planetary waves are global in nature and therefore the determination of their parameters requires a global scale observation. Programs such as Atmospheric Tides Middle Atmosphere Program (ATMAP) have been involved in a globally coordinated study of atmospheric tides (see the special issue on *Atmospheric Tides* from the *Journal of Atmospheric and Terrestrial Physics* 51). Turbulence is random motion which, like gravity waves, has small scale variations in time and space and therefore is local in nature.

Whereas at lower altitudes periodic wind components are to some extent small perturbations of the background wind motion, in the meteor region planetary waves, tides and gravity waves have

amplitudes that are comparable to the prevailing wind (Cevolani *et al.,* 1983). Also, this region is a transitional region in the sense that it is between an upper ionized region in which the dynamics are governed by electromagnetic processes and a lower neutral region in which radiative processes play an important role (Darn *et al.,* [1]983).

1.3.2 PREVAILING WIND AND ATMOSPHERIC TIDES

As we shall see in Chapters 4 and 5, prevailing wind and atmospheric tides play an important role in the dynamics of the meteor region. The prevailing wind is primarily zonal with a generally weak meridional component, and is important in tidal mode coupling. This is a process by which tidal modes that were not originally excited by any forcing are generated by the coupling of forced modes. The introduction of the zonal prevailing wind in the theoretical development of tidal theory renders the governing equations of motion inseparable in height, the physical manifestation of which is the coupling between atmospheric layers. Although a concrete theory has not been developed, the prevailing wind also seems to influence or at least coincide with the phase transitions of tides especially the semidiurnal tide .

The ATMAP community (see Forbes' 1986a report of the ATMAP Workshop held in Kyoto, Japan on December 5 - 6, 1984) agreed that a *tide* should only be considered to be a global oscillation with spatial coherence in the form of modes in a classical tidal theory sense and having 12- or 24- h periodicities. It was noted however, that there was energy at or near tidal frequencies which was not global, but was due to synoptic scale variations of local propagation conditions, or sometimes to the diurnal modulation of upward propagation of gravity waves and momentum deposition.

A question that arose at the workshop was whether a global tide does ever reach a steady state with the changing propagation condition. Linked to this was the question of suitable time scales over which observations can be considered to represent a tide in a global sense and thus be compared with steady state models. Bernard (1981) and later Vial *et al.* (1991) computed tidal set up time - the time required for the establishment of the stationarity of the tide around the Earth. Though these authors found different times, at least 10- day observations seem more appropriate for the extraction of tidal components (Forbes, 1986a; Vial *et al.,* 1991). Therefore in this thesis tidal parameters will be deduced from observations of at least 10 days, with the

exception of the study of day-to-day 'tidal' variability.

Tides are essentially atmospheric waves excited at lower altitudes primarily due to insolation absorption by water vapour and ozone. They then propagate upwards, if propagating at all. An upward propagating wave is indicated by a downward phase progression. The thermotidal energy in the tide is transported upwards as tide propagates and the amplitude of the associated wind grows in amplitude with increasing height. Tidal components can also consist of non-propagating *(evanescent)* modes the energy of which resides near the region of injection. For such modes there is a more rapid upward deCay of energy density compared to the gas density decay and consequently, the amplitude of the associated wind decreases above as well as below the excitation level (Hines, 1972). Depending on the background propagation conditions, some modes can be evanescent within a certain region but propagate otherwise. A good example of these is the (2, 2) mode (see later in Section 1.3.3), which tends to be evanescent between 50 and 70 km as a result of the atmospheric background thermal structure (Forbes, 1982 b).

The gross structure of tides has been extensively studied at both practical and theoretical levels and generally, tides have regular behavior from year to year with a few deviations partly due to global effects like stratwarm (Manson and Meek, 1984), and also due to local effects. Lately the attention of tidal study has turned towards short-term tidal variabilities.

A tide generally consists of a superposition of different modes and depending on season, latitude and height, there are characteristic dominant modes. The semidiumal tide consists of at least five modes, namely (2, n) for n = 2, 3, 4, 5, 6 (see next section for nomenclature). The (2, 2) mode is generally dominant but at midlatitudes (30 - 60 $^{\circ}$) higher order modes especially the (2, 4) mode can be dominant. The diurnal tide is characterized by propagating modes and evanescent modes, with the former being dominant near the equator and the latter toward the poles. At midlatitudes a mixture of these can exist making it difficult to define a typical diurnal tidal structure in this region. Also, the dependence of the diurnal tide on both propagating and evanescent modes make the tide more sensitive to local solar variation (Poulter, 1980). The dominant modes for the diurnal tide are the propagating (1, 1) mode and the evanescent (1, -2) mode. The superposition of modes results in interference effects and tend to complicate the tidal structure. This superposition of modes is one of the possible causes of short-term tidal variability.

As mentioned earlier, tides are excited by insolation absorption by water vapour and ozone. These agents of excitation are subject to temporal and spatial variation which, apart from being another possible source of the short-teim variability, also result in the generation of non-migrating modes (see next section). These modes are the sources of longitudinal tidal variability.

1.3.3 TERMINOLOGY AND NOTATION

1.3.3.1 TIDAL TERMINOLOGY AND NOMENCLATURE

Let a be the number of oscillations per solar day. Then S_c is the a diurnal solar tidal field. S. can be expanded in terms of a *wave family S:* (or S(a,$)) for s = 0, 1, 2, ... where s is the zonal wave number. The wave family can be expressed in terms of Hough functions e:'^{s} (see Fig. 1.3 and Chapter 2) as a *wave type S.%* (or S *(a ,s,n))* where n = *+1,* ±2, ±3, ... For *migrating modes* (i.e. modes that follow the Sun) s = a and for *non-migrating modes s* a. Since we deal mainly with migrating modes, for brevity we omit a and express the wave type as S *(s, n)* and the corresponding mode as *(s, n).* Therefore, we talk of the *(s, n)* mode of the s -diurnal tide (where s = a). For example, for the semidiurnal tide, s = 2 and therefore we have among others the (2, 2), (2, 3) and (2, 4) modes.

The notation used here is the one reported by Forbes (1984) to have been used by Flattery (1967). According to his notation we have (2, *n)* for the *semidiurnal tide (a* = 2) where n = 2, 4, 6, ... for modes symmetric about the equator, and n = 3, 5, 7, ... for antisymmetric modes. The *diurnal tide (a* = 1) consists *of propagating modes (n* > 0) and *evanescent (trapped, n* < 0) *modes.*

Propagating diurnal modes are denoted by (1, *n)* (Forbes, 1984) where n = 1, 3, 5, ... for symmetric modes and n = 2, 4, 6, ... for antisymmetric modes. Evanescent diurnal modes are denoted by (1, *-n)* where n = 2, 4, 6, ... for symmetric modes and n = 1, 3, 5, ... for antisymmetric modes.

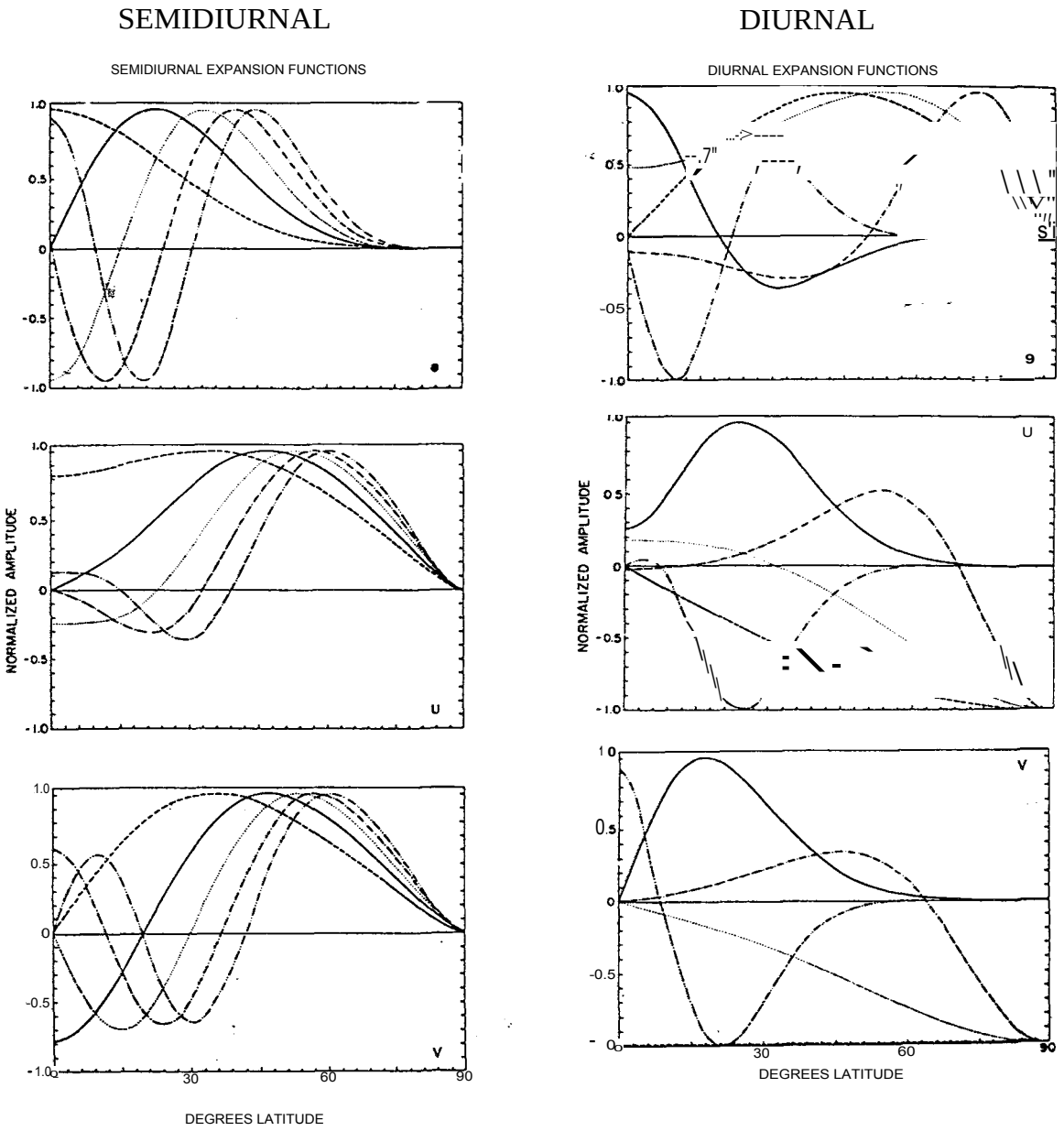

FIGURE 1.3 (Top) Hough expansion function. (Middle) Zonal velocity expansion function. (Bottom) Meridional velocity expansion function (after Forbes, 1984 - see this reference for normalization details)

1.3.3.2. GENERAL CONVENTION

* Zonal or EW refers to east/west; eastward positive

* Meridional or NS refers to north/south; northward (equatorward for our case) positive

*Time quoted - unless otherwise stated all times in this thesis are local time (LT)

* SH - southern hemisphere
* NH - northern hemisphere
* MIA - the *Monthly Interannual Average* is the average taken over a number of years for a particular month
* AA - *Annual Average*
* AAA - *Average of the Annual Averages* is the average of the AAs taken over a number of years
* UN(MIA) - is the uncertainty in MIA (i.e. standard deviation of the mean)
* UN(AAA) - is the uncertainty in AAA (i.e. standard deviation of the mean)
* SD(MIA) - is the percentage standard deviation in MIA
* SD(AAA) - is the percentage standard deviation in AAA.
* GT - Grahamstown

Frequently used references will be identified by suitable abbreviations after initial citing.

SEASONS: I divided my seasons as follows

(1) Summer (December, January, February)

(ii) Autumn (March, April, May)

(iii) Winter (June, July, August)

(iv) Spring (September, October, November)

In each case the early, mid- and late part of that season refers to the first, second and last month of that season respectively. For example early, mid- and late summer refer to December, January and February respectively. I decided to sometimes use this convention instead of quoting the actual months to be able to easily compare my results with other stations, especially those in the NH.

1.4 THESIS FORMAT

The thesis is organised into six chapters including the current one. In Chapter 2, I will review the theoretical work that has been done in the study of prevailing and tidal atmospheric dynamics.

Chapter 3 deals with the equipment, data acquisition and mathematical procedures. The results of my research are given in Chapters 4 and 5. The former deals with the different components of wind motion in the meteor region in a broad sense, with special emphasis on the prevailing wind made towards the end of the chapter. Chapter 5 deals with tides and then everything is summarised in the last chapter (Chapter 6) which also includes comment on possible future research.

CHAPTER 2
TIDAL THEORY

2.1 CLASSICAL TIDAL THEORY

2.1.1 INTRODUCTION

Tidal theory is divided into classical tidal theory (CL) and nonclassical tidal theory (e.g. Lindzen and Hong, 1974) depending on the assumed properties of the background atmosphere. Classical tidal theory considers linearized fluctuations on an inviscid, axisymmetric and hydrostatically balanced background atmosphere with a temperature field that has no horizontal dependence so that there is no background motion.

The advantage of the idealized classical approach is the simplification of the governing equations of motion but, at the same time, being able to explain the gross structure of atmospheric tides. However, there are some discrepancies between observations and classical models which cannot be explained by the theory. These discrepancies are largely due to the fact that classical theory does not consider physical processes like interaction with mean winds and meridional temperature gradients, eddy and molecular diffusion of heat and momentum, electrodynamic forces, Newtonian cooling and variation in atmospheric composition, which have important effects on tides especially above 70 km.

Nonclassical tidal theory, which takes these processes into consideration, has successfully explained most of the discrepancies found between classical theory and observations, such as the dominance of higher order modes at midlatitudes (Lindzen and Hong, 1974). Another major difference between classical and nonclassical tidal theories is that in the former the equations of motion are separable in height and latitude with the eigenfunctions (Hough functions) defining the horizontal structure of a given mode while the eigenvalues (equivalent depths) fix its vertical structure. The inclusion of mean winds and some dissipative processes in nonclassical theory renders the governing equations inseparable.

Nonclassical tidal models are divided into *"invi.scid"* and *"viscid"* models depending on the parameterization of the dissipative mechanisms. "inviscid" models, while including mean winds and meridional temperature gradients either neglect eddy and molecular diffusion and only include Newtonian cooling and, possibly, 'Rayleigh friction' for the filtration of small-scale noise or the ease of application of upper boundary conditions , or alternatively, include eddy and molecular diffusion using transformation terms (Vial, 1986, hereafter V86; Forbes and Hagan, 1988 hereafter FH). The exclusion or the transformation of dissipation terms makes it possible for the equations of motion to be reduced to a single second order partial differential equation for the perturbation geopotential. The "viscid" models (Forbes, 1982a,b; V86), on the other hand, include realistic parameters of eddy and molecular diffusion. The inclusion of these parameters results in four coupled second order partial differential equations.

2.1.2 BACKGROUND ATMOSPHERE

Atmospheric tidal phenomena are characterized by many complex physical processes which complicate the mathematical development of tidal theory. To simplify the problem a number of assumptions are made. These are

(a) The governing equations of motion are the Navier - Stokes equations.

(b) The atmosphere is heated in sequential equilibrium states hence it maintains a state of local thermodynamic equilibrium.

(c) The unperturbed atmosphere is a perfect gas such that

$$p_o = \frac{\rho_o R T_0}{M} \tag{2.1}$$

where p_o, ρ_0 and T_o are the static pressure, density and temperature of the basic state respectively.

(d) The atmosphere is a thin layer with dimensions that are small compared to the Earth's radius *a*. Consequently terms of the order of z/a where z is the height above the Earth's surface are

negligible hence gravitational acceleration g is taken to be constant.

(c) The atmosphere is in hydrostatic equilibrium such that for an infinitesimal layer with unit cross section the upward force due to pressure gradient is equal to the weight of the layer (Iribarne and Cho, 1980). This implies that

$$\frac{1}{\rho_o}\frac{dP_o}{dz} \quad g \tag{2.2}$$

(f) The Earth is not elliptical but spherical

There are four significant additional assumptions:

(g) The Earth is smooth and the land-sea distribution is disregarded.

(h) Dissipative processes like eddy and molecular diffusion of heat and momentum, infrared cooling and ion drag are not considered.

(i) Tidal fields (e.g. velocity, temperature, pressure) are linearized perturbations about an unperturbed basic state and are of the form

$$f = f_0 + f' \tag{2.3}$$

where f_o and f' are the basic field and the tidal field, respectively. The linearization of the oscillation implies that higher order terms of the oscillation are negligible.

(j) The basic fields p_o, ρ_o and T_o have no horizontal (latitude and longitude) dependence and only depend on altitude. Consistent with such a basic state, the background atmosphere is static.

2.1.3 EQUATIONS OF MOTION

An air parcel moving in the Earth's atmosphere is acted upon by a number of forces resulting in its acceleration given by (Siebert, 1961)

$$a_a \quad \frac{DV}{Dt} - g - \quad ^1 \qquad 21\ VV(I) \qquad (2.4)$$

where 1 is the tidal gravitational potential and the terms on the right are acceleration terms due to Earth's gravitational force, the pressure gradient force, Coriolis force, and gravitational tidal force respectively. *D/Dt* is the Lagrangian time derivative given by

$$\frac{D}{Dt} = \frac{a}{at} + v.v \qquad (2.5)$$

From (2.4), the zonal and meridional momenta are expressed (in spherical coordinates) as (Siebert, 1961; CL)

$$\frac{au}{at} - 2 \quad ucos8 \quad \frac{1}{a} \frac{a}{ae} \left| \frac{8p}{p} + O \right| \qquad (2.6)$$

and

$$\frac{av}{at} + 2\ Qucose - \frac{1}{asine} \frac{a}{a4)} \left| \frac{8p}{p_0} + O \right| \qquad (2.7)$$

where 0 is the latitude, (1) is the longitude, a is the Earth's radius and we have used $p = p_o + Sp$ and $p = p_0 + S\ p$ where $8p$ and 6 p are the perturbations in pressure and density respectively. The hydrostatic pressure relation is given by (Siebert, 1961)

$$\frac{a\ op}{az} \quad gsp \quad p_\circ \frac{}{az} \qquad (2.8)$$

Mass is conserved and hence we have the equation of continuity

$$\frac{Dp}{Dt} = \frac{\partial \rho}{\partial t} + \frac{\partial \rho w}{\partial z} \quad \rho X \tag{2.9}$$

Nvhere

$$x = v.v - \frac{1}{a \sin 0} \frac{\partial}{\partial t}(it \sin 0) + \frac{1}{a \sin e} \frac{\partial u}{\partial aq} \frac{\partial w}{\partial z} \tag{2.10}$$

The thermotidal processes are governed by the thermodynamic energy relation given by (CL)

$$-0P - \frac{\partial P}{\partial t} \frac{1}{\partial z} \frac{1v}{dpo} \quad ygH \frac{DP}{Dr} + (y-1)\rho of \tag{2.11}$$

Equations (2.8) to (2.11) are reduced (see CL for details) into the tidal response equation

$$\frac{Ha^2}{az^2} \frac{G''s}{+} \left(\frac{dH}{dz} - 1 \right) \frac{aG - 's}{az} \; to \quad \frac{g}{g} \frac{}{az^2} \quad \frac{g}{4a^2 0^2} \quad \frac{dH}{dz} + K G^{cr's} \quad \frac{}{y gH} \Bigg| \tag{2.12}$$

where x = (y - 1)/ y = 2 /7 , J is the tide generating heating, and

$$G = \frac{1}{yp_o} \frac{}{Dt} \tag{2.13}$$

Equation (2.12) is solved by the method of separation of variables and yields (see CL for details)

$$F \quad - \frac{4a^2 Q^2}{gh_n^{'s}} 8^{o's}{}_n \tag{2.14}$$

and

$$\frac{d^2 y_n^{a's}}{dx^2} \quad 4 \left[1 \quad \frac{4}{} \quad KT/ \quad \frac{dH}{dx} \right] \Bigg| \quad \frac{K}{y} e^{-x12} \tag{2.15}$$

where $h_n^{a's}$ is the separation constant and

$$x = -\log \left(\frac{P,}{p_o(0)} \right) \tag{2.16}$$

where $p_0(0)$ is the background pressure at ground level.

The set { 9:^{s} } is bounded at the poles (i.e. at 6 = 0,7t) such that (2.14) is an eigenfunction-eigenvalue problem which gives the horizontal tidal -structure and is called the *Laplace's tidal equation.* The eigenvalues 17:$_{\mathbf{1}}$ are called the *equivalent depths* and the eigenfunctions 8:^{s}} are the Hough functions discussed in Section 1.3.

Equation (2.15) is called the *vertical structure equation.* For two boundary equations (see Wilkes, 1949; CL for details), this equation gives the vertical tidal structure for a given Hough mode.

To get the solution for a specific case, *H, I* and (1) must be known and Laplace's tidal equation together with the vertical structure equation must be solved for certain boundary conditions. The reader is referred to CL for a detailed discussion.

2.2 NONCLASSICAL TIDAL THEORY

2.2.1 BACKGROUND ATMOSPHERE

The nonclassical background atmosphere is similar to the classical background atmosphere with only two major differences. First, the temperature field of the latter only depends on altitude whereas that of the former is dependent on both altitude and latitude. Associated with a temperature field with a horizontal dependence are meridional temperature gradients which induce mean background motion as opposed to the static classical background atmosphere. Secondly, nonclassical theory includes dissipative processes like eddy and molecular diffusion of heat and momentum, infrared cooling and ion-drag which are ignored classically.

The models for the mean background motion (prevailing wind), background temperature and dissipative processes are discussed in the next section together with their effects on atmospheric tides.

2.2.2 PREVAILING WIND AND TEMPERATURE.

2.2.2.1 THE GEOSTROPHIC ZONAL PREVAILING WIND MODEL.

The atmosphere is in hydrostatic equilibrium such that the vertical component of equation (2.4) is zero implying that there is no vertical atmospheric motion in the basic state (Iribarne and Cho, 1980; Beer, 1976). There are, however, meridional pressure gradients (Hines; 1972) caused by meridional temperature gradients resulting in horizontal motion. Due to the Earth's rotation this motion is also affected by the Coriolis force and hence is governed by geostrophic balance

$$\frac{1}{p_0}\frac{aP^\circ}{a80} = -2\,CI\,U\cos e \qquad (2.18)$$

By using this balance, Forbes and Vial (1989) related the prevailing zonal wind and temperature above 80 km by

$$2\,S2\cos^\circ \frac{aO}{az} = R\frac{aT}{ae} \qquad (2.19)$$

By integrating (2.19) and using zonal prevailing wind values at 80 km (based on satellite data and analytical computations), the zonal prevailing wind is given by

$$71(z,0) = T1(80,6) + \frac{R}{2\,Q\cos e}\int_{J8^\circ}^{r} zaT_{dz} \qquad (2.20)$$

The resulting geostrophic zonal prevailing winds are good in the meteor region especially in the SH.

2.2.2.2 THE EFFECTS OF ZONAL PREVAILING WIND.

For the static classical background atmosphere, the atmospheric tidal response relation (equation (2.12)) is separable in height and latitude. In this case, the latitudinal structure of the atmospheric response is characterized by Hough modes and its vertical structure is characterized by the equivalent depths (CL). The inclusion of zonal prevailing wind renders the tidal response inseparable. However, it is customary to continue using Hough functions for modal

decomposition even though, in this case, they are not eigenfunction of the response equation (see FH). The physical consequence of the inseparability of the response equation is the coupling between atmospheric levels (Vial and Teitelbaum, 1984, hereafter VT) and the following tidal features: the enhancement of higher order modesTor the semidiurnal tide hence their dominance at midlatitudes (Lindzen and Hong, 1974; Aso *et al.,* 1981); mode coupling (i.e. the generation of secondary modes which were not originally excited thermotidally); and the introduction of seasonal asymmetry of the diurnal tide structure (FH).

2.2.3 DISSIPATION

2.2.3.1 CONDITIONS OF EFFECTIVE DISSIPATION

CL point out that according to Wilkes (1949) atmospheric tides are effectively dissipated if $\tau_d < \tau_t / 27$ where τ_d is the time scale of dissipation and τ_t is the tidal period. The *residence time* which is the time it takes the waves to cross a dissipative region, is also of importance (CL). According to these authors

$$\tau_r \propto \frac{D}{a_H} \qquad (2.21)$$

where D is the depth of the dissipative region, λ_H and λ_z are the horizontal and vertical wavelengths of the tide, respectively. For sufficiently large D we have $\tau_r > \text{IV } 27$ and under these conditions dissipation can be significant even if $L_i > \tau_t / 27$, $\tau_d < \tau_r$. Given the inverse proportionality of λ_z to τ_r, it follows that for fixed τ_d, a and s, the shorter vertical wavelength (higher order) modes of any tide will be significantly damped neglecting the possible dependence of z_d on λ_z (CL).

2.2.3.2 THE EFFECTS OF DISSIPATION

As discussed in Section 1.2.3., the important atmospheric dissipative processes are eddy and molecular diffusion of heat and momentum, ion drag and infrared cooling.. However the most important ones for tides in the meteor region are the eddy and molecular diffusion of heat and momentum. Hence in this section I will concentrate more on these.

Due to the short vertical wavelengths of the diurnal tidal modes (-27 km for the dominant (1, 1) mode), the diurnal tide is more sensitive to dissipation than the semidiurnal tide which has long (>30 km for the (2, 6) and lower order modes (Phillips and Vincent, 1987)) vertical wavelength modes. The semidiurnal tide is insensitive to dissipation until about 100 - 110 km (FH) which is more or less above the height of my present study (± 95 km). Hence I intend to concentrate on the effects of dissipation on the diurnal tide.

Eddy diffusion is the major dissipative process affecting the diurnal tide due to its strong effect on the (1, 1) mode (V86) which is the dominant mode of the diurnal tide in the 70 - 120 km altitude range (FH). Molecular viscosity and thermal conduction, on the other hand, have a weak effect on the diurnal tide below 100 km (Forbes 1982a; VT). The diurnal tide is more sensitive to 'Rayleigh friction', which is used to simulate mechanical damping, than to Newtonian cooling which is used to simulate thermal damping (V86; FR), leading to the conclusion that this tide is more sensitive to mechanical damping than to thermal damping.

The effects of dissipation on the diurnal tidal structure are: the increase of phase difference* at 35 ° latitude (VT); the intensification of the seasonal asymmetry introduced by the prevailing wind (see Section 2.2.2.2) (FH); and the seasonal enlargement of the vertical wavelength as a result of the seasonal variation of eddy diffusion coefficient (VT).

2.2.4 NONCLASSICAL TIDAL MODELS

There are two types of nonclassical models, namely, *"viscid" ("eighth order")* models and the *"inviscid" ("second order')* models (V86; FH). These are classified according to the parameterization of eddy and molecular diffusion of heat and momentum. Following V86 eddy and molecular diffusion terms are of the form

$$\frac{\partial}{\partial z}\left(K\frac{\partial \psi}{\partial z}\right) \qquad (2.22)$$

where K is an appropriate " diffusion coefficient" and ft is the tidal field.

* Phase difference between the zonal and the meridional wind components.

For "viscid" models, the dissipative terms have the foi in

$$\left| \frac{a}{az} \left| (K_{eddy} + K_{mol} \frac{af'}{az} \right| \right. \tag{2.23}$$

This results in a motion governed by four coupled second order partial differential equations in altitude and latitude (V86; FH). These models are unpopular because of the amount of numerical computation required.

For "inviscid" models, the viscous terms are expressed by the transformation.

$$\frac{a}{az} \left| (K_{eddy} \quad \nu_{mo/\rho} \frac{afi}{az} \right| \; --' — V_{eff} \tag{2.24}$$

This transformation makes it possible for the set of governing equations of motion to be reduced to a single second order partial differential equation for the perturbation geopotential c (V86; FH). Numerically these are more efficient than the "viscid" models. The reader is referred to V86 for a detailed description of these models.

2.2.5 TIDAL EXCITATION

Atmospheric tides are primarily excited by two mechanisms: gravitational excitation and thermal (thennotidal) excitation. Gravitational excitation is weak and will therefore not be dealt with. Therrnotidal excitation is due to the Earth's daily rotation in the solar radiation field resulting in the periodic heating of the Earth's surface and atmosphere. Associated with this periodic heating are two excitation mechanisms: heat transfer between the Earth's surface and the atmosphere; and direct insolation absorption by atmospheric constituents.

2.2.5.1 SURFACE - ATMOSPHERE HEAT TRANSFER

Most of the incident solar radiation is absorbed by the ground and sea resulting in the periodic variation of the ground and sea temperatures. The absorbed heat is then transferred to the troposphere by turbulence and infrared radiation. This results in the excitation of upward propagating tides (CL). However, these authors point out that this tidal excitation is small

especially if the heating is averaged over land and sea which have different heating rates. Also this differential heating results in non-migrating modes.

2.2.5.2 DIRECT ATMOSPHERIC ABSORPTION

Mesospheric and lower thennospheric (80 - 110 km) tides are primarily excited by the absorption of solar near - infrared radiation by water vapour (H_20) in the troposphere and the lower stratosphere, and by the absorption of solar ultraviolet radiation by ozone (0) in the stratosphere and mesosphere. After being excited at these regions, the tides propagate upwards to the mesosphere and lower the thermosphere regions (i.e. the meteor region).

Tidal excitation has been considered by a number of researchers (e.g. Siebert (1961), CL and Forbes and Gareth (1978)) but the most accurate results are those of Groves (1982a,b). In Groves' (1982a) study on tidal excitation due to ozone, he used an updated latitudinal and seasonal ozone model and also took into consideration the theory of the longitudinal variation of ozone distribution, surface and lower atmospheric (cloud) reflection layers. However, his work was hampered by insufficient data on the longitudinal variations. Groves (1982b) evaluated Hough components of water vapour excitation using realistic water vapour densities and also taking into consideration cloud-related scattering and longitudinal dependences. More recently Sivkov and Shved (1993) (hereafter SS) modelled the excitation of the semidiumal tide due to ozone and water vapour heating using more up-to-date ozone and water vapour models. They obtained results that are similar to Groves' for the semidiumal tide. Groves' results are discussed below.

A. SEMIDIURNAL EXCITATION

The tide-generating Hough heating components are represented by $J_{\text{ь}}^{0\text{'}\text{S}.}$ For the migrating (s = a = 2) symmetric (n even) components, J_2^{22} is generally larger than J_4^{22} and $J_6^{2}2$ For ozone heating $J_2^{2\text{ᵓ}}$ is generally constant for all four seasonal representative months (January, April, July, October) possibly due to the form of $\text{O}_{2^{\cdot 2^{1}}}$. However, for water vapour heating the equinoctial months have larger values. J_4^{22} and J_6^{22} are generally enhanced during the equinoxes for both ozone and water vapour heating except that $^{J62'2}$ is negligible for the latter. Antisymmetric (n odd) components $^{J32'2}$ and J_5^{22} are smaller than the $J_2^{2\text{-}2}$ component for both excitation sources.

Asymmetric components are larger during the solstices than the equinoxes with the solstitial values being larger in winter than in summer due to shorter duration of daylight and hence the generation of larger Fourier components. Non-migrating modes (s a) which are due to longitudinal variations of excitation sources are < 3% of the corresponding migrating components for ozone heating while for water vapour heating their amplitudes are <15 % of those of J_2^{22}.

B. DIURNAL EXCITATION

For the diurnal tide a = 1. The major migrating (s = a = 1) symmetric components are: $J_1^{1,1}$ and $J_3^{1,1}$ and these are of importance at low latitudes; J_{-2}''' and $J_{-4}^{1,1}$ and these are of importance at high latitudes. The J_{-2}''' is the largest of all symmetric components. J,'''' islarger than J31'' and is comparable to $J_{-4}^{1,1}$. For ozone, all components are smaller in July than in January, but this is only true for symmetric modes in the case of water vapour. $J_1^{1,1}$ and $.1_{-2}$'°' are generally larger during the equinoxes than the solstices for water vapour.

The largest antisymmetric component is the $.1\text{-}_1^{1,1}$ component and the other components are J_{-3}'•'; $J_2^{1\text{-}1}$, and J_4'•'. J_,'•' is smaller than $J_{-2}^{1,1}$ but is comparable to the other symmetric components. $J_{-1}^{1,1}$ mainly accounts for the high-latitude symmetry. Longitudinal variation in the excitation sources and reflection layers especially cloud cover produce non-migrating (s # a = 1). The amplitude of these components is < 14 % of the amplitude of J,'•'

2.2.6 LONGITUDINAL TIDAL VARIATION

Longitudinal tidal variation is due to non-migrating secondary modes caused by longitudinal variation of the thermotidal source and/or the background atmosphere (temperature, wind and pressure) (SS). Bernard (1981) used a second order perturbation approach and found that the semidiurnal tidal modes interacts with the background atmosphere yielding non-migrating modes with $s = 0, 1, 3, 4$.

Secondary modes can sometimes be comparable to primary modes which would result in significant longitudinal tidal variability. According to Bernard coupling is more effective for non-solar modes with $s > 2$, that is, modes with zonal phase velocity less than the apparent velocity of

the sun (Bernard, 1981). Consequently, the phases will be later in local time for areas to the west. For a longitudinal difference of 90° they will be 3 and 6 h later for s = 3 and 4 respectively (see also Table 5.17 in Chapter 5). SS concentrated on the longitudinal variation due to variation of the theimotidal sources (ozone and water vapour) only. They found that the amplitude contribution of non-migrating modes resulting from longitudinal variation was small (<2 ms -) compared to migrating modes (Fig 2.1).

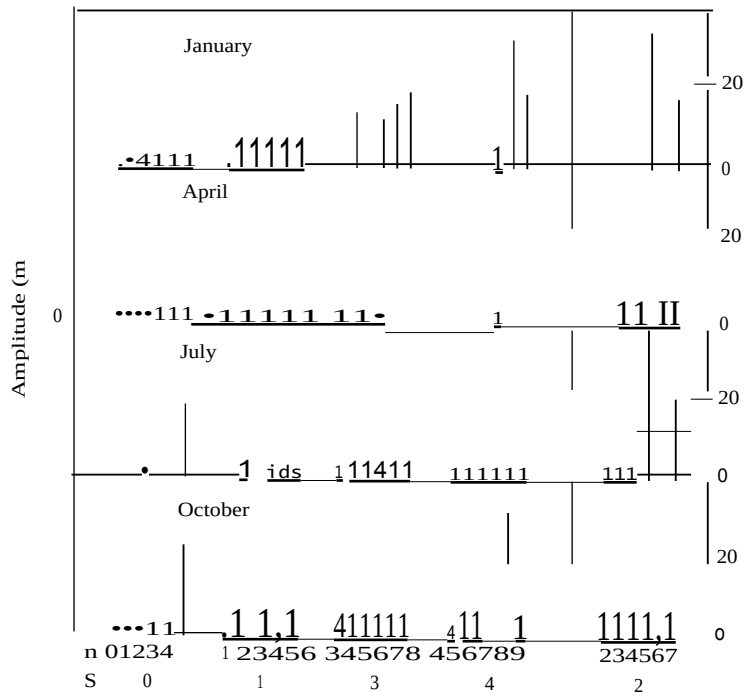

FIGURE 2.1 Maximum amplitude for the zonal component of the semidiurnal tide at 95 km. The left-hand scale is for the non-migrating modes and the right-hand scale for the migrating modes (after SS).

SS also found that the non-migrating modes were primarily due to water vapour and that maximum longitudinal amplitude variations are -2 ms^{-1} and -10 ms' for the NH and SH respectively, with corresponding phase variations of - 0.2 - 0.5 h and 1.5 h.

2.2.7 DAY-TO-DAY TIDAL VARIABILITY

Atmospheric tides characteristically show great day-to-day variability. Sometimes these variabilities can be as large as the magnitudes of the tidal components themselves (Waltersheid, 1981). Tidal variability is linked to the *tidal set up time.* This is the time required for a tide to be stationary around the Earth (Vial *et al.* 1991). Though this is not immediately clear to me from Bernard's (1981) paper, Forbes (1990) points out that Bernard argues that if the intrinsic time required to establish stationarity around the Earth for a given mode is greater than the characteristic time of its variability, the 'tidal' structure will be influenced by transient effects.

Waltersheid pointed out that the variability can be local as indicated by lack of spatial correlation and can also be random. However it is not yet known to what extent these variabilities are caused by global changes, local effects or synoptic scale disturbances. Also, the mechanisms governing these variabilities are not yet clearly known and understood. Some of the suggested mechanisms associated with the variability are discussed below.

(a) VARIABILITY OF THE EXCITATION SOURCE: The spatial and temporal variation of ozone and water vapour results in variations in insolation absorption hence thermotidal excitation (Bernard, 1981; Canziani, 1994): Cloud cover also changes the heating rates of both ozone and water vapour with changes as high as 48% at times (Groves, 1982a,b). Forbes (1984) points out that source variation is likely to influence the diurnal tide (especially where propagating modes are concerned) more than the semidiurnal tide.

(b) VARIATION OF PROPAGATION CONDITIONS (BACKGROUND ATMOSPHERE): Tidal mode amplitudes and phases are sensitive to variations in background atmospheric temperature, prevailing wind and the associated mode coupling (Bernard, 1981). Fellous *et al.* (1974) suggested that rapid variation of wind and temperature may cause partial tidal reflections which might change the tidal structure as explained in (c) below.

(c) MODE SUPERPOSITION: Temperature discontinuities and negative temperature gradients result in the partial or total reflection of tidal modes (Poulter, 1980). The

superposition of these modes even if the relative phase shifts between them are slight (1 - 2 h), can cause considerable day-to-day changes on the tidal structure (Forbes, 1990; VT).

(d) NON-LINEAR INTERACTIONS: The non-linear interaction between the diurnal and the semidiurnal tide produces a secondary downward propagating_diumal wave and a secondary upward propagating 8-h wave (Fellous *et al.,* 1974, 1975). The downward propagating secondary diurnal wave has similar effects as a reflected wave (see (c) above) and hence cause day-to-day variability especially at midlatitudes in winter (Teitelbaum *et al.,* 1989).

(e) INERTIA - GRAVITY WAVE INTERACTION: Walterscheid (1981) suggests that the semidiurnal tide modulates the non-linear interaction between the mean flow and gravity wave spectrum. This results in a the forcing of the mean flow near semidiurnal frequencies. The magnitude of this forcing depends on phase velocities, intensities, and coherence of the interacting waves and may have great daily variability. Hence the resulting variable secondary wave contributes to the day-to-day changes of the semidiurnal tide.

CHAPTER 3
EQUIPMENT, DATA ACQUISITION AND MATHEMATICAL TECHNIQUES

3.1 INTRODUCTION

In this chapter I will describe the meteor radar that is used at GT to obtain the wind data. I will also describe the deduction of the relevant wind parameters from the radar observations. Finally, I will describe the mathematical principles involved in analyzing the data With the specific applications of these left to the relevant subsequent sections.

3.2 EQUIPMENT AND DATA ACQUISITION

3.2.1 EQUIPMENT

The GT monostatic all-sky meteor radar has been described in detail by Poole (1988) and a brief description will be given here. The radar is situated at coordinates 33'19'S, 36°30'E and has an observing region with a radius of -200 km. The observing height range of -85 - 105 km is centered on a nominal height of 95 km. The transmitter is operated at a mean power of -30 W, a fixed frequency of 29.99 MHz and square-wave modulated at 500 Hz. The receiver tuning is offset such that an echo from a stationary target produces a 40 Hz output signal.

There are two receivers, each serving two antennas. Each receiver input is switched at 250 Hz between its two antennas and is synchronized with the switching of corresponding outputs between two low-pass filters. To compensate for a delay in the receivers, mainly due to crystal filters in the IF stages, a similar delay is introduced between the inputs and outputs of the receivers. The low-pass filters have a cut-off frequency of -100 Hz which ensures the removal of switching frequencies and higher harmonics leaving a meteor echo appearing as a pure audio tone.

In addition to the four receiving antennas there is a transmitting antenna. All antennas are simple half-wave dipoles and are mounted one-third of a wavelength above level ground. Their axes are aligned along the north-south meridian, resulting in the two broad lobes of the beam aligned in the east and west directions causing a system anisotropy. This arrangement is capable of providing the azimuth and elevation of meteor echoes.

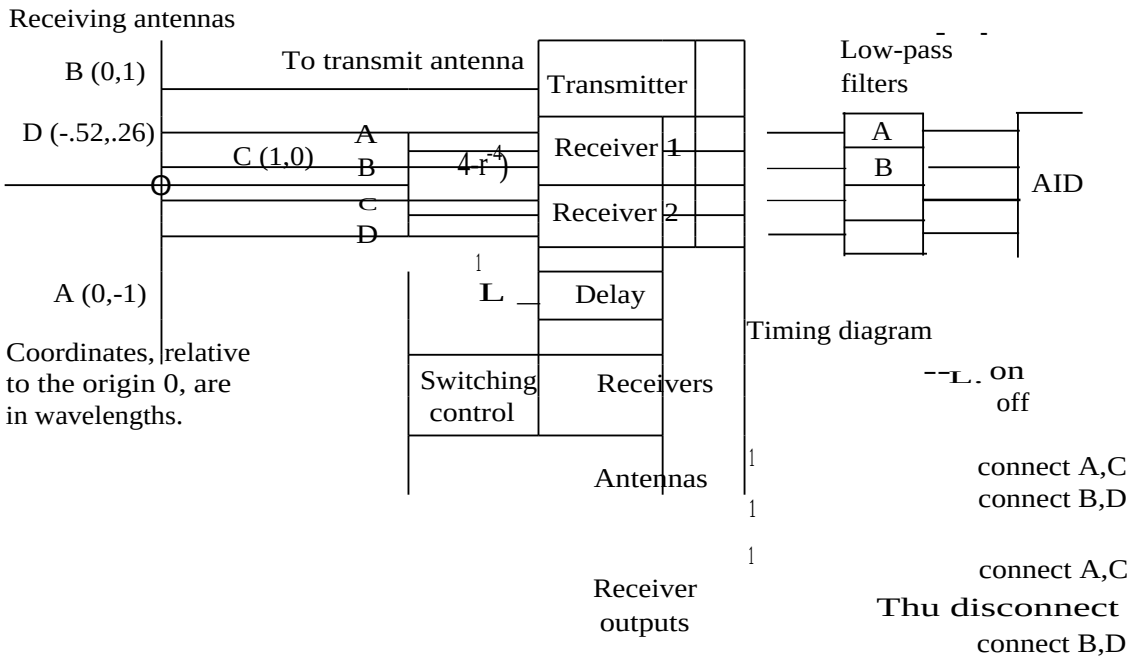

FIGURE 3.1 The schematic diagram of the GT meteor radar (after Poole, 1988)

3.2.2 DATA ACQUISITION

A signal with a frequency f_0 is transmitted and is reflected by the meteor train. Due to wind in the meteor region the train drifts, causing the reflected signal to be Doppler-shifted by an amount proportional to the drift velocity. From this the line-of-sight velocity can be computed from

$$u_r = \frac{c\,(f_r - f_o)}{2f_0} \tag{3.1}$$

where f is the frequency of the reflected signal and c is the phase velocity of the incident signal and can be taken to be equal to the velocity of light for our purposes.

The vertical wind is assumed to be zero and therefore we only consider the horizontal drift which is given by

$$1.1_{h} \quad {}_{r}\cos 8 \tag{3.2}$$

where 8 is the elevation (Fig 3.2) (measured by the system)

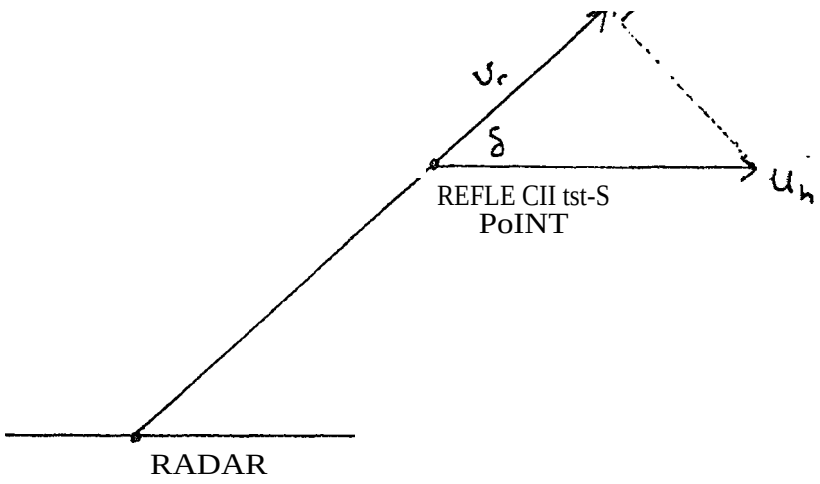

FIGURE 3.2. Line-of-sight drift velocity

On the horizontal plane we have the situation shown in Fig 3.3. (The angle c1)„. is effectively measured by the system)

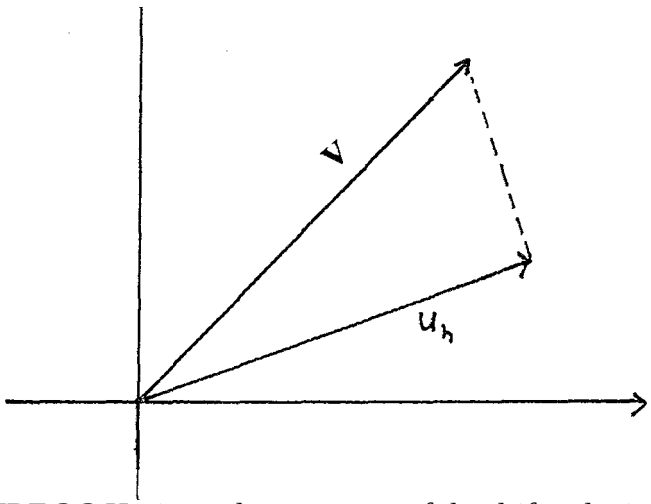

FIGURE 3.3 Horizontal component of the drift velocity and the actual wind vector V.

From Fig 3.3 we have

$$u_h = V\cos(e_w - \quad (3.3)$$

where V is the mean horizontal wind speed. We can also write

$$_{uhX} = \cos(O_w - \quad) \text{ co } s(1)_{,,}$$
$$= V(\cos e \cos^2 4)_{,..} + \sin e \quad \cos(\%) \quad (3.4)$$

similarly

$$= V(\cos e \cos(I) \quad slnl \quad + \sin e_x \text{ sing } (k_w)) \quad (3.5)$$

for the orthogonal axes x and y. To find V we have to compute the averages of $u_{h,,}$ and $u_{h,,}$ (W_{hx} and L_{hy}) for a given time bin. In obtaining these averages, values of u_h are weighted to correct for system anisotropy. The averages of cosil), $\sin^2 4)_w$ and cos (t.,,, sin c:D,,, are given by half, half and zero respectively, and we obtain

$$_{fl\ Az} = \frac{1}{2} VCOSO \quad (3.6)$$

$$= Y2\ V\sin e_w \quad (3.7)$$

If they axis corresponds to the geographic meridian, equations (3.6) and (3.7) gives, respectively, the zonal and meridional wind velocity components (u and u)

Due to the fact that the GT meteor radar does not have a height resolution the measured parameters have an error caused by the height integrating. By modeling the meteor height distribution $q(z)$ as a Gaussian and assuming that the amplitude of the oscillation is an exponential function of height, Poole (1990) found that the observed complex amplitude is related to the actual amplitude at a reference height (z = 0, taken to be 95 km in our case) by

$$A = \int q(z)\exp[(cci - ilc_u)z]clz \quad (3.8)$$

where a = H, $k_v = 27/A_u$, A.„ = vertical wavelength. For a propagating wave this yields

$$IAA = \exp[d^2(a^2 - k^2)/47z, \quad \text{tis} \tag{3.9}$$

where d is the equivalent width of the gaussian..

For d = 20 km and H = 7 km Poole obtained the correction factors given in Table 3.1.

A_U/km	ial			1P·M		
	x = 0	0.30	0.50	0	0.30	0.50
50	0.61	0.64	0.71	0	2.62	4.37
100	0.88	0.94	1.04	0	1.31	2.18
	1.00	1.06	1.18	0	0	0

TABLE 3.1. The correction factors for the magnitude and phase of IA l for different wavelengths where I Al = fal (after Poole, 1990).

3.3 MATHEMATICAL TECHNIQUES

3.3.1 HARMONIC ANALYSIS

In Section 4.3.1 we describe the extraction of the prevailing wind and amplitudes and phases of oscillatory components using the guidelines suggested at the AYMAP Workshop on Atmospheric Tides (Forbes, 1986b). This method uses harmonic analysis as described below. Harmonic analysis is generally applied to a discrete time series y of N data points corresponding to times t spaced at $7'/N$ where T is the period of the data interval (e.g. a solar day).

Lety(t) be a continuous physical process where t is the time. Also let $y(t_n) = y_n$ be the discrete samples of $y(t)$ where t_n is the time given by

$$t = \frac{nT}{N} \qquad n=1,-,N \tag{3.10}$$

In practice, y(t) is not usually periodic from day to day but it has a non-cyclic component, taken

to be linear throughout *T*, given by (CL)

$$1 \; *v^{-} y1 \tag{3.11}$$

This implies that the periodic variation can be represented as

$$y_n = Y_n \quad \frac{ti}{T} \tag{3.12}$$

y_n can be represented as a series of harmonic teims

$$y' = A_0 + E \; S_0 \tag{3.13}$$

where *r* is the number of harmonics and

$$S_o = \quad \cos \frac{2n \, ot}{T} + 13_0 \sin \frac{2n \, o \, t_n}{T} \tag{3.14}$$

The coefficients A_o, a_0 and p_o are given by

$$A, = \frac{1}{N} \; N, \; v_n - \frac{(N+1)1}{2N} \tag{3.15}$$

$$cc_0 = \frac{2}{N}_{n=1} \; y \cos \frac{2n \, an}{} \quad 1 \tag{3.16}$$

$$13_{\sigma} =-- \frac{2}{N} \underset{n=1}{Y-} L: y \, sm \frac{2Z \; an}{N} \quad \frac{1}{N} \text{ cat } \frac{an}{N} \tag{3.17}$$

S_o is compounded into

$$S = A_0 \cos \left| \frac{2 \quad \pi}{T} (t_{,,} \; _o) \right| \tag{3.18}$$

where $A_{\circ}$ and $4)_0$ are the amplitudes and phases given by

$$A_\sigma = \sqrt{\alpha_\sigma^2 + \beta_\sigma^2} \tag{3.19}$$

and

$$4). = \arctan(p_a /.o(,) , \quad o\ 4). s\ 2\ n \tag{3.20}$$

respectively for a = 1, 2, 3, 4 (in our case - see Section 4.3.1).

3.3.2 MAXIMUM ENTROPY METHOD

Before we go into the computation of the power spectral density (PSD) let us briefly consider the concept of power for a time series y *(t).* This power can be expressed as

$$power\ of\ y(t) = \sum_{j=-71} [power\ of\ y(t)\ at\ frequency\ i] \tag{3.21}$$

This equation implies that the power of *y(t)* is the additive contribution at all its frequency components, with the contribution of each harmonic being independent of the amplitude, phase and frequency of the others. The power spectrum of *y(t)* is its power at every frequency as a function of frequency.

Coming to the methods used to estimate the PSD we find that there are conventional and modern methods. Examples of the conventional approaches are the Blackman -Tukey method and the direct fast Fourier transform (FFT) method. Examples of the modern approaches are the maximum entropy method (MEM) and the maximum likelihood method (MLM). There are a number of disadvantages with the conventional methods which are not necessarily common to all of them. These include the following: they require long data sets; they require a good window to reduce leakage but this can be done at the expense of spectral resolution.

On the other hand, MEM and MLM can be used for shorter data sets and do not use windowing. In addition these two methods are data adaptive (Childers, 1978) in the sense that when power is being computed at any given frequency, they are accordingly adjusted to minimize influence by power at other frequencies. MEM has an added advantage in that zeros are not added to increase the length of the estimate of the autocorrelation function but instead it is extrapolated beyond the range of data. This extrapolation has the maximum entropy in an information theory sense (Press

et al., 1986). The objective of this is to avoid adding infolination due to the extrapolation process. This leads to the superior spectral resolution for MEM compared to other methods. However, this superiority is marred by the lack of an objective criterion for the choice of the length of the prediction error filter *M.* Smaller values of *M* result in a highly smoothed PSD whereas large values lead to spurious details.

Mathematically, the MEM power spectrum is given by (Press *et al.,* 1986)

$$P(f) \qquad \frac{a_o}{+ \sum_{k1} a \; z^k} \tag{3.22}$$

where

$$e^{2nifAt} \tag{3.23}$$

and At is the sampling interval,fthe frequency within the Nyquist interval, and a_0 and a_k are coefficients obtained from

$$\begin{vmatrix} c(0) & c(1) & c(2) & & c(M) \\ c(1) & c(0) & c(1) & \ldots & c(M-1) \\ c(2) & c(1) & c(0) & & c(A4-2) \\ & & & & \\ c(A4) & c(M-1) & c(M-2) & \ldots & c(0) \end{vmatrix} \begin{vmatrix} \\ a_t \\ a_2 \\ \\ a_m \end{vmatrix} = \begin{vmatrix} a_o \\ 0 \\ 0 \\ 0 \\ 0 \end{vmatrix} \tag{3.24}$$

where *c(i)* is the autocorrelation at lag 7.

3.3.3. LINEAR CORRELATION

The zonal and meridional components of the tides *(u* on u, respectively), although having the same frequency, have different amplitudes and phases. We thus expect that $u = cu$ where c is a complex constant. To test for this linear dependence (correlation) between these components we use the *correlation coefficient.*

We are going to use the notation X_i to represent the values of the variables being correlated. The correlation coefficient is derived from the Pearson's product moment formula (Worthing and Geffner, 943) and for any two components X_1 and x_2 is given by

$$r_{12} \qquad \sum X_1 X_2 - N\bar{X}_1\bar{X}_2 \qquad (3.25)$$

$$\sqrt{k2d \quad 2 - N./V_1)(E\ X_2^2 - NX_2^2}$$

where the overbar terns are the means, N is the number of data points and the-summation is done over N.

3.3.4 COMPUTER PROGRAMS

A number of computer programs were used in implementing the above mathematical techniques and other procedures used in the subsequent sections. These programs can be obtained on request via E-mail from phsm@ruchem.ru.ac.za.

CHAPTER 4

GENERAL WIND CIRCULATION

4.1 INTRODUCTION

As mentioned earlier, the GT meteor radar has been in continuous operation since October 1986. Echb data have been collected and processed since then to yield the zonal and the meridional velocity components of the wind as described in Section 3.2. In this thesis I will concentrate on seven years of data obtained between 1987 and 1993 with a detailed analysis of 1987 and 1988 which have enough data for monthly analysis throughout the year. The radar was not always operational within this period, and to avoid unbalanced weighting of data for any particular interval I used a rejection criterion described in Section 4.3.1. To study the gross structure of the prevailing and tidal dynamics I used monthly intervals and to study short term variations like the day-to-day tidal variability I used 1-day intervals.

In this chapter I will discuss the gross structure of the prevailing and tidal wind motions in the meteor region specifically under the following headings:

(i) Wind spectra
(ii) Wind components
(iii) Prevailing wind

Tides will be discussed in detail in the next chapter.

4.2 WIND SPECTRA

4.2.1 RESULTS

Fig. 4.1. is an example of the time series of wind in the meteor region. Sometimes the wind shows clear solar harmonic periodicities as it is the case in this figure. However, the behaviour

sometimes becomes more complicated.

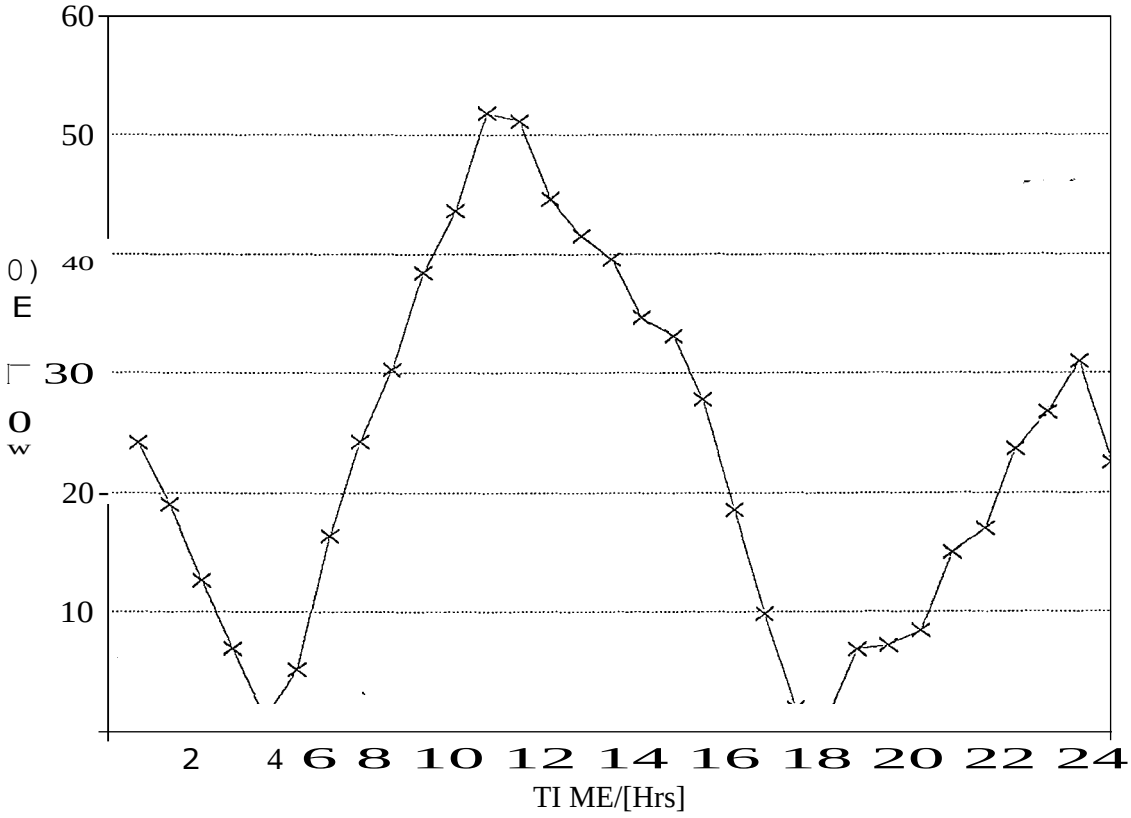

FIGURE 4.1 The mean time series of the neutral wind for February 1987.

Whether showing obvious periodicity or not, the time evolution of the wind is not random but is characterized by variations with solar harmonic periods. Such periodicity has been widely studied (e.g. Manson *et al.,* 1987) and hence it would be of interest to do a similar study in order to see how the winds above GT compare with other areas. Fig. 4.2 and 4.3 show the monthly PSD obtained by using MEM (see Section 3.3.2) for the zonal and the meridional winds respectively for 1987 and 1988. I used a 100th order spectral analysis with a 0.1 cycles/day frequency resolution. I chose a 100th order analysis because a 50th order tend to produce a smooth spectrum while a 200th order spectrum is not very different from a 100th order one but has a longer computational time.

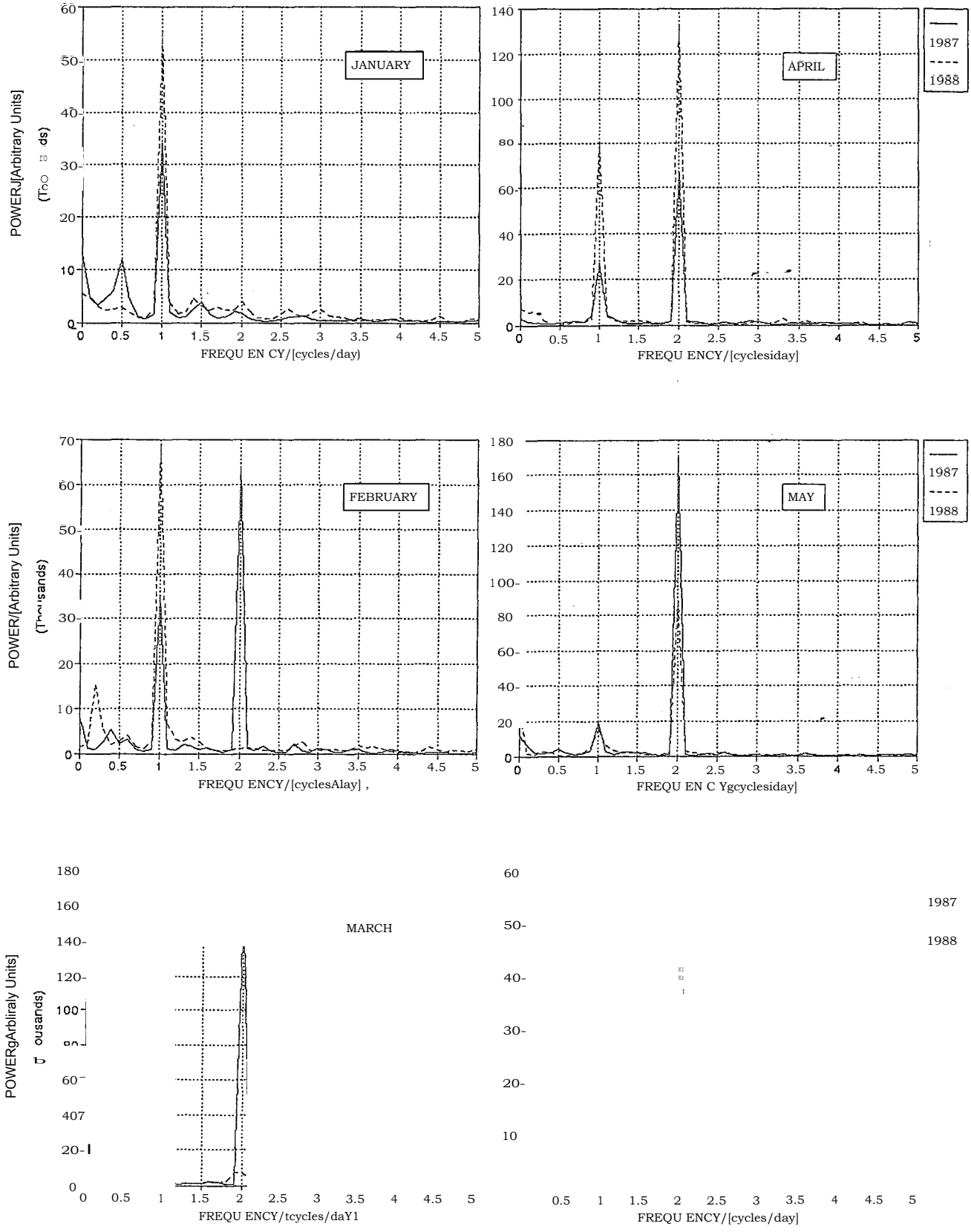

FIGURE 4.2 The zonal spectra for 1987 and 1988.

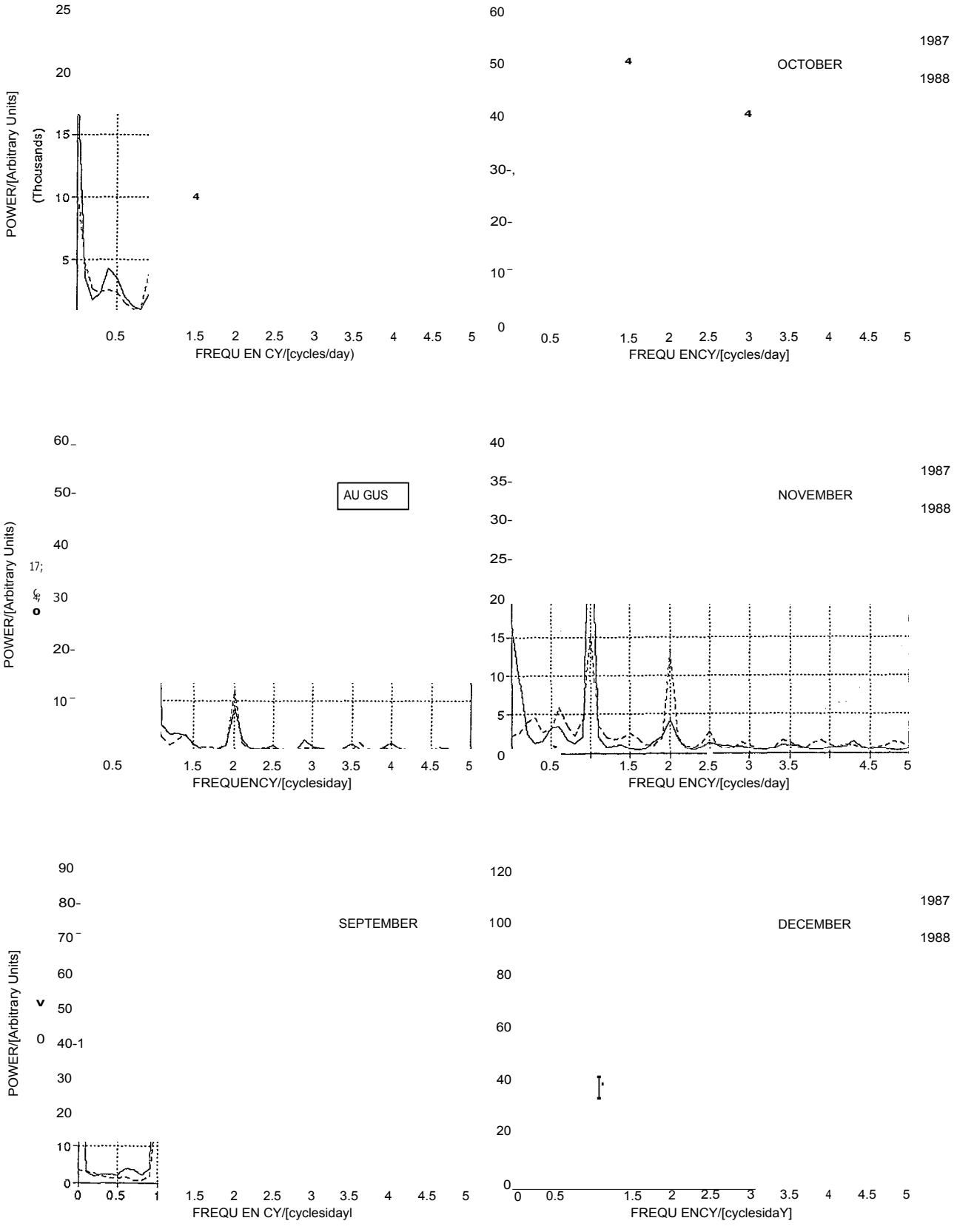

FIGURE 4.2 (Continue)

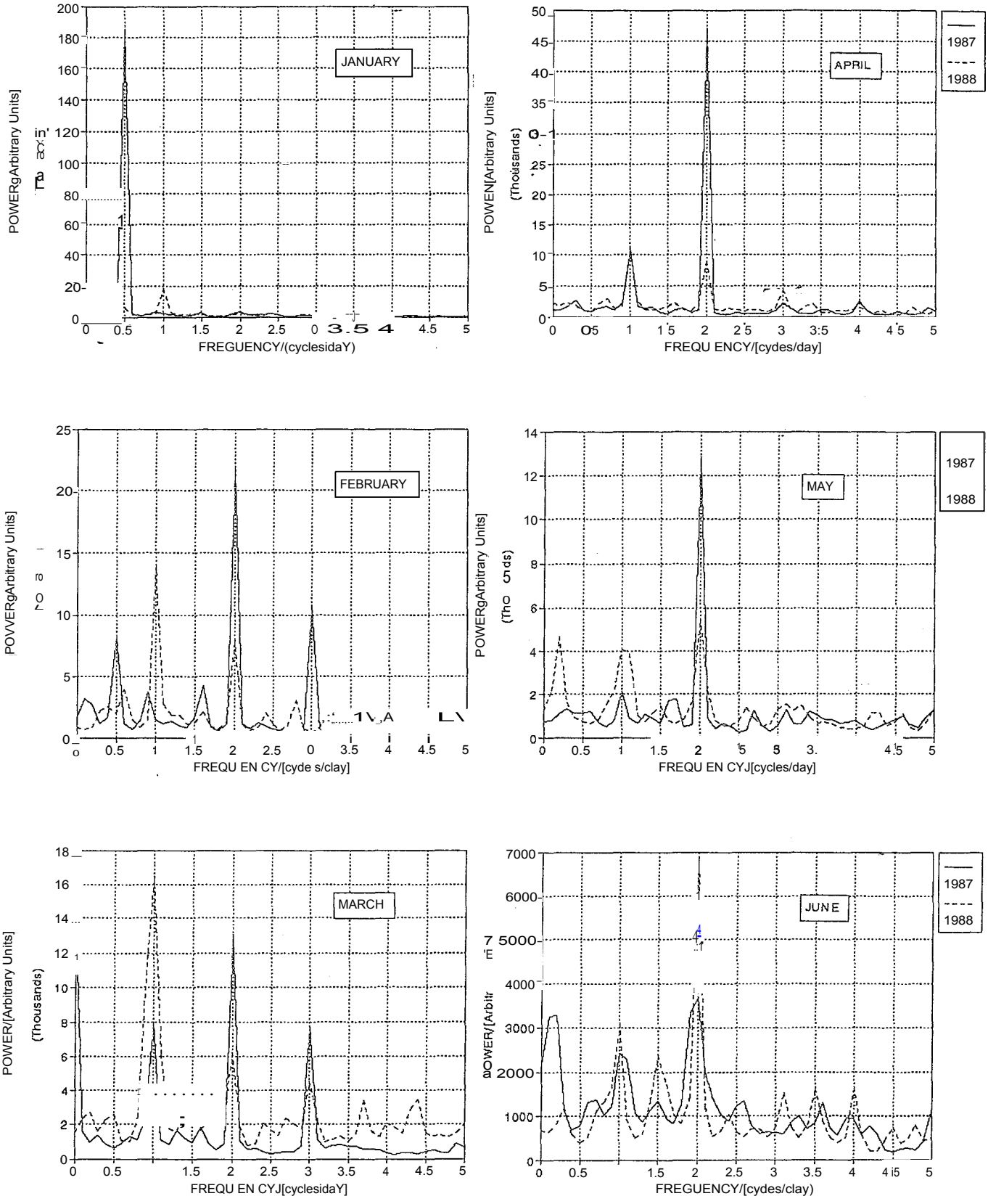

FIGURE 4.3 The meridional spectra for 1987 and 1988.

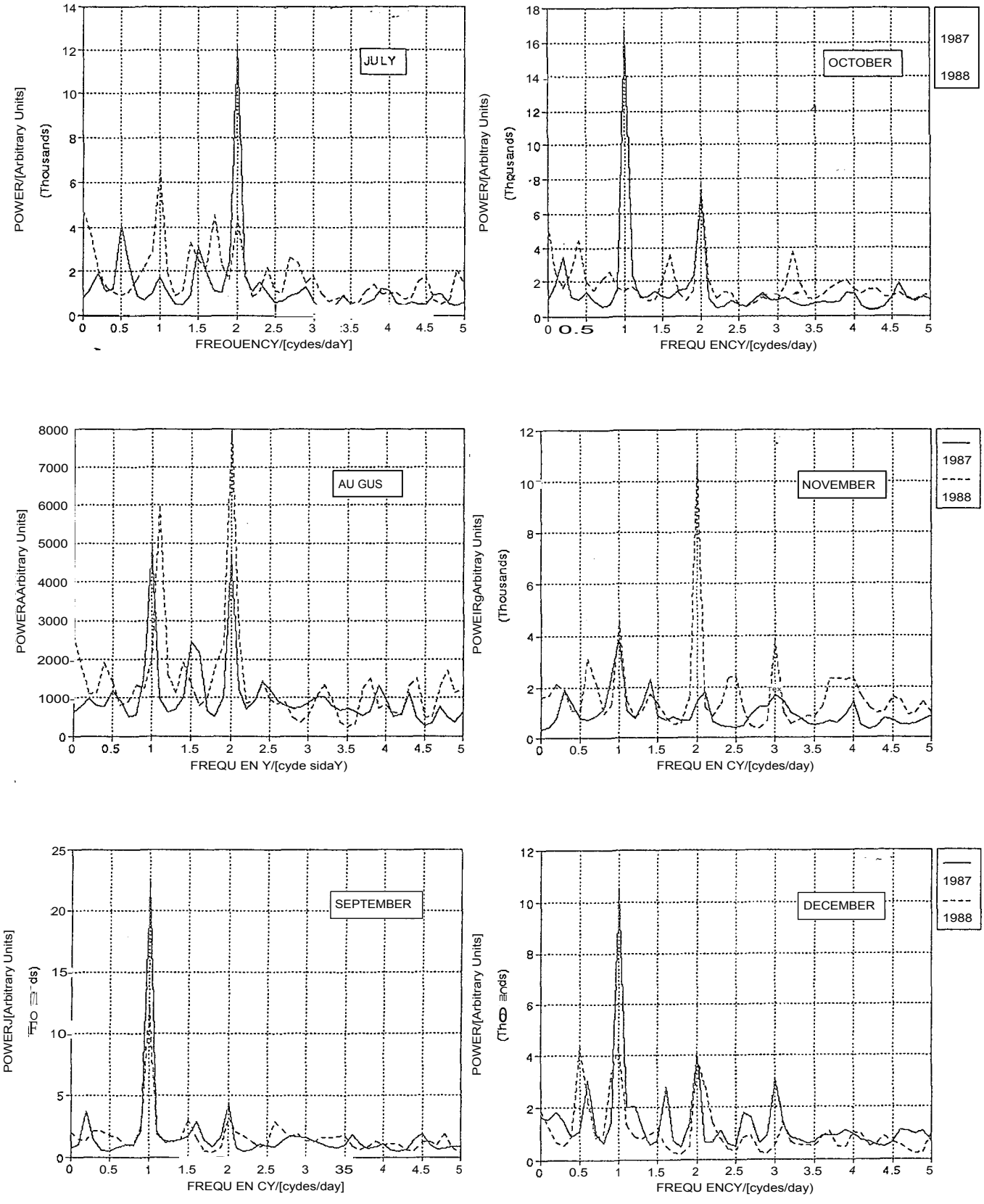

FIGURE 4.3 (Continue)

What is clearly evident in these figures is the dominance of the diurnal and semidiumal spectral components over other spectral components. However, in January 1987 there was a strong 48-hour component. This spectral component is the quasi 2-day wave which has been studied by a number of authors (e.g. Poole, 1990). This wave is strong in summer, and this also confirmed by my results for December, January and February for both the zonal and the meridional spectra. However this behaviour is more pronounced in the meridional spectra than in the zonal ones. While the zonal spectra is completely dominated by tidal spectral components, the meridional spectra, apart from the evidence of the 2-day wave, also show other spectral components. The most-important of these is the 8 hour (terdiurnal) component. There is also evidence of a lbh (1.5 cycles/day) periodicity which seems to be more pronounced in autumn and winter. The 6h (quaterdiurnal) component is very weak for most of the months.

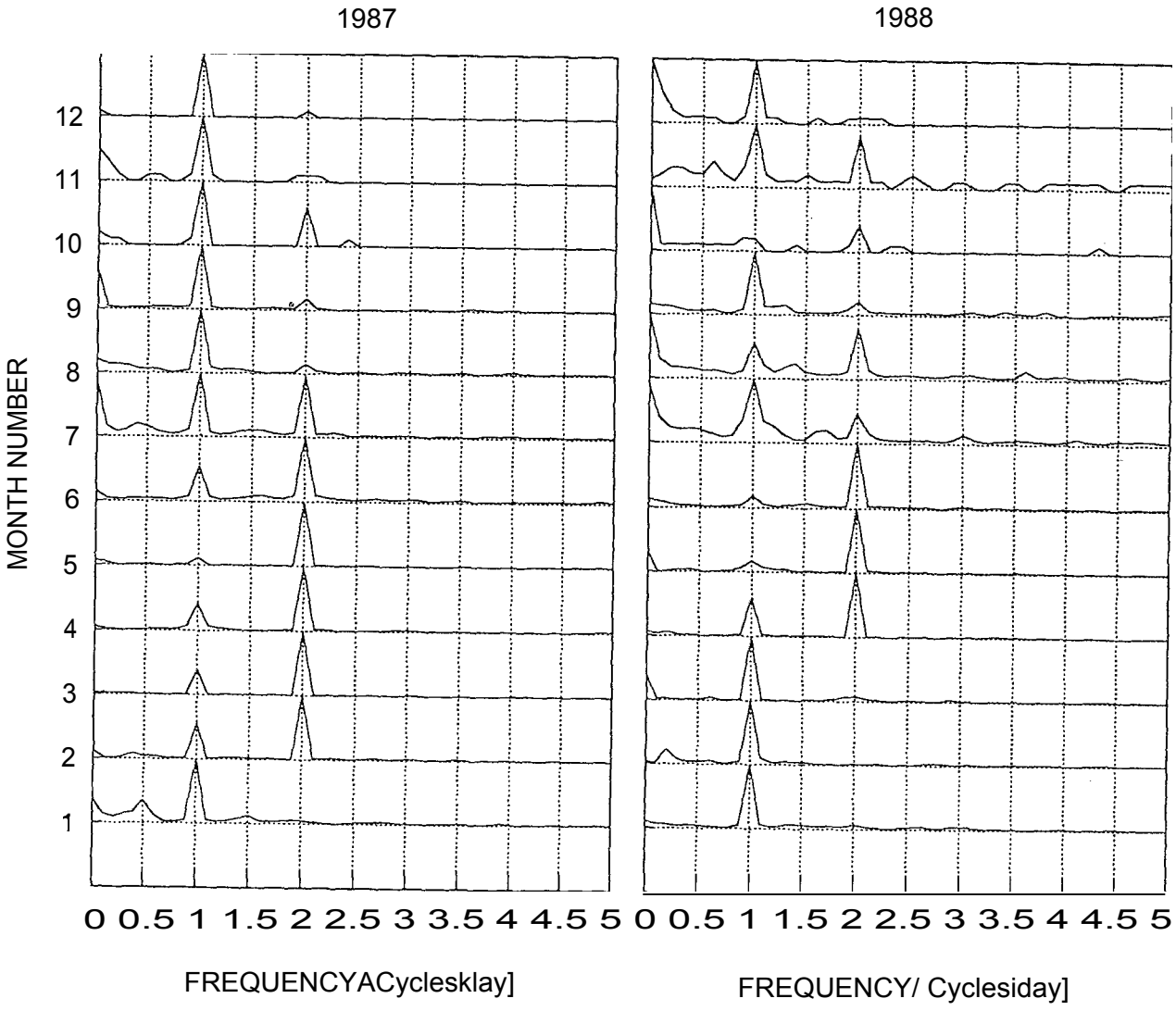

Figure 4.4 The normalized zonal spectra for 1987 and 1988.

The meridional spectra are more noisy compared to the zonal spectra. This is due to the orientation of the antenna of our radar which is more sensitive in the zonal than in the meridional direction (see Section 3.2). Fig 4.4 and 4.5 show the noinialized zonal and meridional PSDs respectively for 1987 and 1988. These figures highlight certain seasonal characteristics of the tidal spectral components. The zonal spectra in 1987 are dominated by the diurnal tide in late winter to mid-summer with a strong semidiurnal tide between late summer and early winter. In July the two tidal spectral components are comparable. The 1988 zonal spectra generally have the same features as the 1987 ones, though the semidiurnal tide generally has a 1 to 2 month lag compared to 1987. For instance, in 1987 the tidal components have comparable power in July and this happens in August in 1988. Also, the onset of the dominance of the semidiurnal tide is in February for 1987 and is two months later for 1988.

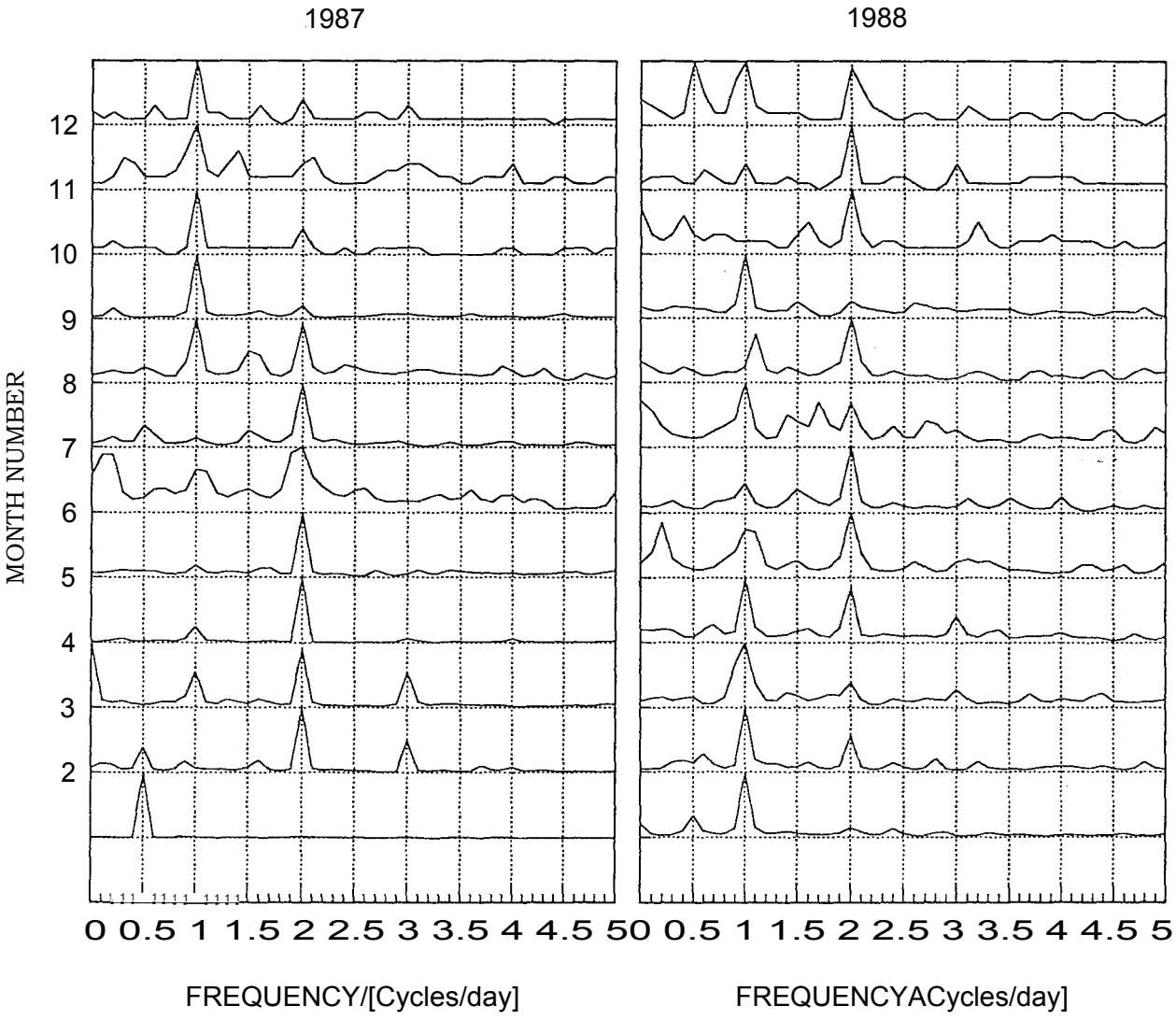

FIGURE 4.5 The normalized meridional spectra for 1987 and 1988.

The seasonal variation of the meridional spectra (Fig. 4.5) are less systematic compared to the zonal variation. However, there is a tendency of the diurnal tide to be more dominant in late winter to mid-summer and for the semidiurnal tide to be strong between late summer to mid-winter for 1987. To a great extent the 187 meridional spectra are similar to their zonal counterparts. The meridional spectra for 1988 are less systematic and very noisy and none of the tidal components is outrightly do.iinant over the other in any season.

4.2.2 COMPARISON AND DISCUSSION

The spectra of the wind above GT show periodicities of 48-, 24-, -16-, 12- and 8-hours with the tidal oscillations (24- and 12-h) being dominant for most of the months of 1987 and 1988. Manson *et al.* (1982) at latitude 52°N reported similar spectra for 30 day intervals. They also observed the unexpected -16 h oscillations. Manson *et al.* (1987) found the semidiurnal tide to be dominant from mid-autumn to early spring for the zonal wind at 106 km (Fig 4.6 (a)). This compares well with my results of a dominant semidiurnal tide for the zonal component as shown by Fig 4.4 (a) and (b). These figures also show a dominant diurnal tide from early spring to mid-autumn which is in agreement with a similar dominance between mid-spring to late summer as found by Manson *et al.* (1987).

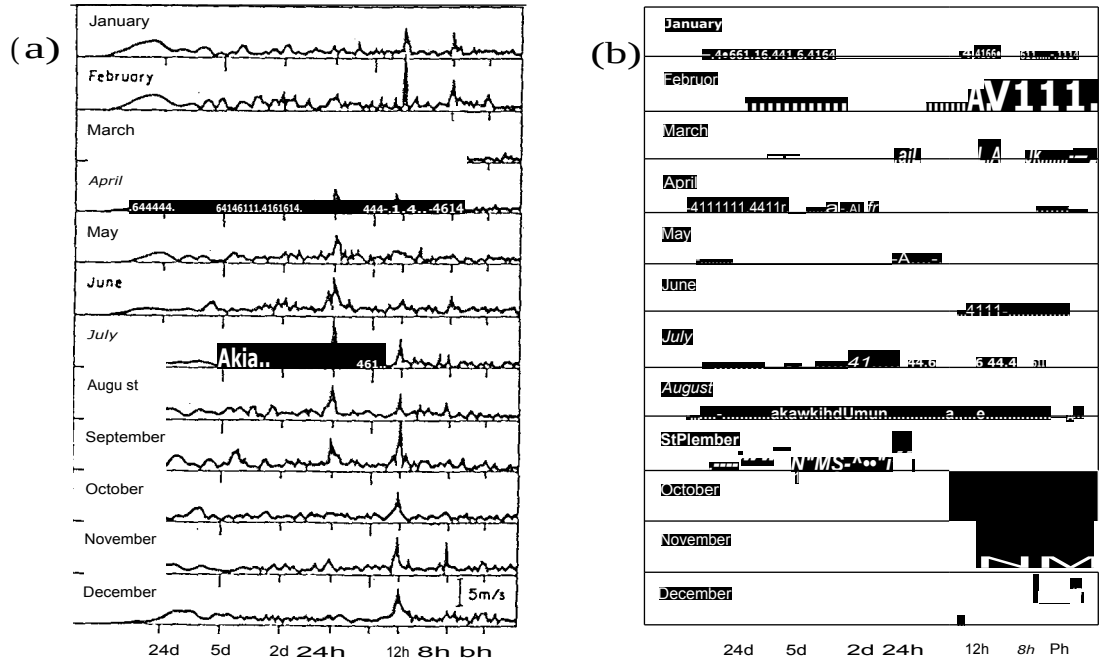

FIGURE 4.6 The power spectra at Saskatoon (52°N) for the (a) zonal, (b) meridional components (after Manson *et al.* (1987)).

The GT meridional spectra for both 1987 and 1988 are very complicated and it is difficult to draw a comparison with Manson *et al.'s* result. Their spectra also do not show a clear systematic seasonal trend. One clear feature in both my results and theirs is that there is no spectral components that has outright dominance over the others.

The above results indicate the fact that the observed spectral components have a systematic seasonal trend, especially the zonal component. The seasonal dependence of the tidal spectral components should be expected especially because of the seasonal variation in their forcing. As reported by a number of authors (e.g. Groves, 1982a,b; Hanīs, 1993) the diurnal and the semidiurnal tides are primarily excited by the absorption of solar radiation by water vapour and ozone, respectively. The distribution of these forcing agents varies with season hence the above seasonal spectral trends may be due to the variation of the source of excitation. For instance, the dominance of the diurnal tide in summer may be due to the movement of water vapour into the summer hemisphere as reported by Groves (1982b). Other factors that might explain the above trends are the seasonal variations in dissipation (VT), the prevailing wind and hence in mode coupling. It will be recalled that mode coupling results in the generation of certain modes which were not originally produced by tidal forcing (Section 2.2.2) and this would be accompanied by spectral changes.

4.3 WIND COMPONENTS

4.3.1 MONTHLY CLIMATOLOGIES

Having discussed the important spectral components of neutral wind we now concentrate on how their combined effects approximate the wind in the meteor region. The important spectral components were deduced by using the guidelines agreed upon at the Workshop on Atmospheric Tides (see Section 1.3.2) for constructing monthly atmospheric climatologies (Forbes, 1986b). The amplitudes and phases of harmonic components are obtained from vector monthly averages, yielding 'tidal amplitude and phase that are consistently present throughout the studied month' (Vial, 1989). To do this I accumulated the zonal and meridional wind components for a particular month into thirty-two 0.75 h time bins and averaged for each time bin according to the number of days for which there is data during that month. This forms an *'equivalent clay'* for that month

(or n-day interval, *n* being and number e.g. 10). In the formation of the 'equivalent day' I applied a rejection criteria in order to try and avoid a largely biased weighting of the monthly (n-day interval) averages. In this criteria I used a 50% threshold in which any time bin that had less than half its potential data values was rejected. Secondly, after all the data values had been accumulated and the above threshold applied the acceptable time bins are counted and if they are less than 16 which is 50% of the maximum number of time bins ti.e. 32) that whole month (n-day interval) is rejected. I then applied a harmonic analysis on this 'equivalent day as described in Section 3.3 to obtain the prevailing wind and the amplitudes and phases of the solar harmonic components.

Having obtained the above parameters I fitted the data in least-squares fashion to harmonic functions

$$u(t) \quad {}_{0} \sum_{a=1}^{4} 21_{a} \text{ COS CD (1 -} \tag{4.1}$$

and

$$u(t) = u_{0} + \sum_{a=1}^{4} D_{a} \cos \quad (t - \tag{4.2}$$

where

t = time in hours

co= 2 TZ 0/24

u_o= zonal prevailing wind

u_o= meridional prevailing wind

u_o= - diurnal zonal amplitude

v_o= G^{-1} - diurnal meridional amplitude

ck_o= 6^{-1} - diurnal zonal phase in hours

6_0= - diurnal meridional phase in hours

The phases are the local times of maximum for that particular component in eastward and northward directions for the zonal and meridional components, respectively. Though the spectra discussed in the previous section do not show a strong 6 h component, it is important to mention that sometimes this component can have an amplitude as large as -9 ms (e.g. see Appendix A, Table 2(b) for 1991). Though this component is, on average, small I have included it in all my calculations (i.e., I have used a = 1, 2, 3, 4).

4.3.2 RESULTS

Fig. 4.7 shows the time series for the zonal wind for each of the months of 1987 and 1988 with the thick line representing the fitted five term approximation described in Section 4.3.1. There are similarities between the wind for the corresponding months of 1987 and 1988 with the only major differences occurring in the summer months. The strong diurnal tide observed in Fig. 4.4 (a) from late winter to mid-summer is clearly reflected in the time series figures for 1.987 from August to January. The onset of the dominance of the semidiurnal tide, in agreement with Fig. 4.4 (a) is in February and lasts until July. The time series for 1988 have a similar behaviour, though the dominance of the semidiurnal tide starts in April which is also in agreement with Fig. 4.4 (b).

For all the months, the fitted five-term smoothing function is a good approximation to the observed wind. The meridional time series (Fig 1 ,Appendix B) are noisy (due to system anisotropy) and do not show a systematic dominance of one tidal component over the other. The similarities between the corresponding months of 1987 and 1988 are mainly between March and September.

The same information is perhaps more effectively presented in the form of surface plots. The monthly smoothed time series for the zonal wind are shown in Fig 4.8 for (A.1) 1987 and (B.1) 1988 with the contours projected onto the time-month plane shown again to the right of the corresponding surface plots ((A.2) and (B.2)). For both years the wind consistently reaches its peak in the eastward direction between 8.0 h and 12.0 h which is clearly evident in the contours for both years. From (A.2) and (B.2) of Fig. 4.8 we see that the wind reach its maximum in the westward direction between 2.0 h and 6.0 h and is centered around May. There is also a secondary westward maximum between 16.0 h and 18.0 h centered around April, though for 1988 this maximum is about as large as the maximum in the morning hours. There is also a secondary eastward maximum between 10.0 h and 12.0 h which is centered between August and September in 1987. This is also observed in 1988 though earlier in time of the day (9.0 h) but later in the year (November). The diurnal tide influence is strongest in summer as shown by the strong single eastward peak during the summer months.

Fig 4.9 is the same as Fig. 4.8 but for meridional wind. The surface plots show great month-to-month variability. The contours for both years show a number of similar features. For both years there is a equatorward maximum between 10.0 h and 12.0 h centered around March and April.

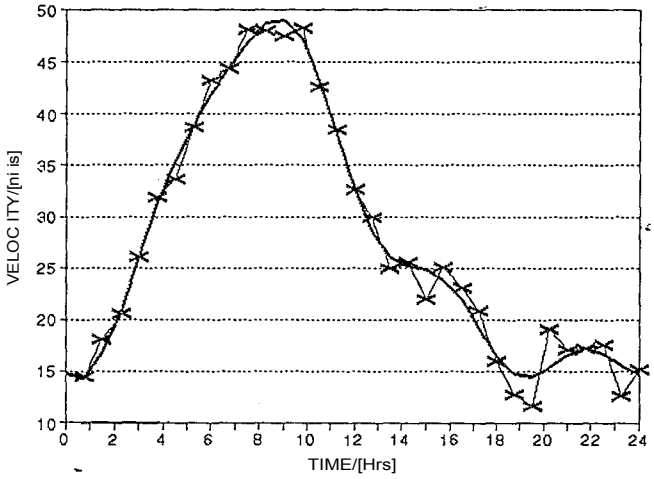

1(a) JANUARY

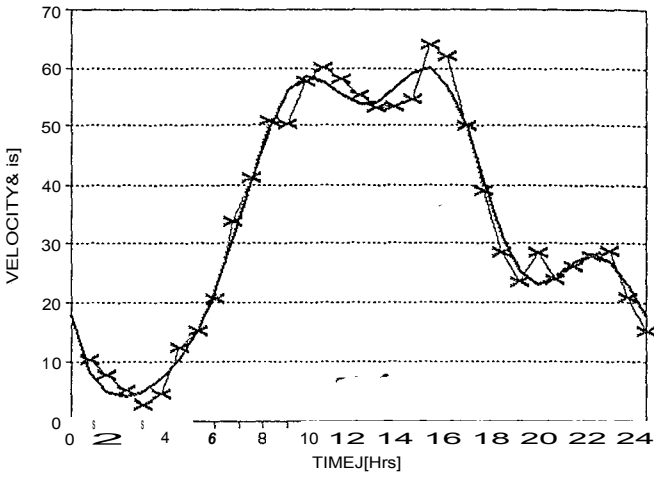

1(b) JANUARY

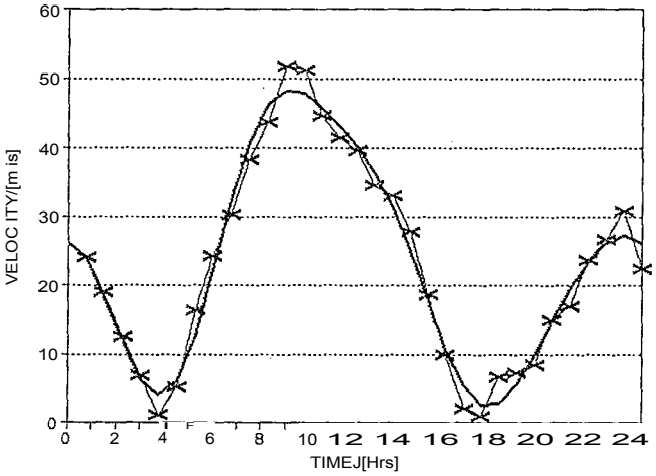

2(a) FEBRUARY

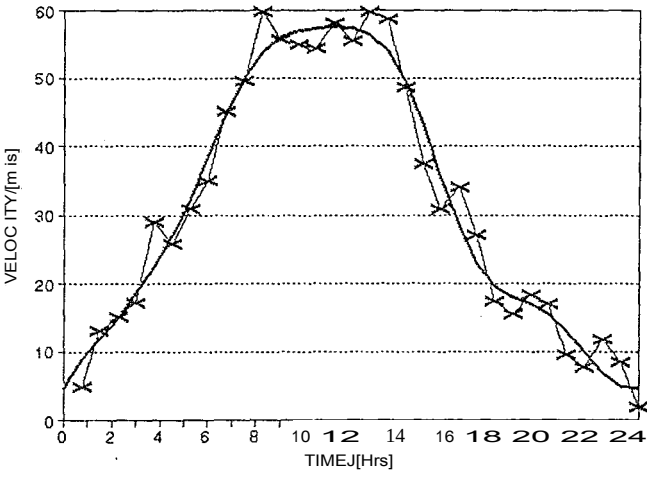

2(b) FEBRUARY

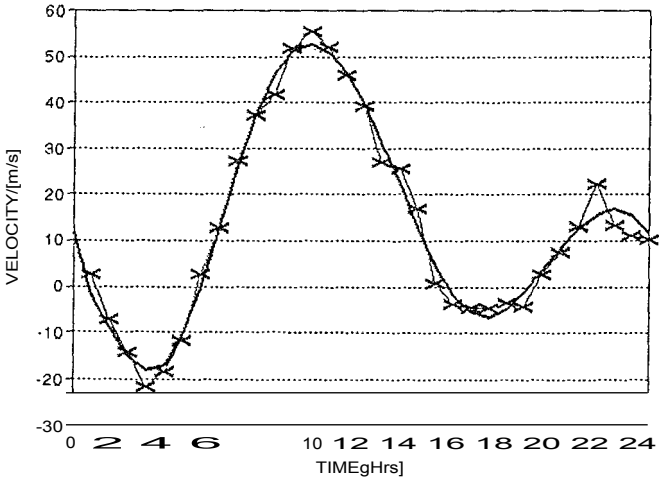

3(a) MARCH

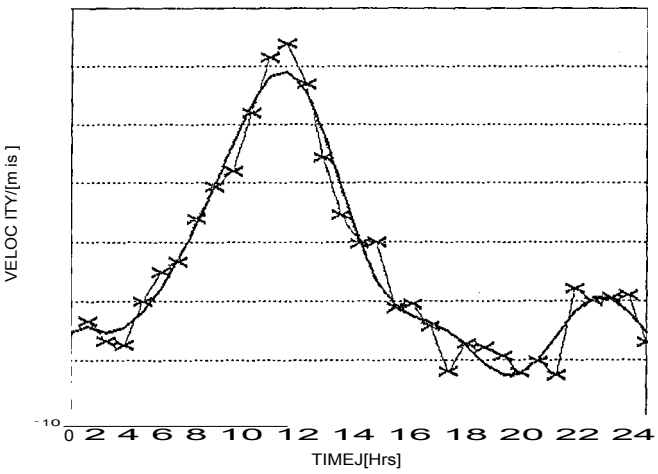

3(b) MARCH

FIGURE 4.7 The zonal time series for 1987 (left) and 1988 (right).

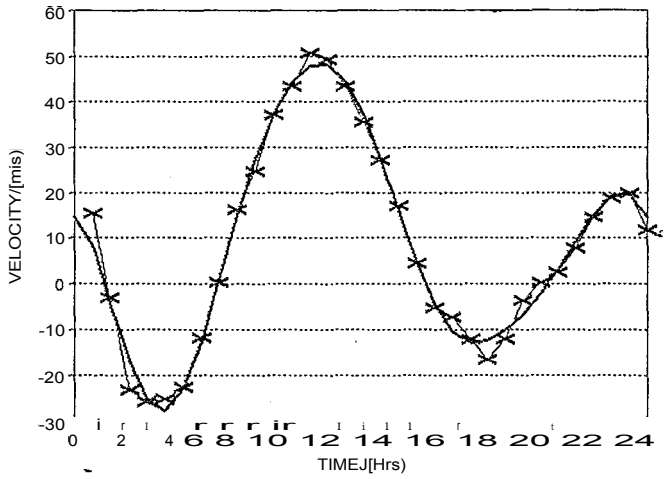

4(a) APRIL

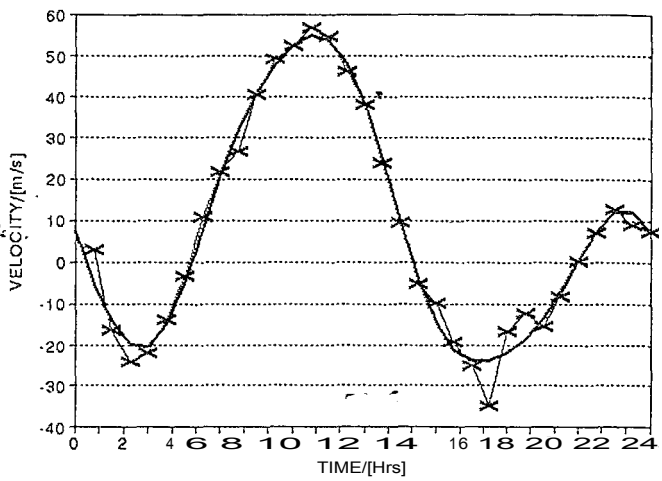

4(b) APRIL

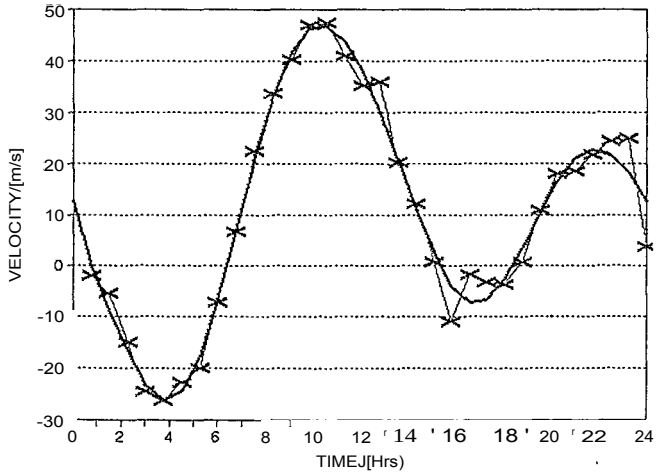

5(a) MAY

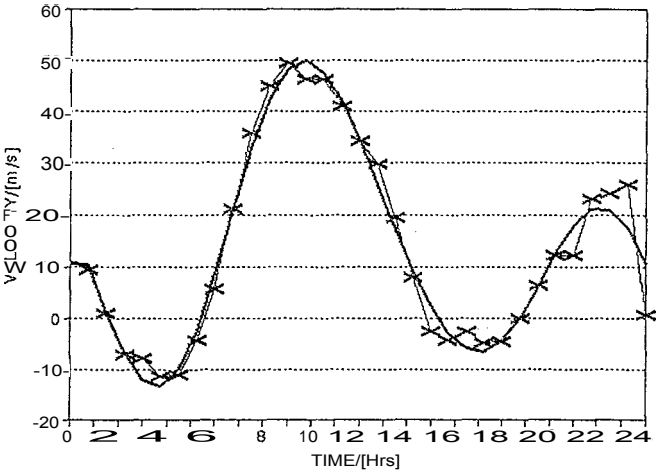

5(b) MAY

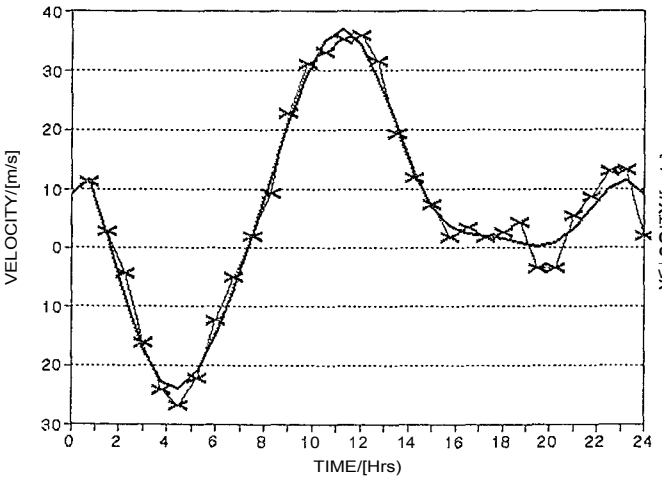

6(a) JUNE

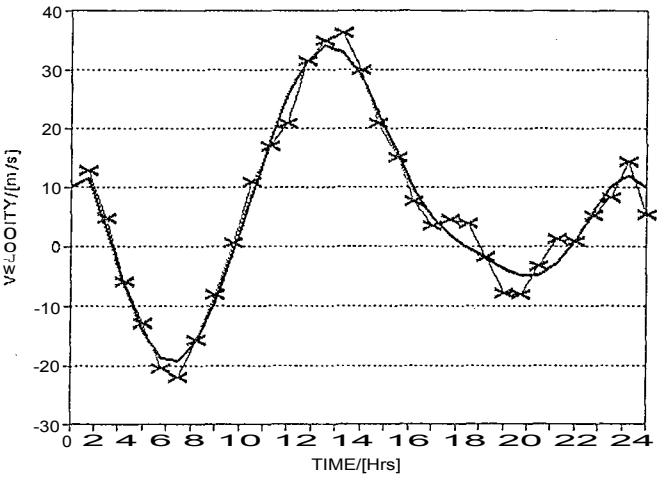

6(b) JUNE

FIGURE 43 (Continue)

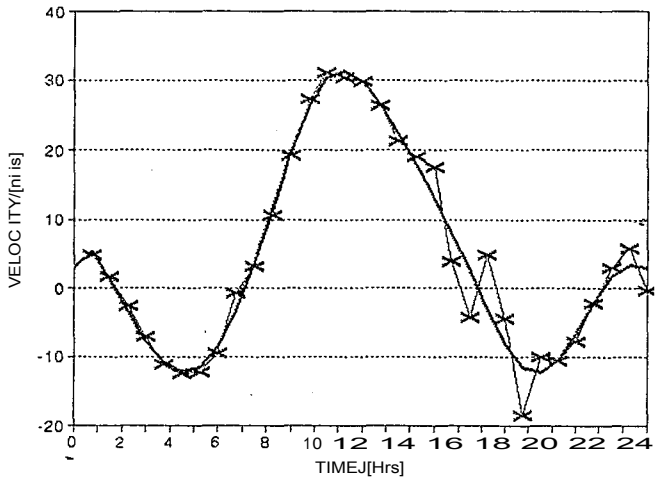

7(a) JULY

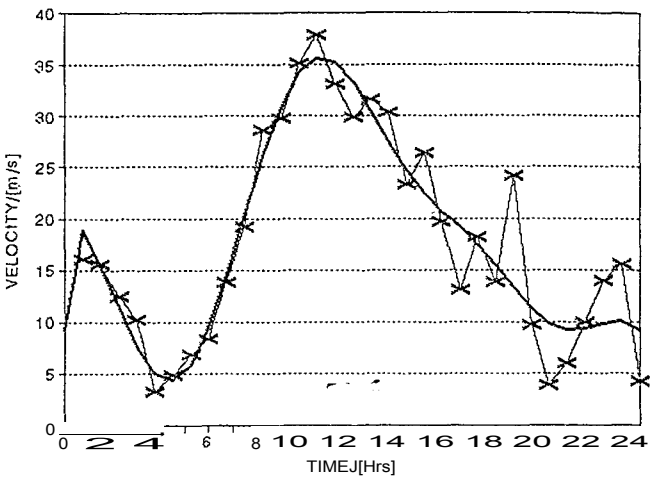

7(b) JULY

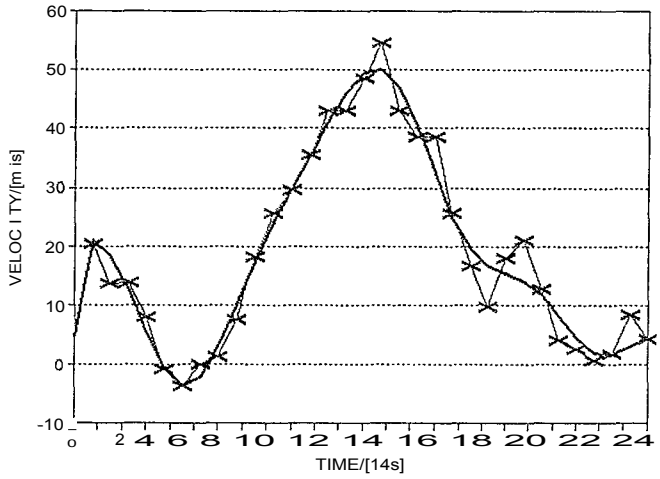

8(a) AUGUST

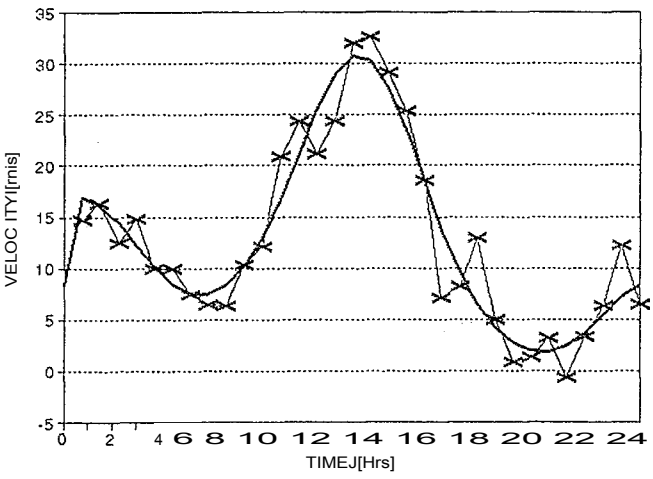

8(b) AUGUST

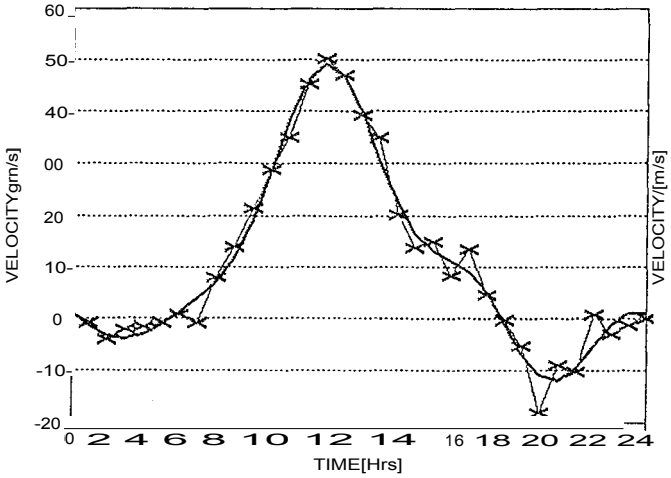

9(a) SEPTEMBER

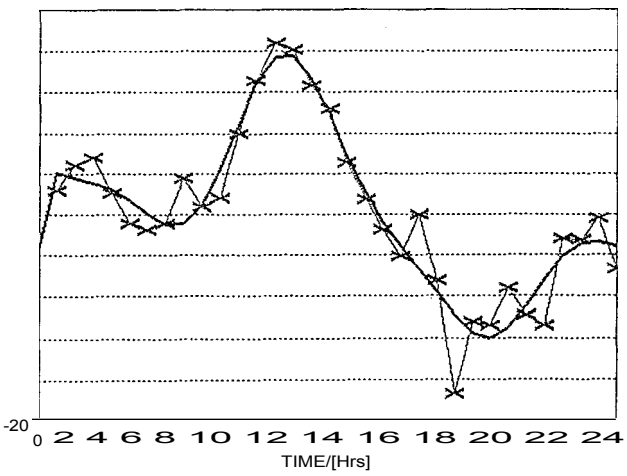

9(b) SEPTEMBER

FIGURE 4.7 (Continue)

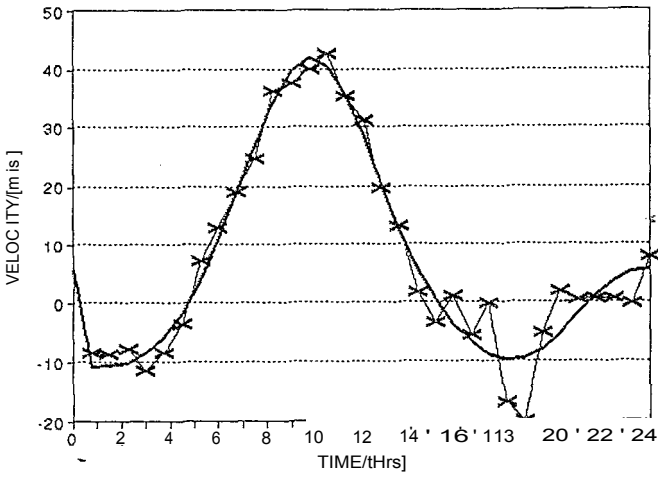

10(a) OCTOBER

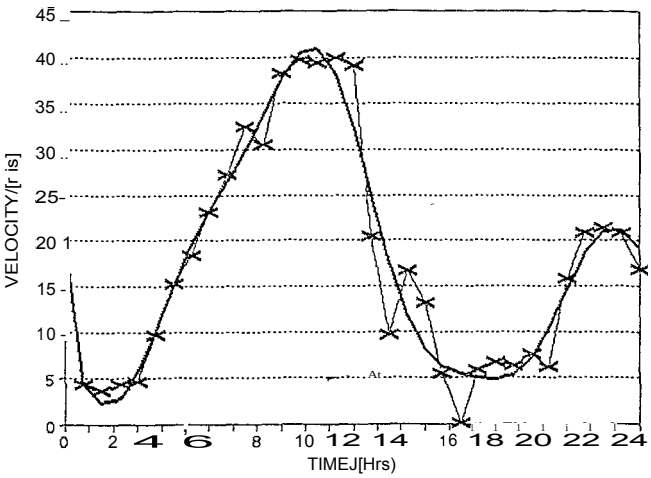

10(b) OCTOBER

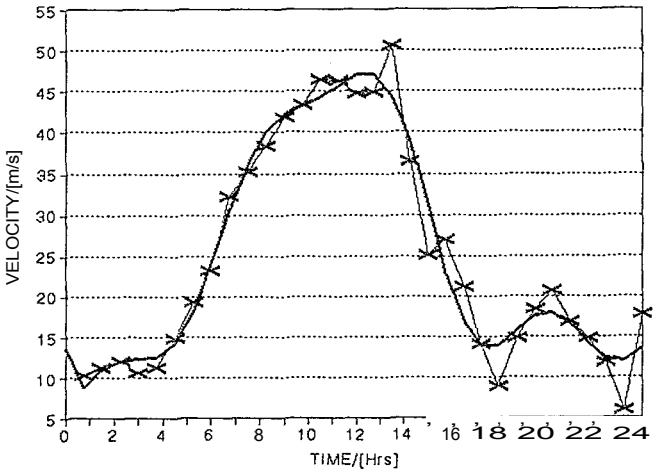

11(a) NOVEMBER

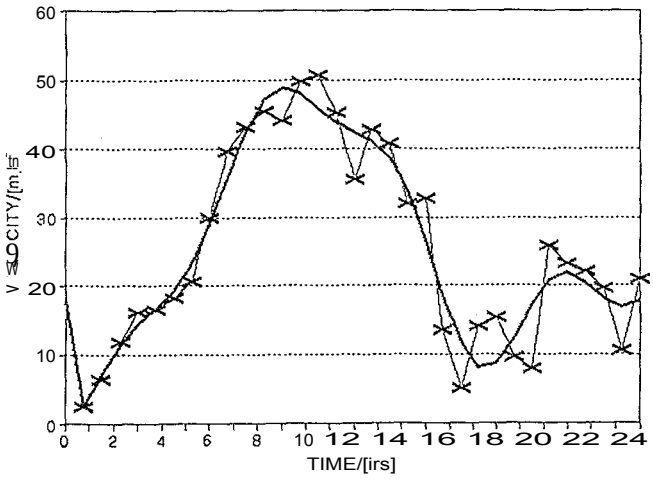

11(b) NOVEMBER

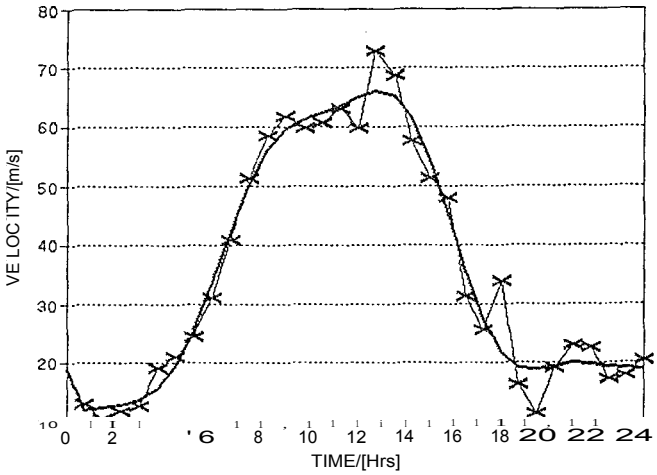

12(a) DECEMBER

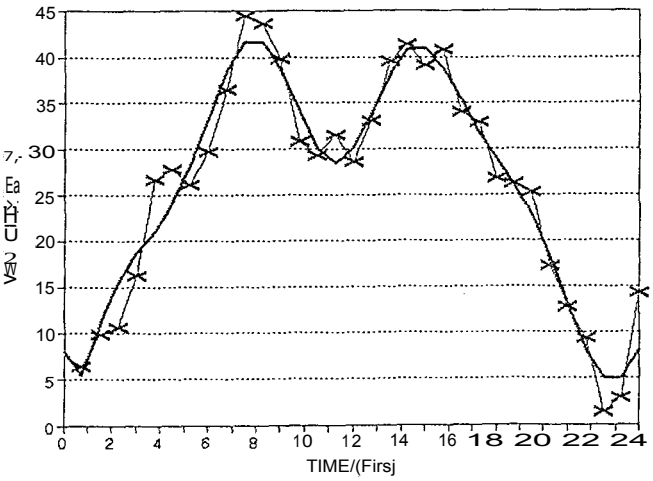

12(b) DECEMBER

FIGURE 4.7 (Continue)

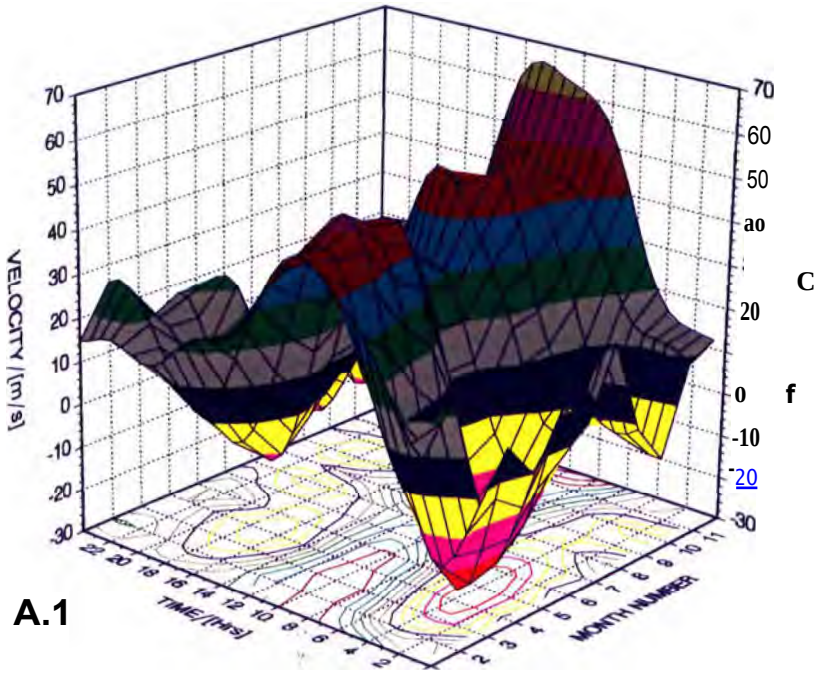

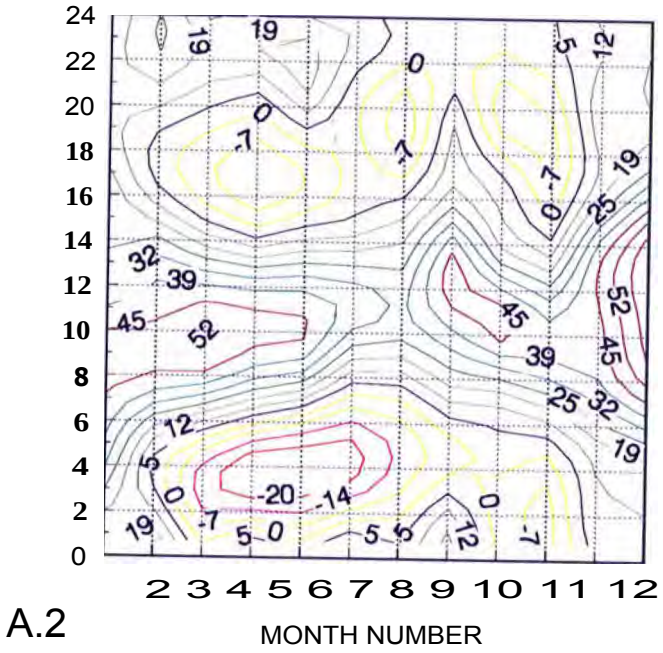

FIGURE 4.8. Surface plots ((A.1) and (B.1)) and corresponding contour plots ((A.2) and (B.2)) of the smoothed time series of the zonal wind for 1987(top **two) and 1988 (bottom two).**

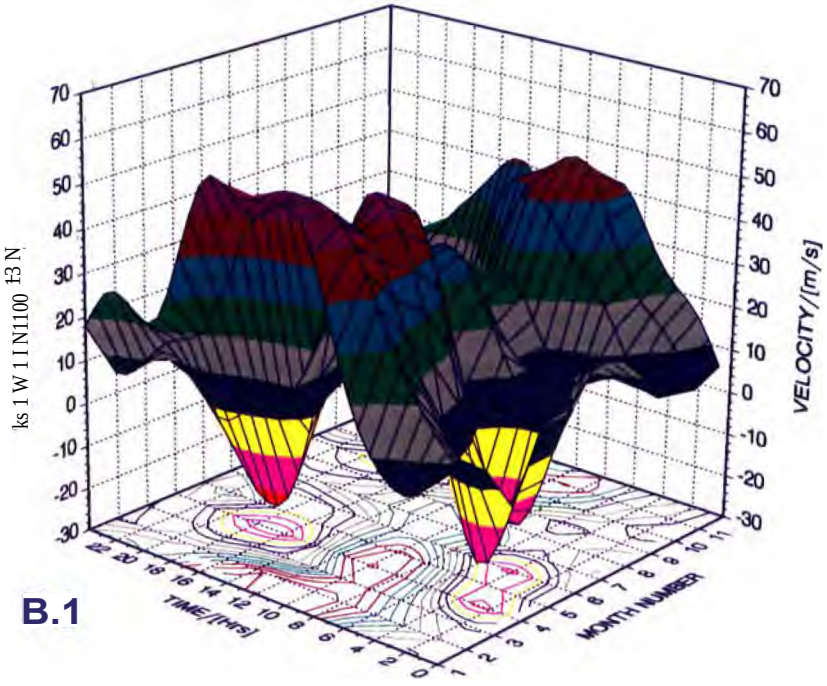

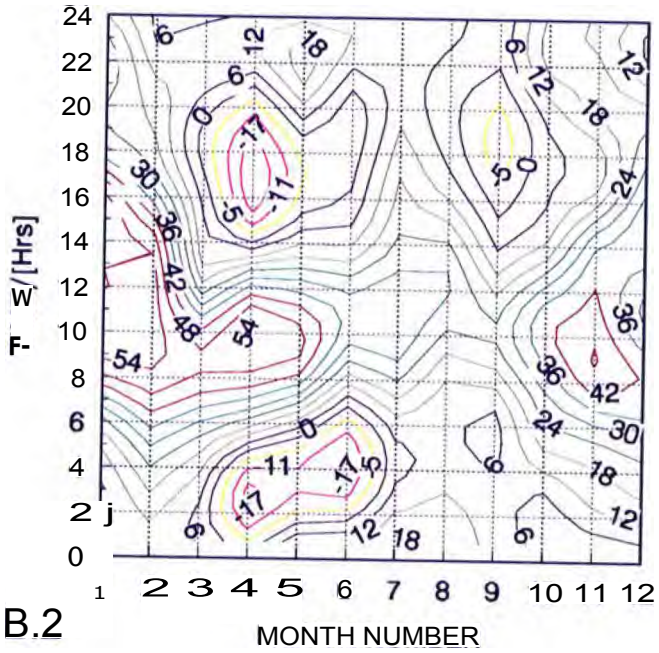

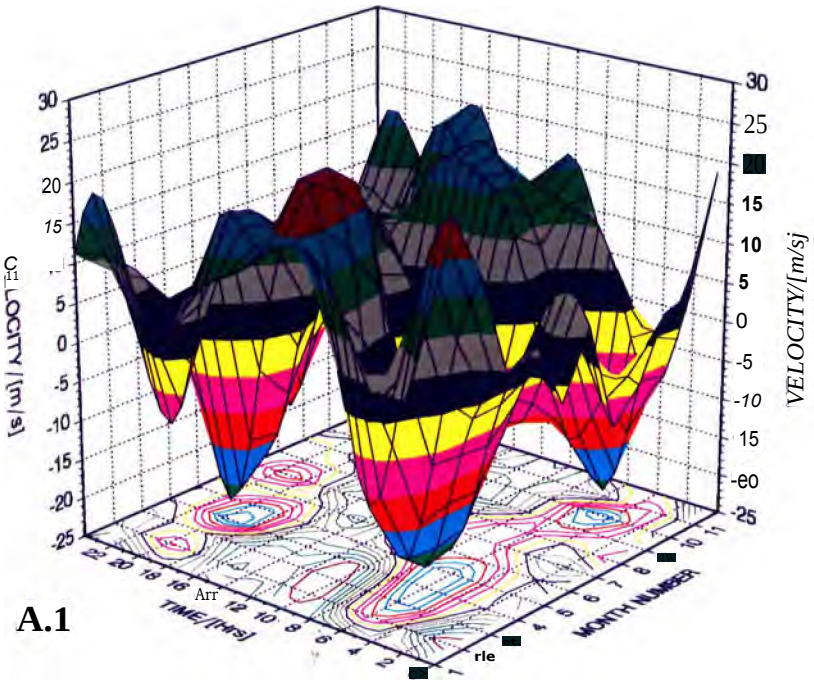

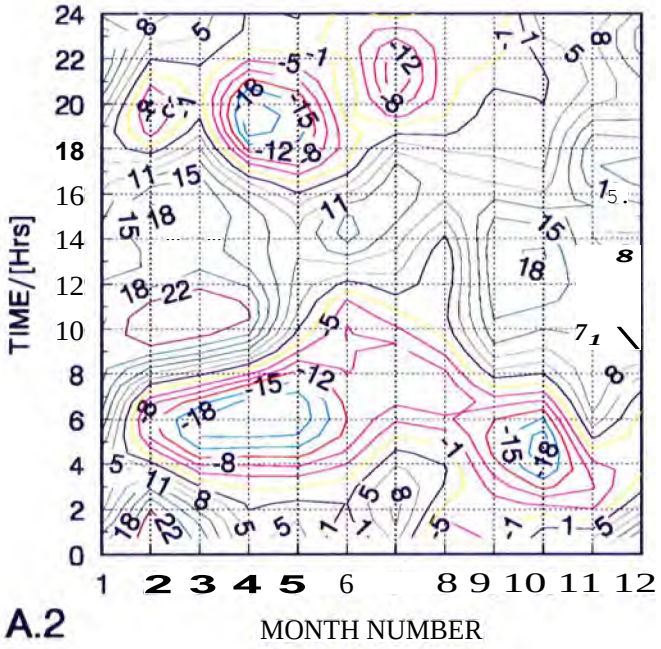

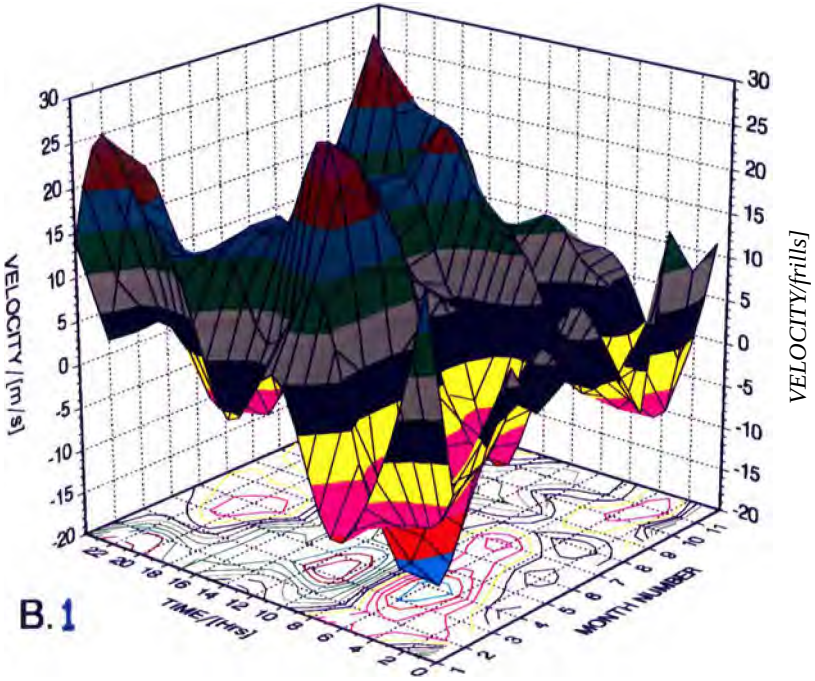

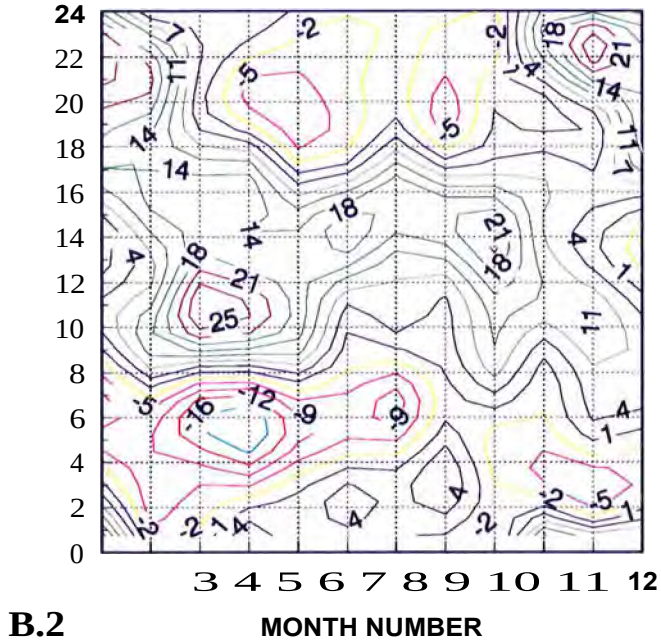

FIGURE 4.9. Surface plots ((A.1) and (B.I)) and corresponding contour plots ((A.2) and (B.2)) of the smoothed time series of the meridional wind for 1987(top two) and 1988 (bottom two).

Also, there is a secondary poleward maximum at - 20.0 h in April and an equatorward peak at -14.0 h in June and another one at -13.0 h in October (September for 1988). Unlike the zonal contours, there is no clear dominance of any of the tidal components which agrees with the spectral observations made in Section 4.2.

4.3.3. DISCUSSION

An important observation made in this section is the similarity of the wind behaviour for corresponding months of 1987 and 1988 especially for the zonal wind. This shows that the physical factors influencing the wind recur from year to year. With the Sun being the main driving force of the wind and tides, such consistency is to be expected. The minor deviations are presumably due to the other physical parameters like the concentration of ozone and water vapour, and dissipative processes which, although recurring from year to year, have greater interannual variability than the Earth's orbital motion around the Sun.

The five-term fitting function confirms the observation made in Section 4.2 that the wind is not random but consists of solar harmonic components and a mean term. In the next few sections I am going to consider in detail the prevailing component. Tidal components, which are the major subject of this thesis, will be dealt with in the next chapter. I am not going to discuss in detail the terdiurnal and the quaterdiurnal components but their parameters are tabulated in Appendix A for reference purposes.

4.4 THE PREVAILING WIND

As discussed in Section 2.2.2, the prevailing wind is governed by the geostrophic balance and consists of both a zonal component and a meridional one. Theoretically, the former is larger than the latter which, as we shall see, is confirmed by the GT results.

4.4.1 THE ZONAL AND MERIDIONAL PREVAILING WIND

4.4,1.1 RESULTS

I deduced the monthly values of the zonal and meridional prevailing winds from an harmonic analysis of the monthly 'equivalent day' for the years 1987 - 1993 inclusive. These are tabulated in Table 4.1 and are graphically shown in Fig. 4.10. for the (a) zonal and (b) meridional components. In an attempt to stack the graphs on top of each other for better interannual comparison, I had to trade off the clarity on the labeling of the axis of the graphs. It is suggested that Fig 4.10 should be used in conjunction with Table 4.1 for even better interannual comparison.

In Table 4.1 and others of the same type that follow, the AAA (see Section 1.3.3.2) is not labelled on the tables, but its value is found where the MIA and the AA columns intersect. UN(AAA) and SD(AAA) are given in the row corresponding to AA but in the columns of U(MIA) and SD(MIA) respectively. In the above figures and the others that follow, the phrase *"real data"* refers to the actual data obtained at GT and *'filled in"* refers to points for which data are missing and are represented on the figures by the MIAs of the relevant months. That is, if ,say there were no data for January 1987 the point that would be indicated on the figure will actually be the MIA for January. Also in these figures y_0 is the first value on the vertical axes, and vs is the vertical grid spacing.

The zonal prevailing wind is strongly eastward (positive) during the solstices with velocities as high as -43 ms". Equinoctial circulation is also eastward but it is generally small (< 20 ms'). The zonal prevailing wind is eastward except in October 1987 when it is westward. The eastward annual averages are - 9 - 23 ins'. The year 1990 has the largest (23.1 ms⁻') annual average but this is probably due to the absence of the minimum values of spring.

The meridional prevailing wind is generally weaker than the zonal component as reflected by its annual averages of < 11 ms⁻' (equatorward) and < 5 ms (poleward). The meridional component is strongly northward in summer and also early autumn and late spring. From mid-autumn to early spring it is generally weak (< 10 ms" except in 1992) and the wind sometimes reverses into a southward (negative) flow.

(a)

	YEAR									
MONTH	1987	1988	1989	1990	1991	1992	1993	MIA	UN(MIA) S	SD(MIA)
1	27.4	31.5	24.6	24.1	11.2	12.1	12.2	20.4	3.2	41.1
2	23.9	33.0	9.1	25.1	16.6			21.6	4.1	42.0
3	9.4	17.7	12.4	18.6	17.0		5.0	- 13.3	2.2	40.3
4	10.4	5.3		20.0	24.3	20.9	0.4	13.6	3.9	71.0
5	7.1	18.2		29.9	22.3	25.1	13.0	19.3	3.4	43.1
6	10.7	9.6	10.9	21.6	7.7	22.3	16.4	14.2	2.3	41.9
7	7.3	23.9	27.7	22.1		42.9		24.8	5.7	51.5
8	27.2	17.2	21.5		25.5	23.6		23.0	1.7	16.8
9	10.4	10.4	17.1		7.1	10.2		11.1	1.6	33.0
10	-1.2	11.2			1.9	6.2		4.5	2.7	118.9
11	20.9	15.7			5.7	19.8		15.5	3.5	44.7
12	31.7	22.1	27.5		12.5	19.2	8.2	20.2	3.6	44.0
AA	15.4	18.0	18.9	23.1	13.8	20.2	9.2	16.9	1.7	26.9

(b)

	YEAR												
MONTH	1987	1988	1989	1990	1991	1992	1993	MIA	UN(MIA)	SD(MIA)	MIA	UN(MIA)	SD(MIA)
1	16.8	14.5	15.8	11.0	14.6	14.7	17.3	15.0	0.8	13.8			
2	16.7	7.4	10.4	15.8	16.8			13.5	1.9	31.8			
3	13.3	5.6	13.4	13.1	10.4		6.9	10.5	1.4	33.0			
4	1.2	7.1		5.7	8.1	4.8	2.7	4.9	1.1	53.2			
5	-1.6	1.5		1.6	2.8	6.8	4.8	3.5	1.0	64.9	-1.6	0.0	0.0
6	-2.1	3.6	-4.9	1.0	-2.5	5.2	6.0	4.0	1.1	55.5	-3.2	0.9	47.9
7	1.1	4.3	-5.5	1.5		13.5		5.1	2.9	113.2	-5.5	0.0	0.0
8	-3.9	2.9	-1.7		1.0	8.8		4.2	2.4	96.4	-2.8	1.1	55.3
9	2.5	3.4	2.7		7.1	7.0		4.5	1.0	50.9			
10	1.2	9.8			6.2	11.5		7.2	2.3	63.4			[1]
11	10.0	10.4			20.1	9.7		12.6	2.5	40.2			
12	15.7	10.6	8.7		15.7	9.3	21.2	13.5	2.0	35.9			
AA	8.7	6.8	10.2	7.1	10.3	9.1	9.8	8.9	0.5	16.2			
AA	-2.5		-4.0		-2.5						-3.0	0.5	28.9

TABLE 4.1 The (a) zonal and (b) meridional prevailing monthly wind components.

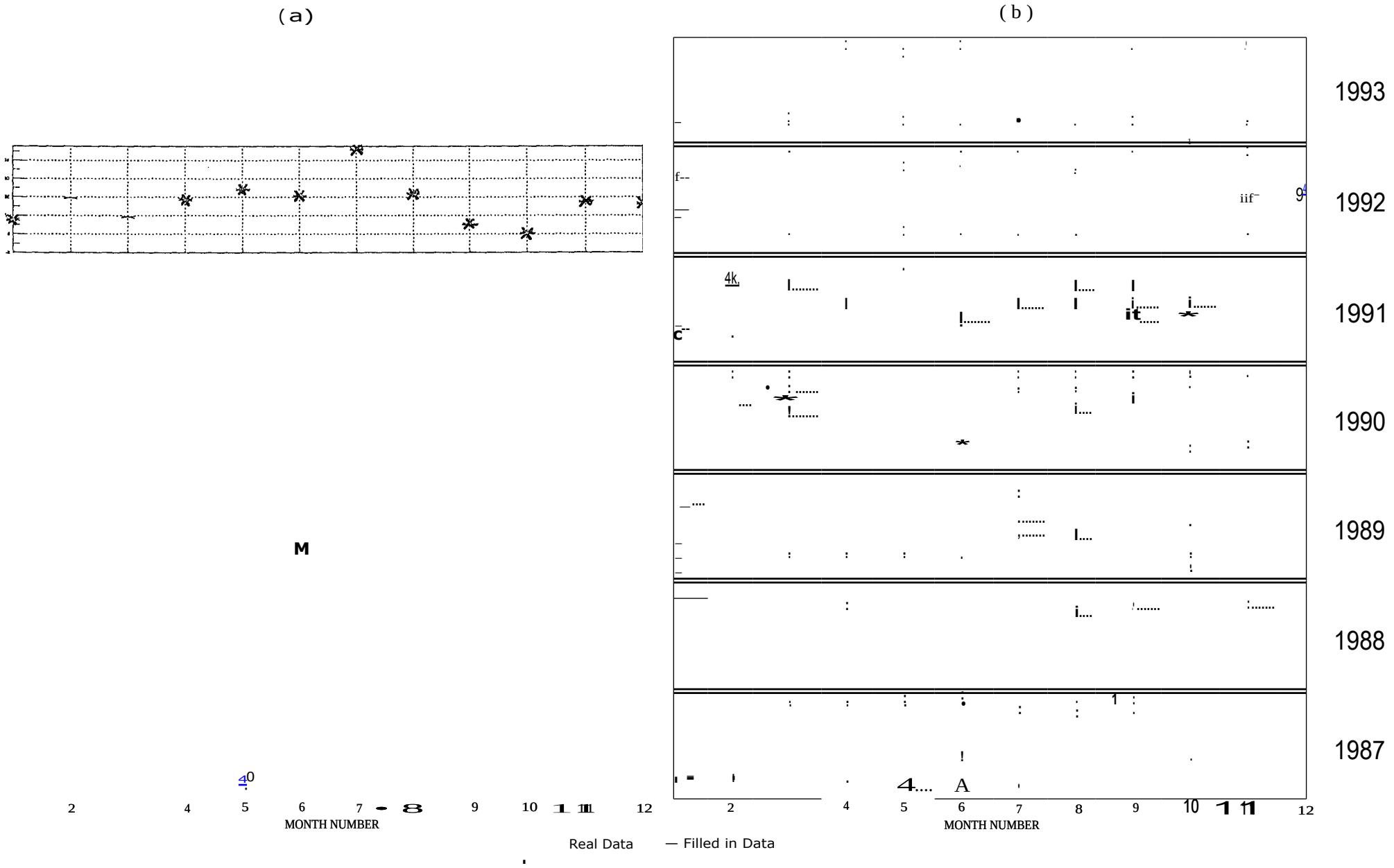

FIGURE 4.10 The (a) zonal (y_o = -2; vs = 8 ms/division) and (b) meridional (y,= -6; vs = 4ms^{-1}/division) (monthly) prevailing wind components.

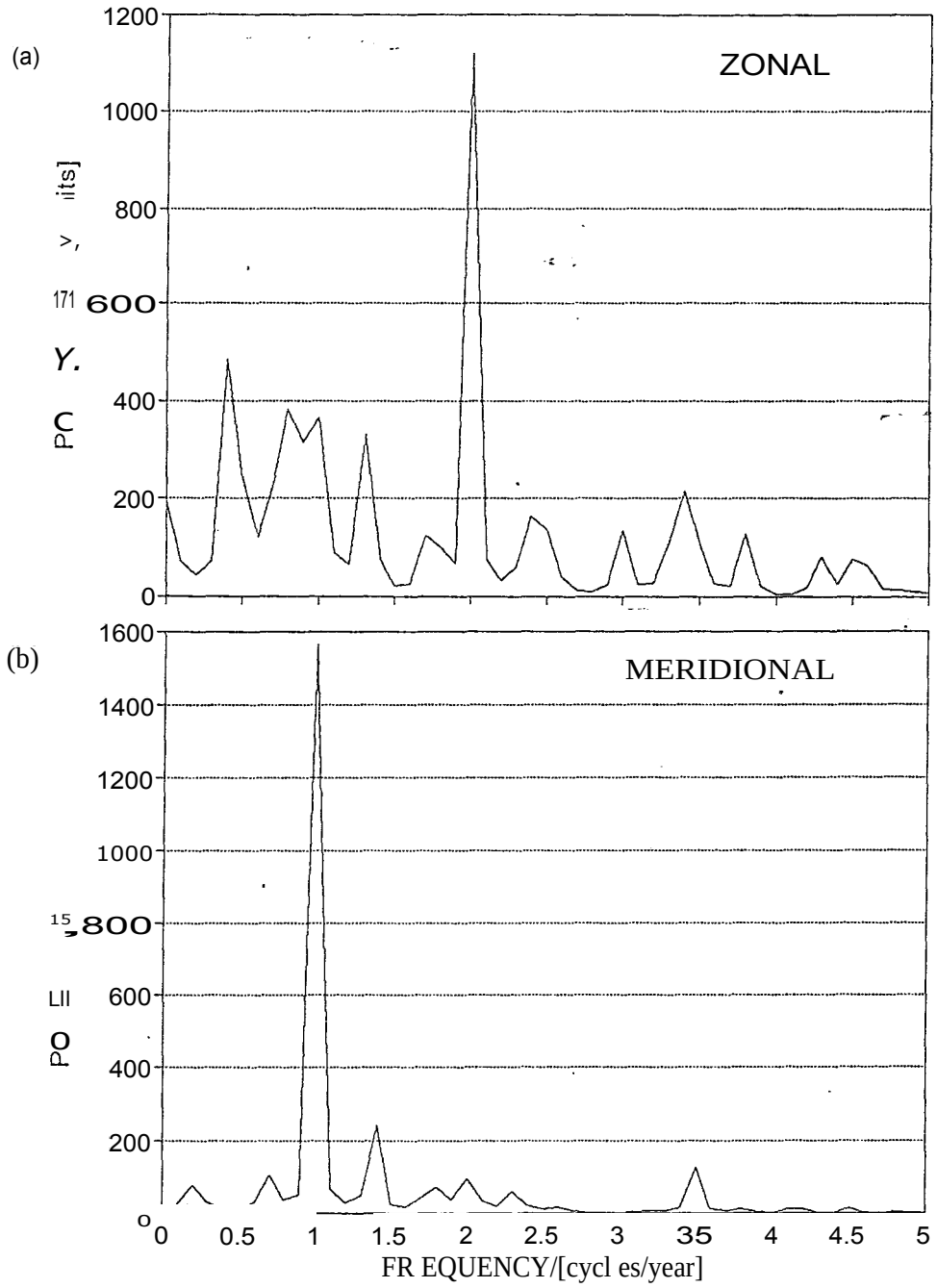

FIGURE 4.11. The seasonal spectra of the monthly averages of the zonal and meridional prevailing winds for the whole seven year (1987 - 1993) period.

Data from Table 4.1 have been used to produce a MEM spectrum of the amplitude sequence covering all the years (1987 -1993). The zonal spectrum (Fig 4.11 (a)) shows spectral components of semi-annual periodicity while the meridional spectrum (Fig. 4.11 (b)) shows annual periodicity. The amplitudes and phases of the spectral components for all the years (1987 - 1993) were obtained by a harmonic analysis and are given in Tables 4.2 and 4.3, respectively. In these tables phases of the zonal and meridional components are the dates of maximum eastward and equatorward flow respectively. I rounded the dates to the nearest day. (However, for 1st January

I took the nearest day to be 1st January even if the number of hours was less than 12 hours to avoid rounding off to January 0 th (December 31st)).

ANNUAL COMP.	YEAR - 1987	1988	1989	1890	1991	1992	1993	MIA
1	7.4	5.4	2.2	7.1	6.9	9.9	2.1	5,9
2	8.4	7.4	12.8	5.1	3.2	8.9	5.7	7.4
3	5.8	0.8	4.6	2.5	6.7	5.6	3.2	4.2
4	4.9	3.2	5.3	1.5	5.0	5.1	-3.1	4,0
5	3.1	4.0	2.1	3.1	2.3	2.6	3.0	2.9
6	3.0	2.4	2.4	2.6	4.1	3.6	0.5	2.7

ANNUAL COMP.	YEAR 1987	1988	1989	1990	1991	1992	1993	MIA
1	9.9	4.9	7.6	3.9	9.3	5.4	- 6.0	6.7
2	2.8	1.6	2.2	2.3	0.7	3.4	5.1	2.6
3	1.3	0.6	1.5	1.6	1.1	1.6	3.9	1.6
4	1.6	1.9	2.3	0.5	1.8	3.1	4.1	2.2
5	1.2	0.7	1.8	0.5	2.3	0.9	2.7	1.4
6	2.1	0.6	1.7	0.1	1.7	1.6	0.2	1.1

TABLE 4.2. The amplitudes of (a) the zonal and (b) meridional seasonal spectral components.

(a)

ANNUAL COMP.	YEAR 1987	1988	1989	1990	1991	1992	1993
1	24/01	06/01	29/10	18/05	23/04	18/07	05/05
2	02/02	02/02	08/02	28/06	30/03	07/01	26/06
3	05/01	08/03	02/01	26/02	10/01	23/04	05/02
4	07/03	24/02	10/01	10/02	03/03	08/02	30/03
5	08/03	01/01	05/01	07/03	25/01	26/02	23/01
6	28/02	31/01	31/01	31/01	01/01	31/01	31/01

(b)

ANNUAL COMP.	YEAR 1987	1988	1989	1990	1991	1992	1993
1	30/01	25/12	25/01	15/02	21/01	17/10	19/02
2	08/02	20/06	04/03	10/03	28/04	28/06	12/01
3	25/03	10/04	19/01	18/03	12/04	06/01	16/01
4	29/03	28/01	30/03	17/03	01/03	01/02	09/01
5	03/03	04/02	13/01	06/03	20/02	14/01	18/01
6	31/01	23/02	31/01	01/01	31/01	31/01	31/01

TABLE 4.3. The phases (play/month) of (a) the zonal and (b) meridional seasonal spectral components.

The MIAs of the amplitudes of the seasonal spectral components (Table 4.2), in agreement with Fig 4.11, show strong semi-annual and annual periodicities for the zonal and meridional winds, respectively. The phase of the meridional annual component is generally in summer (Table 4.3.) whereas that of the zonal semi-annual component shows interannual variability with a tendency to be in summer.

4.4.1.2. COMPARISON AND DISCUSSION

For the whole 7 year period the zonal prevailing wind is eastward except in October 1987. This observation is interesting in the light of results reported by Dartt *et al.* (1983) who found the wind to be eastward except in October for which they got a velocity of -1 ms^{-1} for the altitude range of 90 - 95 km at 35°S. What is striking is that even the magnitudes are approximately equal. Equinoctial circulation is also eastward but it is generally small (< 20 ms^{-1}) which agrees with the findings of Tsuda *et al.* (1987). The AAA of the eastward zonal flow is 16.9 ± 1.7 ms' which is somewhat smaller than the long term average of 20.0 ± 1.1ms at 89-93 km at Adelaide (Dartt *et al.,* 1983).

The meridional prevailing wind is generally weaker than the zonal component in agreement with theory. Dartt *et al.* found an equatorward average of 3.9 ± 0.9 at 89 - 93 km for Adelaide._ This average is small compared to my AAA of 8.9 ± 0.5 ms' . However it is not clear whether Dartt *et al.* performed a simple averaging of both the positive (equatonvard) and negative (poleward) velocities which might explain their small average, or they followed my method of separating the two directional components before averaging. It should be noted that the method of averaging is not so crucial for the zonal wind which is strongly eastward, but is crucial for the meridional component for which the negative and the positive velocities are comparable. The month-to-month meridional wind reversal is similar to Adelaide observations (Stubbs, 1976). The wind reversal occurs between autumn and winter which agrees with Darn *et al.'s* results though in their results the wind is just poleward within this period whereas in my results there is a month-to-month reversal.

The GT the zonal seasonal spectra has a semi-annual variation. On the other hand, Stubbs found an annual variation at 80 - 85 km and a semi-annual variation at 95 - 100 km. The meridional spectrum shows a strong annual component which is similar to Stubb's results at 85 - 90 km. The AAA of the amplitude of the zonal semi-annual component is 7.4 ms 'which is in good agreement with the corresponding value of approximately 8 ms 'reported by Dartt *et al.*. The meridional annual wave amplitude has an AAA of 6.7 m⁻' whilethese authors found approximately 13 ms at 35°S. They also got a meridional semi-annual amplitude of -2 ms 'which compares very well with my AAA of 2.6 ms^{-1}. In agreement with these authors, the phase of the meridional annual and the zonal semi-annual components tend to be at summer (Table 4.3).

4.4.2 THE PREVAILING WIND VECTOR

Tables 4.4 (a) and (b) show the magnitude and the azimuth of the prevailing wind. The corresponding vectors are shown in Fig. 4.12. For most of the months the vector is directed north-east which confirms the dominance of the eastward zonal prevailing wind and the equatorward meridional prevailing wind. The vectors show that these two components become very strong starting from spring to mid-autumn. From late autumn to late winter the prevailing wind vector is sometimes directed south of east due to the reversal of the meridional wind into a southward direction for some of the months during this period.

(a)

	YEAR									
MONTH	1987	1988	1989	1990	1991	1992	1993	MIA	UN(MIA)	SD(MIA)
1	32.1	34.7	29.3	26.5	18.4	19.0	21.2	25.9	2.5	25.1
2	29.1	33.8	13.9	29.7	23.7			26.0	3.5	29.6
3	16.3	18.5	18.2	22.7	19.9		8.6	17.4	2.0	27.8
4	10.4	8.8		20.8	25.6	21.5	2.7	15.0	3.6	59.5
5	7.3	18.2		29.9	22.5	26.0	13.9	19.6	3.4	42.2
6	10.9	10.3	11.9	21.7	8.1	22.9	17.5	14.8	2.2	39.9
7	7.4	24.3	28.3	22.1		44.9		25.4	6.0	53.1
8	27.5	17.5	21.6		25.5	25.2		23.5	1.8	16.9
9	10.8	11.0	17.3		10.1	12.4		12.3	1.3	23.8
10	1.7	14.9			6.5	13.0		9.0	3.0	67.4
11	23.2	18.8			20.9	22.1		21.2	0.9	8.8
12	35.4	24.5	28.8		20.1	21.3	22.7	25.5	2.3	22.5
	17.7	19.6	21.2	24.8	18.3	22.8	14.4	19.8	1.3	17.4

TABLE 4.4 The (a) magnitude and (b) azimuth of the prevailing wind.

MONTH	YEAR						
	1987	1988	1969	1990	1991	1992	1993
1	55.5	65.3	57.2	65.5	57.4	39.5	35.3
2	55.0	77.3	41.1	57.8	44.7		
3	35.4	72.5	42.9	54.7	59.4		35.8
4	63.6	36.5		74.0	71.5	77.0	9.3
5	102.4	95.2		57.0	62.9	74.6	70.0
6	100.9	69.4	114.1	67.3	108.3	76.8	69.9
7	51.5	79.5	101.3	66.0		72.5	
8	96.2	80.5	94.5		87.8	69.5	
9	76.4	72,1	51.0		44.9	55-9	
10	-43.5	48.0			16.9	28.2	
11	54.4	56.4			15.8	63.9	
12	63.7	64.4	72.4		30.5	64.2	21.0

TABLE 4,4 (Continue)

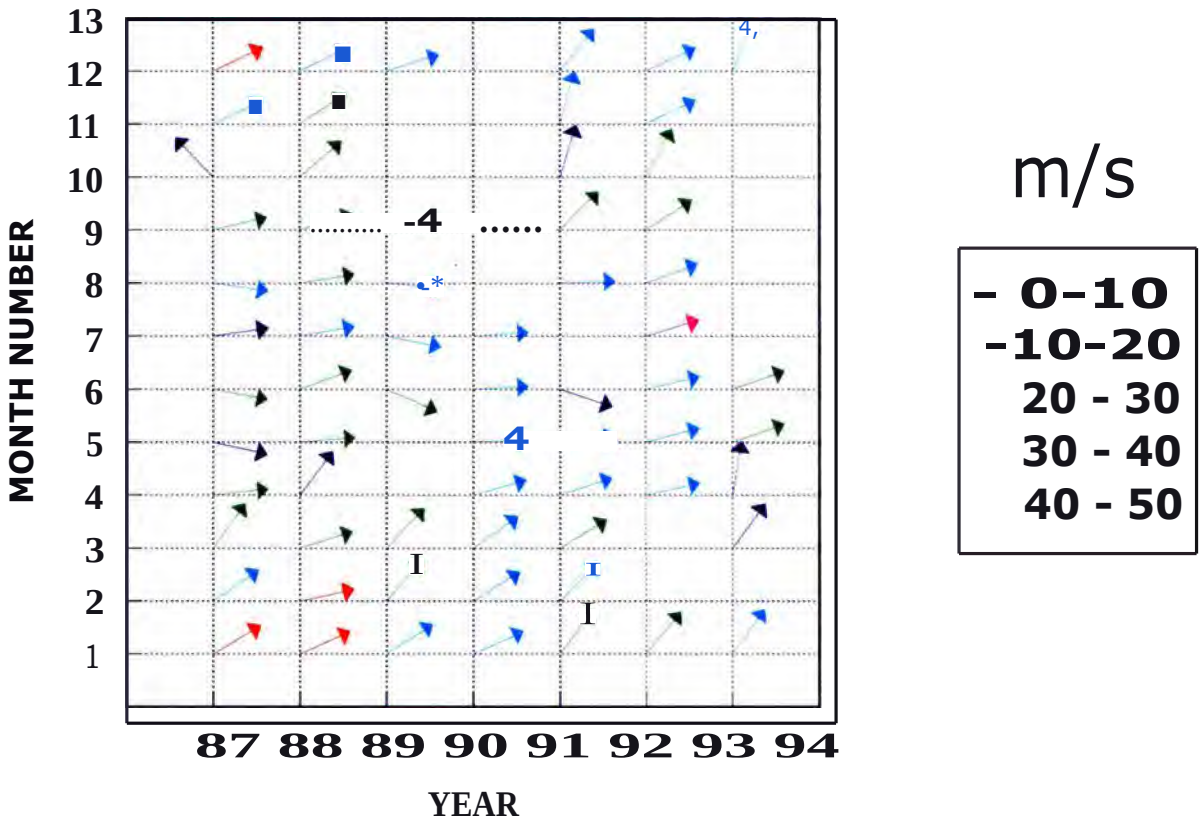

FIGURE 4.12 The prevailing wind vector.

The wind vector between mid-autumn and early spring is approximately eastward for most of the months indicating a stronger eastward zonal component compared to the meridional component. This is in contrast with the wind between mid-spring to early autumn in which the meridional component is comparable to the zonal component. The magnitude of the prevailing wind vector is generally >10 ms' with only eight months having a vectors with magnitudes of 0 - 10 ms^{-1}. For all the years there is month-to-month magnitude variation except 1990 for which the magnitudes are ¯20 - 30 ms' for all the months for which there is data. For most months there is great interannual magnitude variation for a given month. However, September has a consistent magnitude of 10 - 20 ms^{-1}. August and December generally have magnitudes of 20 - 30 ms".

CHAPTER 5

TIDAL DYNAMICS

5.1. INTRODUCTION

As I mentioned in the introductory chapter (Chapter 1), tides are regular dynamical phenomena in the meteor region and are of comparable magnitudes to the prevailing wind in this region. In this chapter I am going to analyse the characteristics of tides above GT. First I will study their monthly climatology in order to delineate their gross structure above GT and then, I will concentrate on their short term variability. Comparison with similar studies elsewhere and theoretical models will also be made.

5.2. THE SEMIDIURNAL TIDE

5.2.1 AMPLITUDE

(a)

	YEAR									
MONTH	1987	1988	1929	1990	1991	1992	1993	MIA	UN (MIA	SD(MIA
1	4.6	5.4	10.0	8.0	2.6	5.0	4.3	5.7	0.9	43.7
2	15.3	2.7	9.4	7.4	8.6			8.7	2.0	52.4
3	21.0	11.1	19.5	9.3	11.3		5.6	13.0	2.5	46.4
4	26.4	24.2		29.9	22.6	26.8	12.5	23.8	2.5	25.4
5	24.7	23.1		29.0	32.0	22.4	19.7	25.1	1.9	18.1
6	18.3	17.1	18.5	19.3	14.7	13.5	11.0	16.0	1.2	19.1
7	13.3	7.1	16.4	14.9		8.3		12.0	1.8	34.1
8	11.1	8.1	13.4		15.6	5.2		10.7	1.9	38.8
9	9.8	8.0	5.5		11.0	4.0		7.6	1.3	38.1
10	11.3	9.2			6.6	8.2		8.8	1.0	22.2
11	5.6	6.1			2.9	7.2		5.5	0.9	33.6
12	6.5	7.6	4.1		2.9	3.7	4.9	4.9	0.7	36.5
AA	14.0	10.8	12.11	16.8	11.9 1	10.4 1	9.7	12.2	0.9	20.1

(b)

	YEAR									
MONTH	1987	1988	1989	19990	1991	1992	1993	MIA	UN(M	SD(MIA
1	7.3	7.9	14.5	15.4	11.3	11.1	12.0	11.4	1.2	26.9
2	12.2	7.5	10.2	7.6	13.6			10.2	1.2	26.8
3	11.1	3.6	12.1	8.5	7.4		6.0	9.0	0.9	25.3
4	14.7	10.0		12.1	9.4	14.5	7.5	11.4	1.2	25.5
5	12.6	8.2		10.9	19.8	9.9	10.3	11.9	1.7	34.5
	6.7	8.2	7.8	5.5	1/0	6.2	6.0	7.5	0.3	29.5
6	11.5	5.5	7.8	8.4		7.6		8.2	1.0	26.2
8	4.3	7.6	7.9		5.2	4.3		5.9	0.8	29.9
9	5.2	3.5	4.5		7.4	3.0		5.7	0.9	33.9
10	9.2	7.3			7.3	7.4		7.8	0.5	12.0
11	4.7	10.4			5.6	11.8		8.1	1.7	43.0
12	5.7	8.9	9.2		4.1	11.6	14.2	8.9	1.5	41.4
AA	8.8	7.8	9.31	9.8	9.4	9.2	9.3	9.1	0.2	7.0

TABLE 5.1. The amplitudes of the (a) zonal and (b) meridional components of the semidiurnal tide.

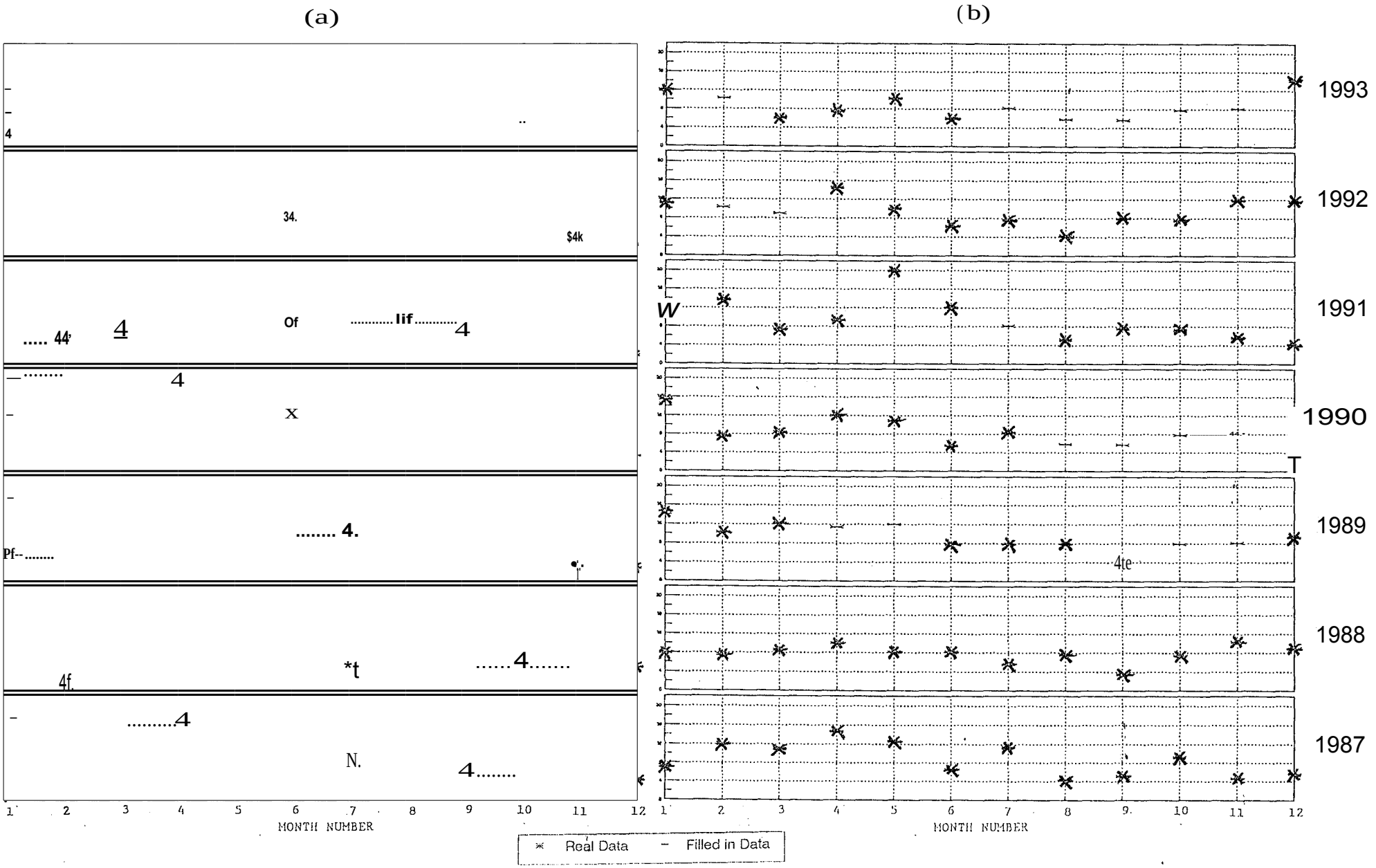

FIGURE 5.1 The monthly amplitudes of the (a) zonal ($y_0 = 0$; vs = 8 ms^{-1} / division) and (b) meridional ($y_0 = 0$; vs = 4 ms^{-1} / division) components of the semidiurnal tide.

Tables 5.1 (a) and (b) show respectively, the zonal and meridional monthly amplitudes for 1987 to 1993. These values are graphically illustrated in corresponding figures (Fig. 5.1 (a) and (b)). From these figures there are a number of observable features and these are discussed below.

The zonal amplitudes are larger (MIAs >10 ms^{-1}) in autumn and winter with a maximum in April/May. Spring and summer have smaller (MIAs <9 ms ') amplitudes. The annual averages are - 10 - 17 $ms^{-'}$ and have an AAA of 12.2 ± 0.9 $ms^{-'}$. The meridional amplitudes (Fig. 5.1 (b)) do not show a systematic annual behaviour but there are a few noticeable features. The amplitudes generally make gentle swings about a mean of - 8 - 9 ms -' (see annual averages). Except for the large (19.8 $ms^{-'}$) amplitude of May 1991, the meridional amplitudes are < 16 ms The meridional amplitudes are smaller than the zonal amplitudes as shown by their MA of 9.1 ± 0.2 ms 'compared to 12.2 ± 0.9 Ins' for the latter.

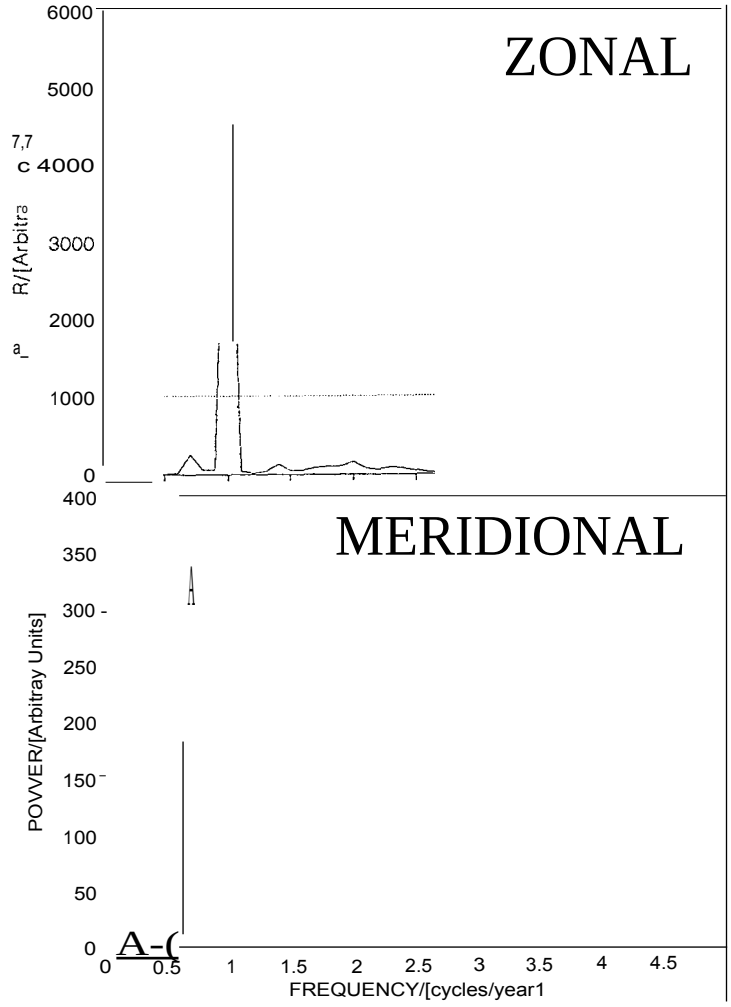

FIGURE 5.2. The seasonal spectra for the zonal and meridional semidiurnal tidal amplitudes

Fig. 5.2 shows the MEM seasonal power spectra for the monthly amplitudes for the whole seven year (1987 - 1993) period . The zonal amplitudes show a dominant annual periodicity. The meridional amplitudes, on the other hand, show unexpected periodicities of approximately one and a half year. This unexpected periodicity cannot be explained,

Interannually, there is great year-to-year variability especially for the zonal component as shown by the respective standard deviations from the MIAs and the AAAs. Genefally, the zonal component is more variable in summer whereas the meridional component does not show a clear seasonal trend but are more variable in November and December.

5.2.2 PHASE.

(a)

	YEAR									
MONTH	1987	1988	1989	1990	1991	1992	19931	MIA 1	UN(MIA,	SD(MIAJ
1	7.7	10.5	6.3	6.7	6.1	7.6	6.7	7.4	0.6	20.6
2	10.5	10.0	73	7.3	9.7			9.0	0.6	15.9
3	10.0	9.0	10.4	9.5	10.6		9.6	9.8	0.2	5.9
4	10.2	9.9		9.9	10.1	10.3	10.7	10.2	0.1	3.0
5	10.2	10.0		10.2	10.0	10.4	10.5	10.2	0.1	2.2
6	10.9	10.8	10.5	10.7	10.4	10.8	11.3	10.3	0.1	2.7
7	11.6	10.9	11.5	10.7		11.0		11.1	0.2	3.6
8	11.8	12.4	11.7		10.9	118		11.9	0.3	6.1
9	11.1	11.1	10.2		10.5	11.2		10.8	0.2	4.2
10	10.1	9.9			9.2	10.2		9.9	0.2	4.9
11	11.0	10.1			9.7	8.2		9.8	0.6	11.8
12	11.4	5.2	7.0		6.8	7.0	7.3	7.5	0.9	27.8
AA	10.5	10.0	9.41	9.3	9.51	10.0	9.4	9.7	0.2	4.8

(b)

	YEAR									
MONTH	1987	1983	1989	1990 1	1991	1992	1993	MIA	UN (MIA1	SD(MIA
1	9.9	10.0	8.7	9.4	10.0	9.9	9.3	9.6	0.2	5.0
2	12.4	9.2	10.1	10.5	10.7			10.6	0.5	11.2
3	11.9	11.6	1/3	11.2	11.6		11.9	11.8	0.2	3.1
4	12.4	12.0		11.5	12.7	12.4	11.7	12.1	0.2	4.0
5	117	12.4		12.4	12.5	115	13.0	12.6	0.1	1.8
6	14.1	13.8	13.8	13.6	14.0	13.6	14.8	14.0	0.2	3.1
7	14.9	14.0	15.1	14.5		13.9		14.5	0.2	3.6
8	15.4	14.5	14.1		12.9	14.8		14.4	0.4	6.7
9	11.8	13.4	10.4		12.0	11.0		11.7	0.5	9.8
10	11.6	11.3			10.1	11.3		11.1	0.3	6.0
11	8.5	9.9			10.4	9.8		9.6	0.4	8.6
12	10.5	8.7	8.8		8.1	8.5	9.1	9.0	0.3	9.1
AA	12.2	11.71	11.7	11.9	11.41	11.8	11.6J	11.7	0.1	21

TABLE 5.2. The phases of the (a) zonal and (b) meridional components of the semidiurnal tide.

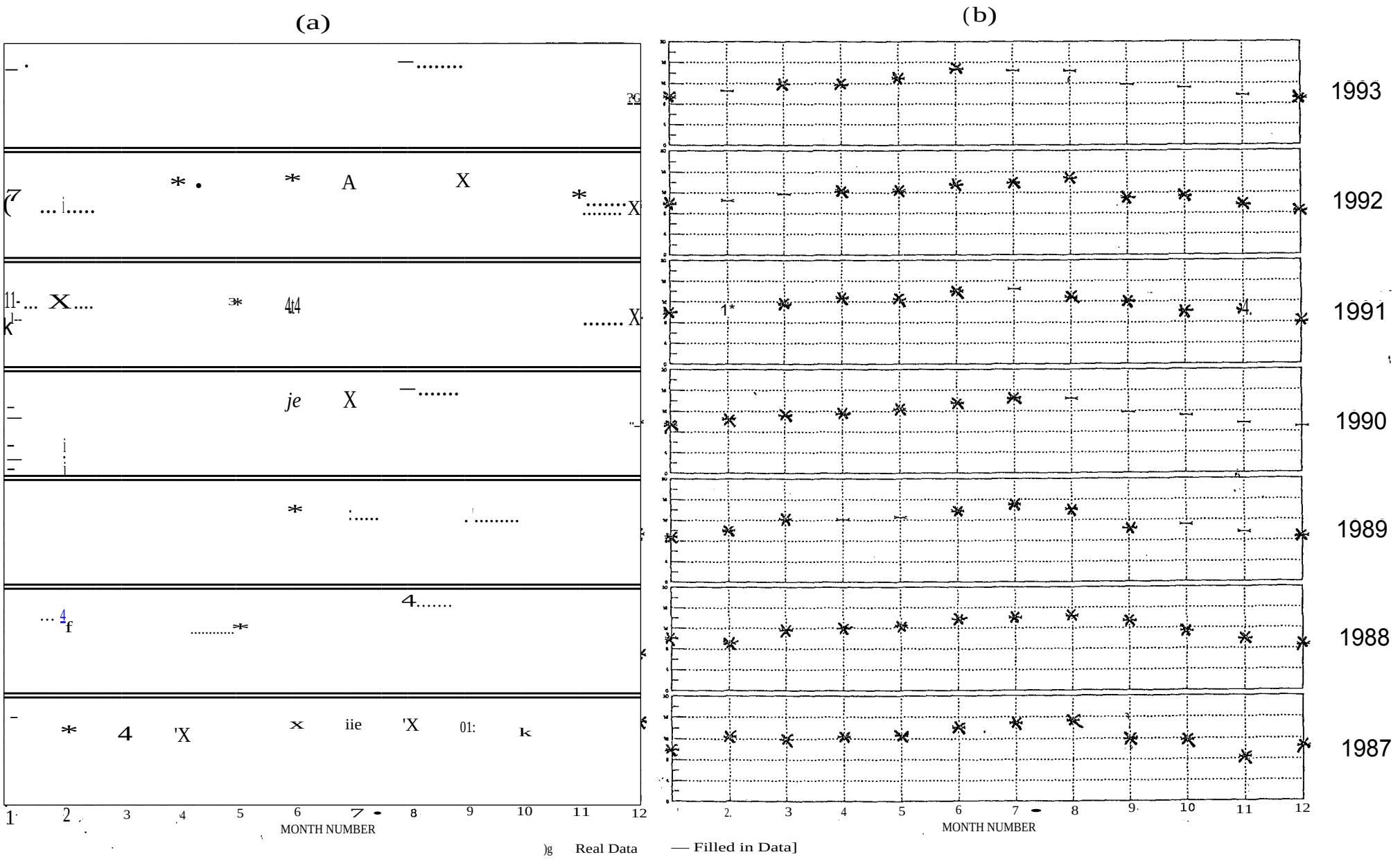

FIGURE 5.3 The monthly phases of the (a) zonal ($y_o = 0$; vs = 3 h / division) and (b) meridional ($y_o = 0$; vs = 4 h/ division) components of the semidiurnal tide.

Tables 5.2 (a) and (b) show the monthly zonal and meridional phases respectively. Fig. 5.3 (a) and (b) are the corresponding graphical presentations. The zonal and the meridional phases are the local times at which the tidal components reach their maxima in the eastward and northward directions respectively. Important features froin these figures and tables are given below.

	YEAR.								
MONTH	1987	1988	1989	1990	1991	1992	1993	- MIA	UN(MLA,
1	2.2	-0.5	2.4	2.7	3.9	2.3	2.61	2.2	0.5
2	2.0	-0.9	2.4	3.2	1.0			1.5	0.7
3	1.9	2.6	1.9	1.7	1.0		13	1.9	0.2
4	2.2	2.0		1.6	2.6	11	0.9	1.9	0.2
5	2.5	2.5		2.2	2.6	10	2.5	2.4	0.1
6	3.2	2.9	3.3	2.9	3.5	2.8	3.5	3.2	0.1
7	3.3	3.2	3.6	3.7		2.9		3.3	0.1
8	3.6	11	2.5		1.9	10		2.4	0.3
9	0.8	13	0.2		1.5	-0.2		0.9	0.4
10	1.5	1.4			1.0	1.1		1.2	0.1
11	-2.5	-0.3			0.7	1.6		-0.1	0.9
12	-1.0	3.5	1.8		1.3	1.5	1.8	1.5	0.6
AA	1.6	1.7	2.3	2.6	1.9	1.8	2.3	2.0	0.1

TABLE 5.3 The phase difference of the semidiumal tide. Positive for zonal component leading.

The semidiurnal phases at GT are close to 0.0 or 12.0 h and thus could give a false 'phase bimodality' (to be described in Section 5.2.4) as shown by Fig 2 in Appendix B. To avoid this, 12 hours were added to phases immediately after 0.0 h resulting in some values >12.0 h. Zonal and meridional phases have annual averages of 9.0 - 11.0 h and - 11.0 - 12.0 h with corresponding AAAs of 9.7 ± 0.2 h and 11.7 ± 0.1 h.

The meridional phases are generally consistent from year to year as shown by the standard deviations of <12% from the MIAs, whereas the zonal phases show great variability especially in summer (SD(MIA)s as high as -28%). The annual phase differences between the zonal and the meridional tides (Table 5.3) have an AAA of 2.0 ± 0.1 h. Fig. 5.4 shows the frequency distribution of rounded-off phase differences. The frequency of the occurrence of a -2 h phase difference is higher for most of the years with a -3 h phase difference next most frequent. Fig. 5.5 shows the distribution for the whole 7 year period. It is interesting to note that there were months in November and summer for 1987 and 1988 when the meridional component is leading.

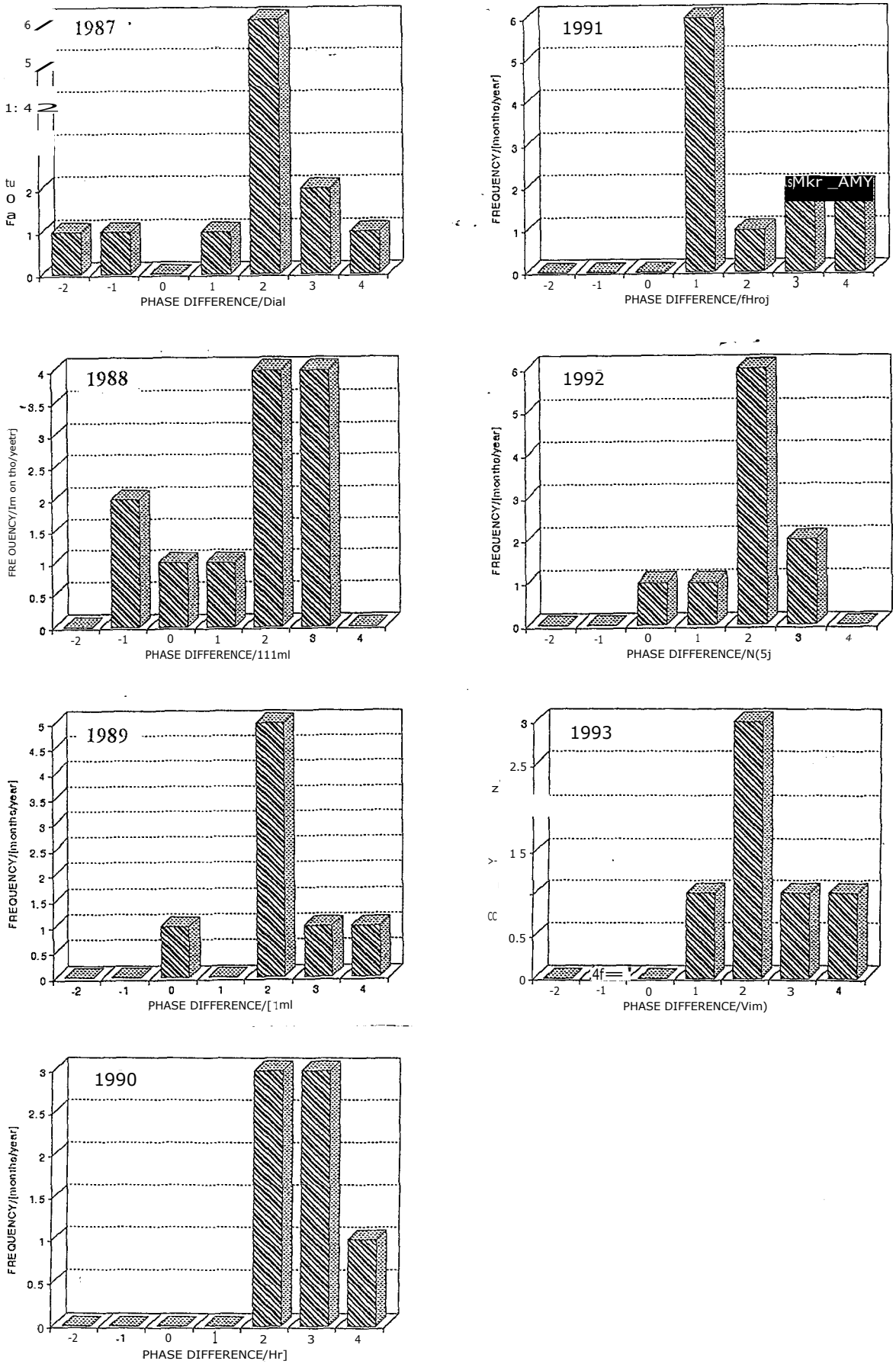

FIGURE 5.4 The annual frequency distribution of the phase differences of the semidiurnal tide.

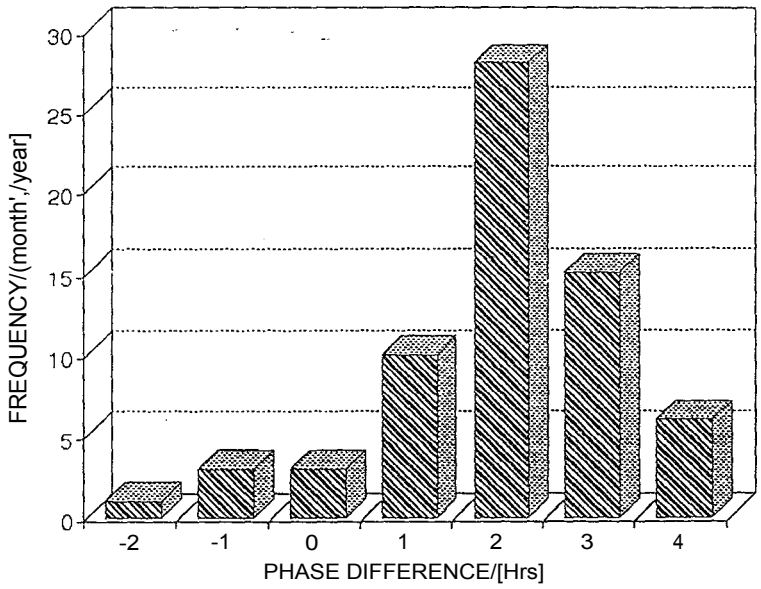

FIGURE 5.5 The frequency distribution of the phase differences of the semidiurnal tide for the whole seven year (1987-1993) period.

5.2.3 OTHER GRAPHICAL REPRESENTATIONS

The above information on semidiurnal tides may usefully be represented in a number of ways which highlight different aspects (Fig. 5.6 - 5.10)

Monthly amplitudes and phases for 1987 and 1988 are shown in the foiin of harmonic dials in Fig. 5.6. The distance of each point on the dial represents the amplitude of the component with the corresponding phase given by the local time on the circumference. The amplitude and phase behavior already discussed in Sections 5.2.1 and 5.2.2 is evident in this figure and also there are clear seasonal zones. These zones are generally consistent between the two years with minor differences as shown by the demarcations. There is, on average, a -3 h phase difference between the zonal and the meridional component. This is clearly seen by the proximity of the corresponding points (months) when the zonal dials are rotated through 3 h (90° clockwise).

The mean monthly behavior of the semidiurnal velocity vector, obtained by the combined amplitudes and phases of the zonal and meridional components, is summarized in Table 5.4 and illustrated on the polar plots of Fig. 5.7 and 5.8 for 1987 and 1988 respectively. The line from

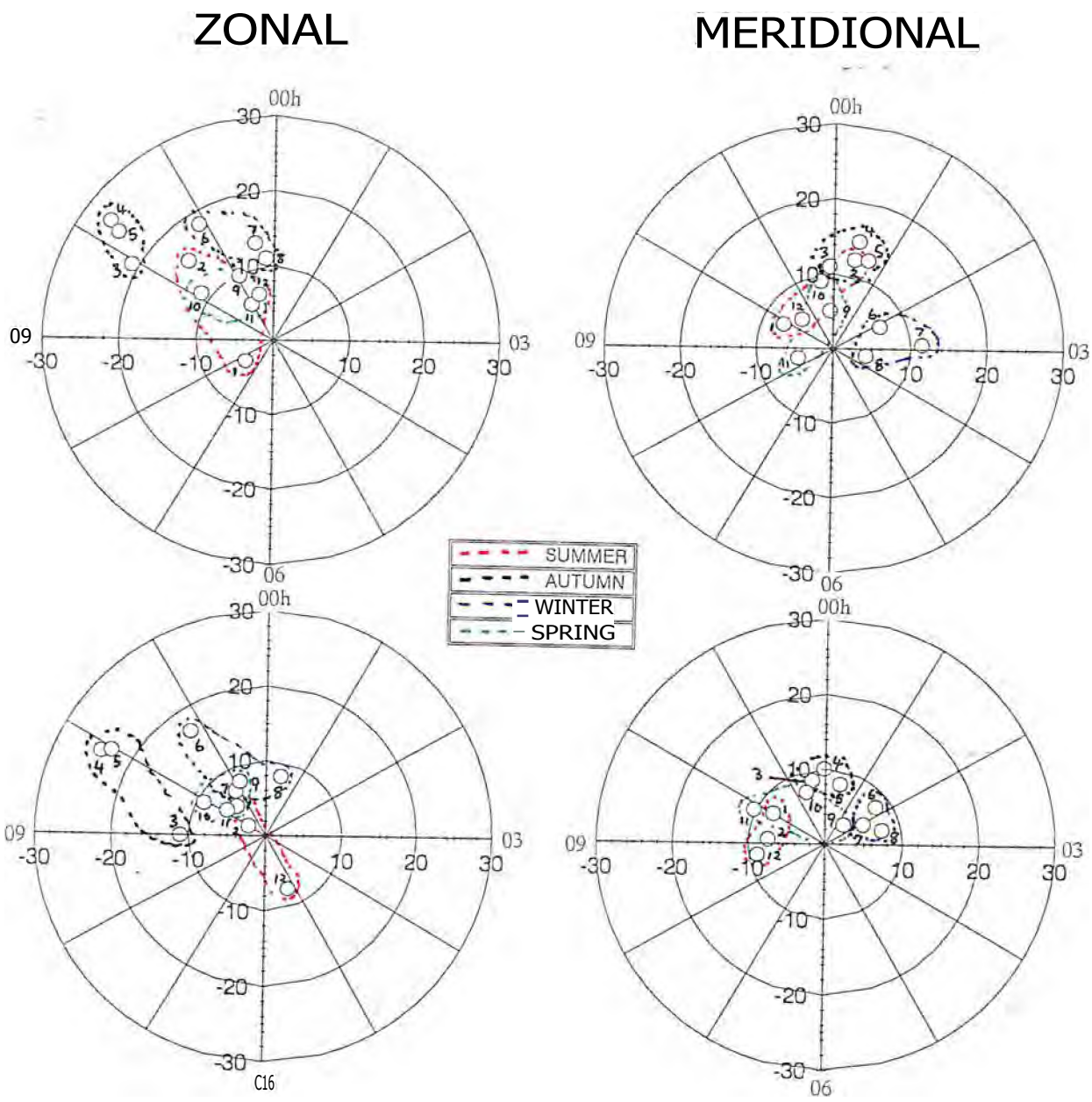

FIGURE 5.6 The harmonic dials of 1987 (top two) and 1988 (bottom two) for the semidiurna! tide. The numbers next to the points indicate the month numbers. Units on the axes are in m/s.

(a)

	YEAR									
MONTH	1987	1988	1989	1990	1991	1992	1993	MIA	UN(MIA)	SD(MIA)
1	7.6	9.4	15.0	15.3	11.2	11.3	11.9	11.7	1.1	23.9
2	17.2	7.8	11.2	7.9	15.7			12.0	1.9	36.4
3	21.7	11.4	20.7	11.2	12.9		6.8	14.1	2.4	41.6
4	27.3	24.4		30.7	22.4	27.8	14.1	24.5	2.4	23.8
5	24.9	22.9		29.2	32.1	23.0	19.9	25.3	1.8	17.8
6	18.0	16.9	18.5	19.2	15.4	13.3	11.2	16.1	1.1	18.4
7	13.6	7.2	16.6	15.3		8.3		12.2	1.9	34.6
8	11.0	9.5	13.6		15.7	5.8		11.1	1.7	34.1
9	10.9	8.1	7.0		12.3	8.9		9.4	1.0	22.7
10	13.5	11.0			9.5	10.5		11.1	0.8	14.9
11	5.9	11.9			6.2	12.8		9.2	1.8	39.8
12	8.3	9.3	9.4		4.7	11.8	14.5	9.7	1.3	34.0
AA	15.0	12.5	14.0	18.4	14.4	13.3	13.1	14.4	0.7	13.6

(b)

	YEAR									
MONTH	1987	1988	1989	1990	1991	1992	1993	MIA	UN(MIA)	SD(MIA)
1	3.8	4.5	2.3	3.0	3.8	3.8	3.0	3.4	0.3	21.3
2	5.3	3.0	3.0	6.0	4.5			4.4	0.6	30.8
3	4.5	3.8	4.5	4.5	10.5		5.3	5.5	1.0	45.4
4	4.5	3.8		9.8	10.5	4.5	11.3	7.4	1.4	47.0
5	4,5	3.8		4.5	4.5	4.5	4.5	4.4	0.1	7.0
6	5.3	4.5	4.5	10.5	3.8	5.3	5.3	5.6	0.8	40.3
7	5.3	4.5	5.3	4.5		5.3		5.0	0.2	8.3
8	6.0	1.5	6.0		5.3	7.5		5.3	1.0	42.9
9	5.3	11.3	4.5		5.3	5.3		6.3	1.2	44.2
10	10.5	10.5			3.8	10.5		8.8	1.7	- 38.3
11	4.5	3.8			4.5	3.8		4.1	0.2	10.5
12	5.3	3.8	8.3		1.5	8.3	9.0	6.0	1.2	50.0
AA	5:4	4.9	4.8	6.1	5.3	5.9	6.4	5.5	0.2	11.1

(c)

	YEAR									
MONTH	1987	1988	1989	1990	1991	1992	1993	MIA	UN(MI A)	SD(MIA)
1	72.7	54.5	69.7	79.6	94.6	78.7	82.4	76.0	4.7	16.3
2	35.6	73.0	49.9	136.7	59.6			71.0	17.5	55.3
3	22.3	25.5	20.3 "	44.7	28.9		56.9	33.1	5.9	43.9
4	16.8	9.6		13.9	9.4	16.3	31.3	16.2	3.3	49.7
5	12.2	3.4		12.0	17.5	13.0	8.1	11.0	2.0	43.6
6	1.6	176.5	176.3	179.3	152.8	8.8	170.9	123.7	30.8	65.9
7	163.6	167.5	168.7	164.8		9,9		134.9	31.3	51.8
8	174.9	43.5	14.8		12.8	34.3		56.1	30.3	120.8
9	26.9	10.8	39.5		34.2	63.3		34.9	8.6	55.0
10	34.6	37.0			48.6	39.8		40.0	3.1	15.3
11	22.9	60.0			64.3	67.0		53.5	10.3	38.5
12	38.7	125.7	69.8		56.0	75.5	77.5	73.9	11.9	39.6

TABLE 5.4 The (a) maximum velocity vector, (b) its time of occurrence and (c) its direction (anticlockwise relative to east) for the semidiurnal tide.

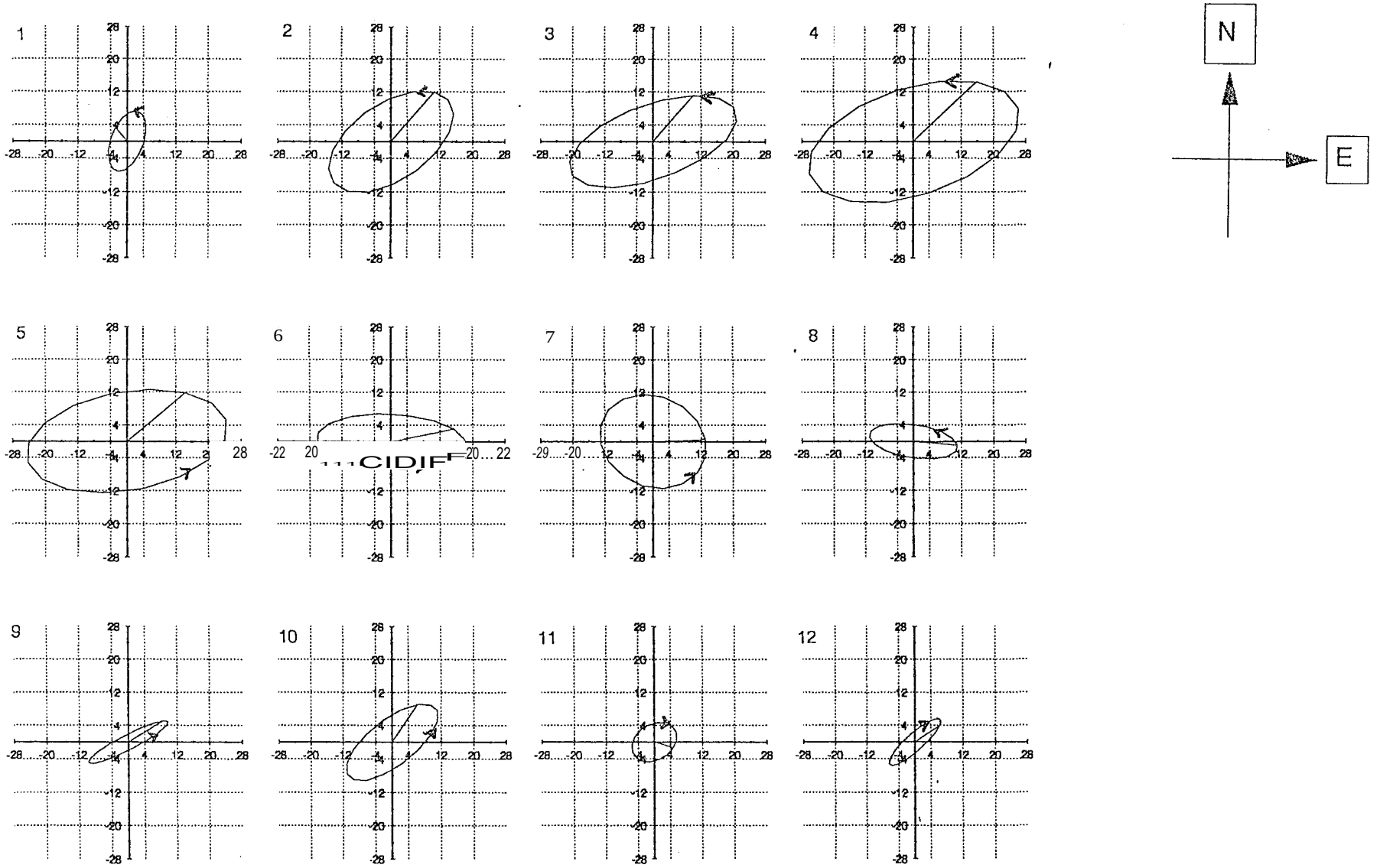

FIGURE 5.7 The monthly polar plots of the semidiurnal tide for 1987. The month number is written on the top left hand corner of the corresponding polar plot. Units for both axes are m/s.

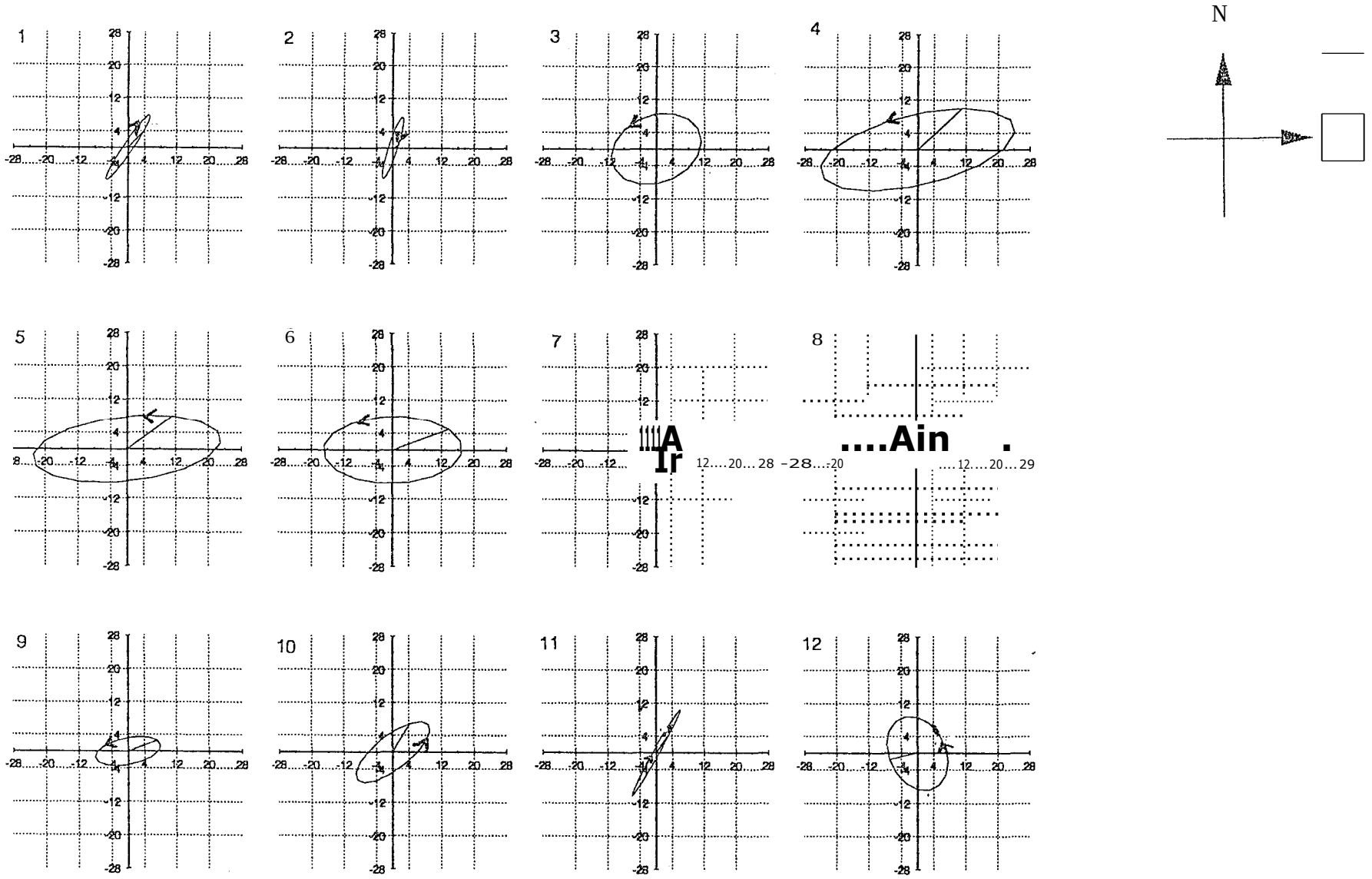

FIGURE 5.8 The monthly polar plots of the semidiurnal tide for 1988. The month number is written on the top left hand corner of the corresponding polar plot. Units for both axes are m/s.

(0, 0) to the ellipse represents the wind vector at 0.0 h. The vector is elliptically polarized and, as expected, is rotating anticlockwise with a few exceptions generally occurring in summer and late spring.

The maximum velocity is largest in autumn and has an AAA of 14.4 = 0.7 ms ^{1}. The AAA of its times of occurrences is 5.5 ± 0.2 h (and 11.6 ± 0.2 h), and the vectors are generally directed northeast (or equivalently southwest) with a few occasions (which are generally in winter) when directed northwest (southeast).

Fig. 5.9 shows the surface plots of the monthly time evolution of the zonal component of the semidiumal tide for (A.1) 1987 and (13.1) 1988, with the corresponding contours shown in (A.2) and (B.2). Fig. 5.10 is the same as Fig. 5.9 but for the meridional component. There are a number of observable features:

1. The zonal surface plots and contours are similar for the two years except the broadened peaks and troughs in 1987. The meridional component, on the other hand, shows greater variability between 1987 and 1988 (cf general comment on interannual variability for all the years as discussed in Section 5.2.1).

2. The peaks on the contours (Fig. 5.9, (A.2) and (B.2)) represent the largest amplitudes for a given year. They are centered on April/May consistent with Fig. 5.1 (a). The meridional peaks (Fig. 5.10, (A.2) and (B.2)) are centered on April (cf. Fig. 5.1(b)). While the zonal peaks are >20 ms^{-1} for both years, there is no consistency on meridional peaks with 1988 peak being -33% smaller than the 1987 ones. The meridional component has secondary peaks in July and October for 1987 and August and November 1988 which shows a month shift.

3. The phases (which we will recall are the local times of maximum of the components eastward and northward) show a systematic behaviour for both components and years. Generally the phases, in particular those of the meridional component, show a progression to later times of maximum as the year progresses, until around August when a negative phase gradient begins.

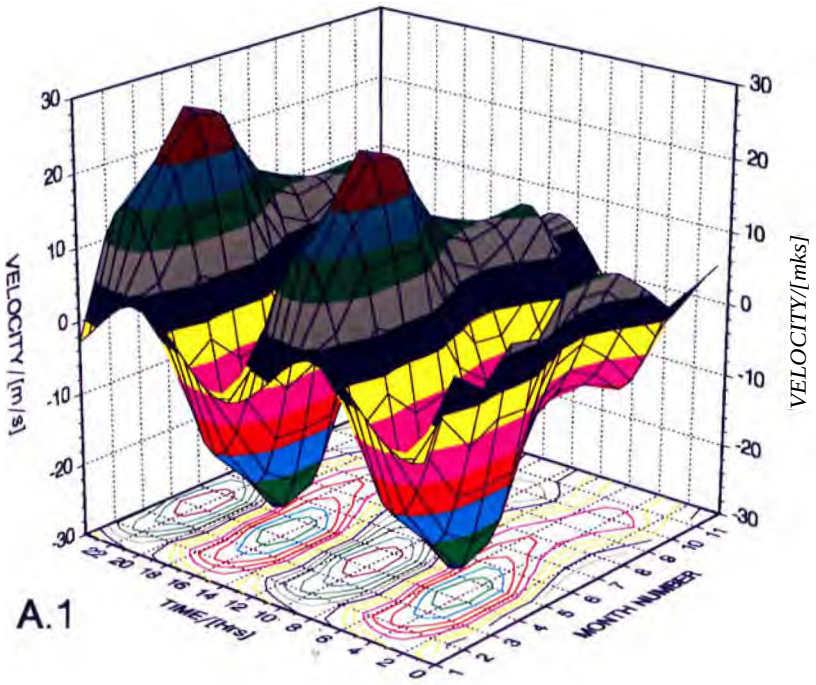

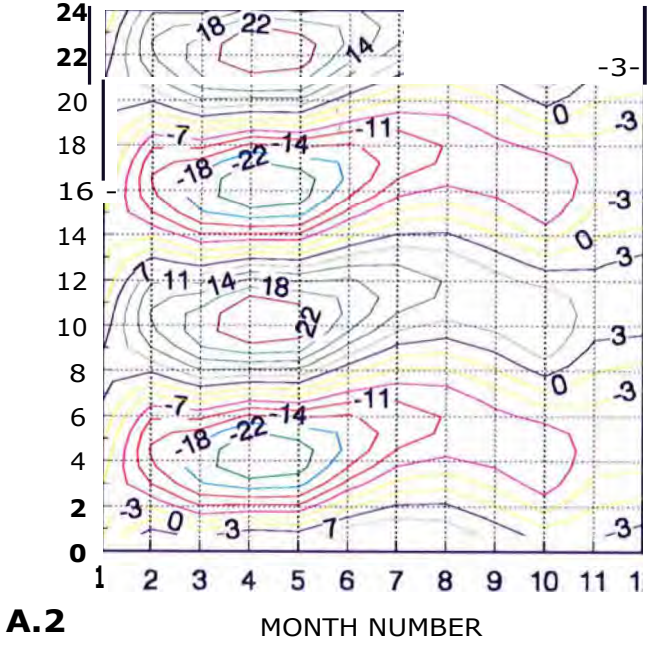

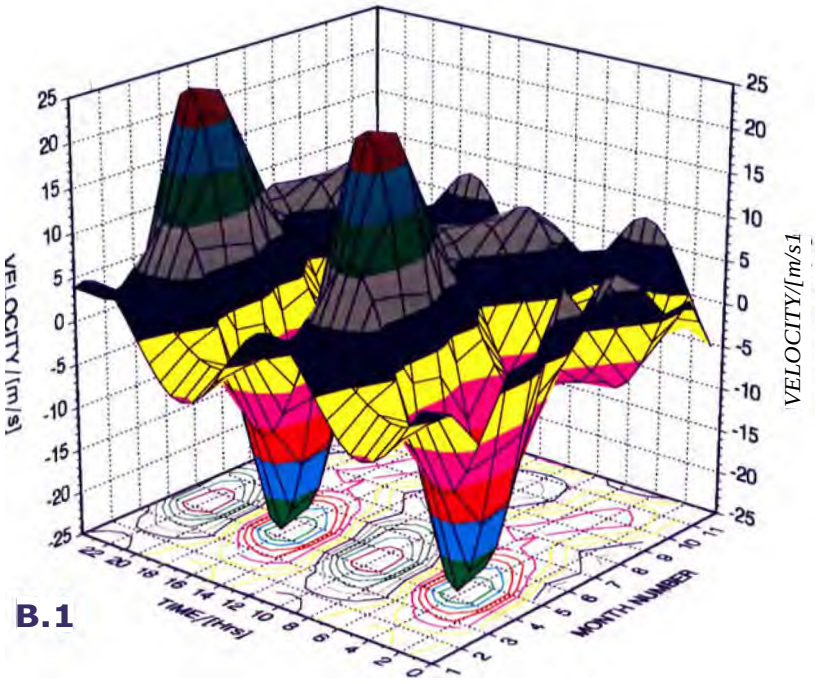

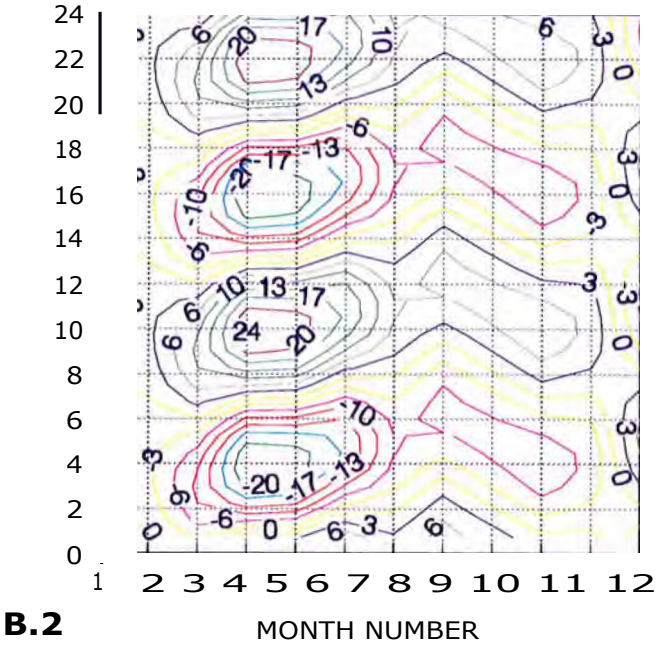

FIGURE 5.9
Surface plots ((A.1) and (B.1)) and corresponding contour plots ((A.2) and (B.2)) for the zonal component of the semidiumal tide for 1987 (top two) and 1988 (bottom two).

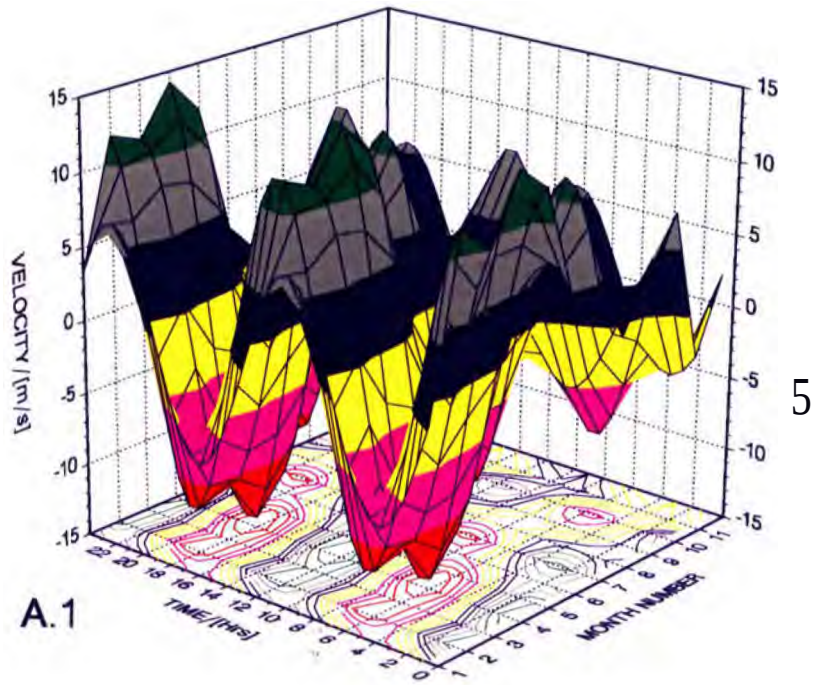

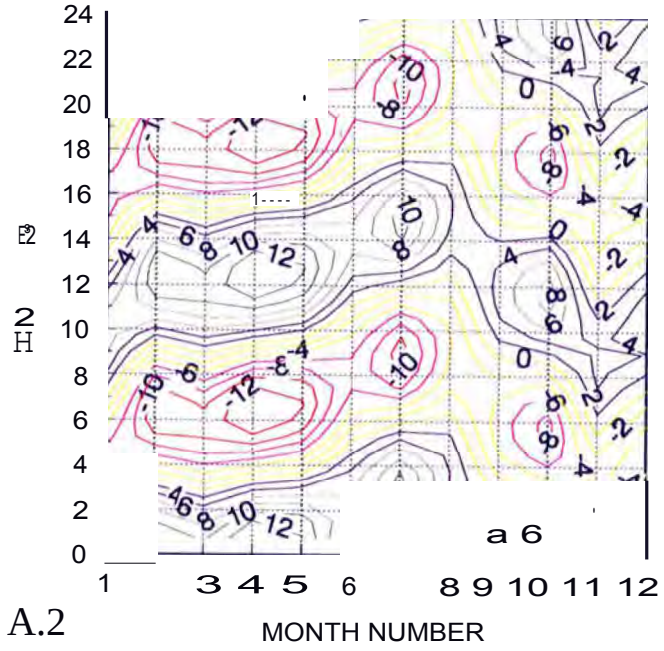

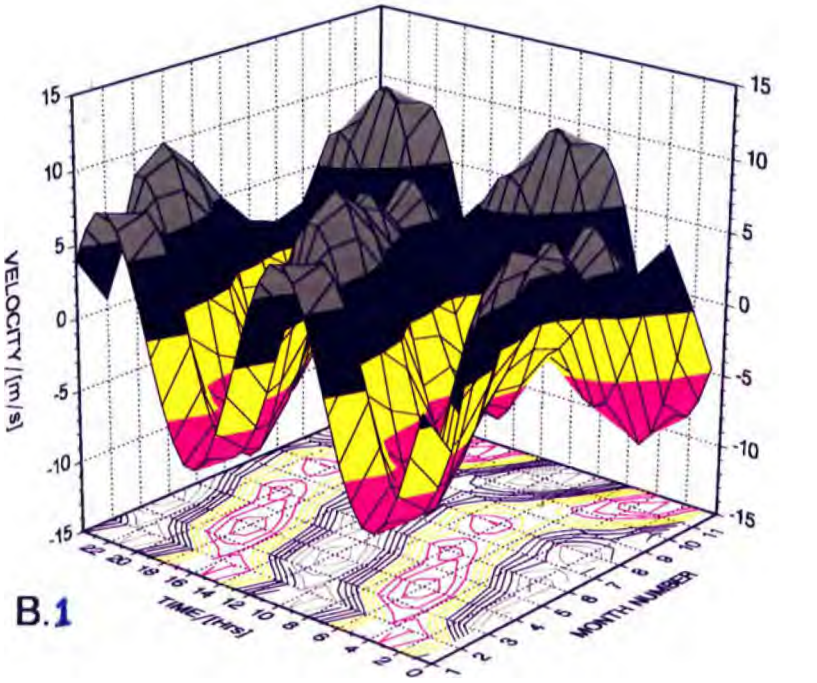

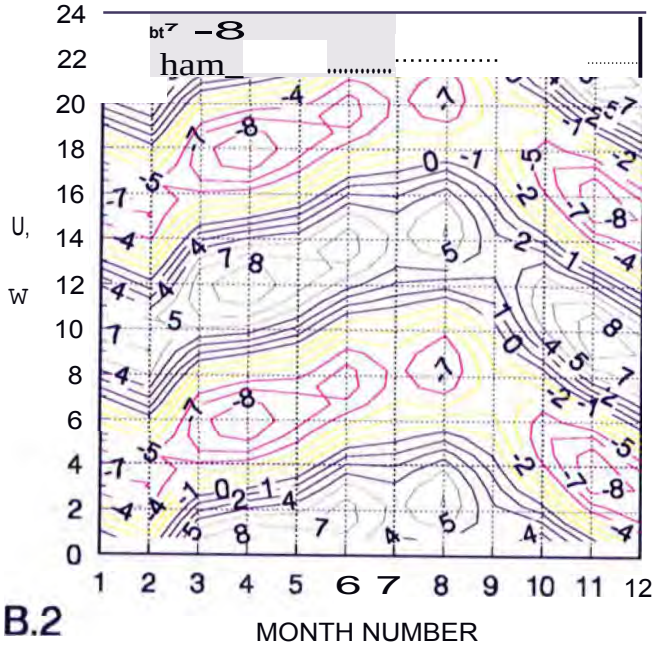

FIGURE 5.10
Surface plots ((A.1) and (B.1)) and corresponding contour plots ((A.2) and (B.2)) for the meridional component of the sem idiurnal tide for 1987 (top two) and 1988 (bottom two).

5.2.4. COMPARISONS AND DISCUSSION

A. AMPLITUDE

The tidal oscillations above GT are generally consistent with observations made at other midlatitude sites and theoretical models.

In agreement with observations at Kyoto (35°N, 136°E) (Vincent *et al.,* 1988, hereafter VTK), the amplitudes of the zonal semidiurnal tide at GT reach their maximum (- 13 - 32 ms^{-1}) in autumn. These maxima are possibly due to the approximately doubled excitation of the (2, 4) and (2, 6) modes during the equinoxes (Forbes and Vial, 1989; Forbes 1982b). This is more important considering the dominance of the (2, 4) mode between 70 and 90 (Forbes, 1982b). However, there are no distinct maxima in spring except for a small hump in 1992. Such behavior might have to do with the seasonal antisymmetry in the phase and amplitude of the (2, 4) temperature mode characterized by a strong maximum in March and a secondary one in September (Forbes and Vial, 1989). Another feature observed at GT is that the maxima are more distinct for the zonal component than for the meridional one. This might be due to two factors:

(a) at the GT latitude (33°) zonal velocity expansion is larger than the meridional one (see Fig.1.3);

(b) at the same latitude the two enhanced modes (i.e. (2, 4) and (2, 6) interfere more with each other for the meridional than for the zonal component.

However, my results do not agree with observations at Adelaide (VTK). These authors found the maxima in summer and early winter. Since Adelaide is on almost the same latitude as GT the tidal behaviour was expected to be similar between the two sites. One possible cause for this difference is the longitudinal variation of ozone and water vapour distribution and therefore the variation of the propagation conditions.

For the solstices, semidiumal amplitude behaviour in the SH sites like Adelaide and Christchurch is characterized by large amplitudes in summer and small amplitudes in winter (Fraser *et al.*, 1989), but this is generally not true at GT. I do not know what could be the cause for this, except the longitudinal variation of the propagation condition as suggested above. In Fig. 5.11, I have compared my results with Forbes' (1982 b) model. The GT results are the averages of the solstice MIAs. The figure shows a discrepancy between my results and the model except for the winter amplitudes and summer phases.

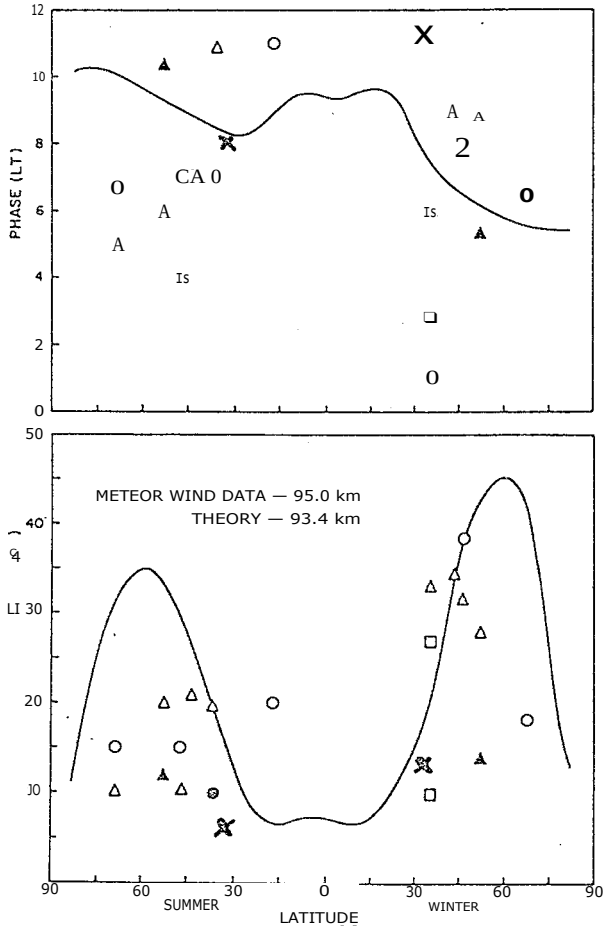

FIGURE 5.11. Comparison of model results (after Forbes, 1982b) and GT results (crosses) for the semidiumal zonal velocity in the meteor region - see this paper for details about the other observations indicated . See Forbes for details of the other observations on the figures.

B. PHASE AND PHASE DIFFERENCE

A number semidiumal phase observations (e.g. VTK) and model results (Forbes and Vial, 1989) show a bimodal feature with summer-like and the winter-like phase modes separated by quick

equinoctial transitions. This behavior is not evident at GT though there is a tendency for the phases to increase by - 1 - 3 h during the equinoxes and winter. There are a number of possible causes for this discrepancy. As pointed out by Forbes (1982b), the semidiurnal tide in the meteor region consists of at least four modes (namely (2, 2), (2, 3), (2, 4) and (2, 5)) whose relative phases and amplitudes are height and latitude dependent. Small (1 - 2 h) relative phose shifts between these modes can significantly alter the phase of the total semidiumal structure with height and latitude from day to day (Forbes, 1984). Therefore averaging over a wide (-_20 km) height range results in an increase or decrease of the phase, depending on the relative phases of the superimposed modes (VT), and this might result in the masking of the phase bimodality.

Secondly, this behavior seems to be affected by propagation conditions as it is reported to coincide with local and global zonal wind reversal (Manson *el ul.* , 1989) and is also suggested to be possibly due to hemispheric/seasonal asymmetry in ozone (SS). According to SS, the asymmetric distribution of ozone results in the generation of asymmetric modes and therefore the structural change of the semidiumal tide. These authors believe that a sharp change of this asymmetry near the equinoxes accompanied by a short duration quasisymmetry might contribute to the equinoctial transitions and phase bimodality. Therefore, it is possible that the absence of the bimodality is due the local behavior of zonal wind and ozone distribution at GT.

As shown in Section 5.2.2, my phase differences between the zonal and the meridional tides are generally -2 h with a -3 h phase approximately half as frequent. Deviations from the expected 3 h phase difference can be attributed to averaging over a height range of -20 km, which as discussed above results in the alteration the tidal phase structure.

C. TIDAL WIND VECTOR

Generally the semidiurnal wind vectors, in agreement with Adelaide results (VTK), rotate anticlockwise, though on average it is elliptically polarized as opposed to the circular polarization at Adelaide. There are some similarities in the behaviour of the semidiurnal wind vector at GT (33°19'S, 26°30'E) and Yambol (42.5°N, 26.6°E; almost conjugate with GT) (Pancheva and

Mukhtarov, 1994): (i) the peak of the maximum velocities is in autumn; (ii) the average maximum velocity at GT has an AAA of 14.4 ± 0.7 ms^{-1}, and at Yambol the average is 13.46 ms^{-1} (18 months average); (iii) local time of maximum velocity at GT has an AAA of 5.5 ± 0.2 h (and 11.6 ± 0.2 h), and at Yambol the 18 months average is 6.03 h; (iv) the polarization is predominantly elliptical. The maximum velocity is predominantly directed northeast (or equivalently southwest) at both sites though symmetry about the equator would lead us to expect one of them to be predominantly southeast(northwest).

5.3 THE DIURNAL TIDE

5.3.1 AMPLITUDE

(a)

	YEAR									
MONTH	1987	1988	1989	1990	1991	1992	1993	MIA	UN(MIA	SD(MIA)
1	16.1	25.1	20.8	17.4	12.7	15.5	14.7	17.5	1.6	23.9
2	12.3	2.5.7	14.7	9.0	21.8			16.8	3.1	40.7
3	21.1	17.7	25.5	18.7	22.4		16.9	20.4	1.3	16.1
4	15.7	27.4		18.0	18.5	19.8	19.5	19.8	1.6	20.2
5	15.2	13.2		6.9	14.2	16.1	13.0	13.1	1.3	25.0
6	15.0	11.9	12.5	8.5	18.0	12.5	10.6	12.7	1.2	24.1
7	14.5	11.7	13.1	14.0		17.8		14.2	1.0	16.1
8	20.2	8.2	14.7		10.6	19.6		14.7	2.4	36.2
9	22.5	8.3	14.9		7.9	11.6		13.0	2.7	45.9
10	23.0	15.2			11.2	14.4		16.0	2.5	31.5
11	18.1	20.4			7.2	7.2		13.2	3.5	53.1
12	27.1	15.5	12.1		6.0	10.4	7.1	13.0	3.1	59.0
AA	18.4	16.7	16.0	13.2	13.7	14.5	13.611	15.2	0.7	12.3

(b)

	YEAR									
MONTH	1987	1988	1989	1990	1991	1992	1993	MIA	UN (M IA	SD(MIA)
1	2.6	18.0	7.9	12.6	12.3	12.0	12.7	11.2	1.8	43.0
2	6.6	11.8	6.7	8.0	19.7			10.6	2.5	52.4
3	13.2	14.4	12.5	19.2	22.6		27.0	18.2	2.4	32.1
4	11.0	14.2		14.2	17.5	10.1	18.4	14.2	1.4	23.4
5	5.3	9.8		7.6	14.5	11.2	11.1	9.9	1.3	32.4
6	6.5	7.0	6.2	4.8	5.3	11.8	5.8	6.8	0.9	34.8
7	4.4	8.9	4.1	5.0		15.5		7.6	2.2	63.5
3	3.3	5.3	4.7		7.3	15.5		7.2	2.2	66.9
9	12.5	11.5	8.5		6.9	15.2		10.9	1.5	30.3
10	11.7	7.4			8.9	13.6		10.4	1.4	26.7
11	8.5	5.6			15.9	5.6		8.9	2.4	54.5
12	10.5	9.8	7.5		8.7	11.8	13.7	10.3	0.9	21.3
AA	8.0	10.3	7.3	10.2	12.7	12.2	14.8	10.8	1.0	24.7

TABLE 5.5. The amplitudes of the (a) zonal and (b) meridional components of the diurnal tide.

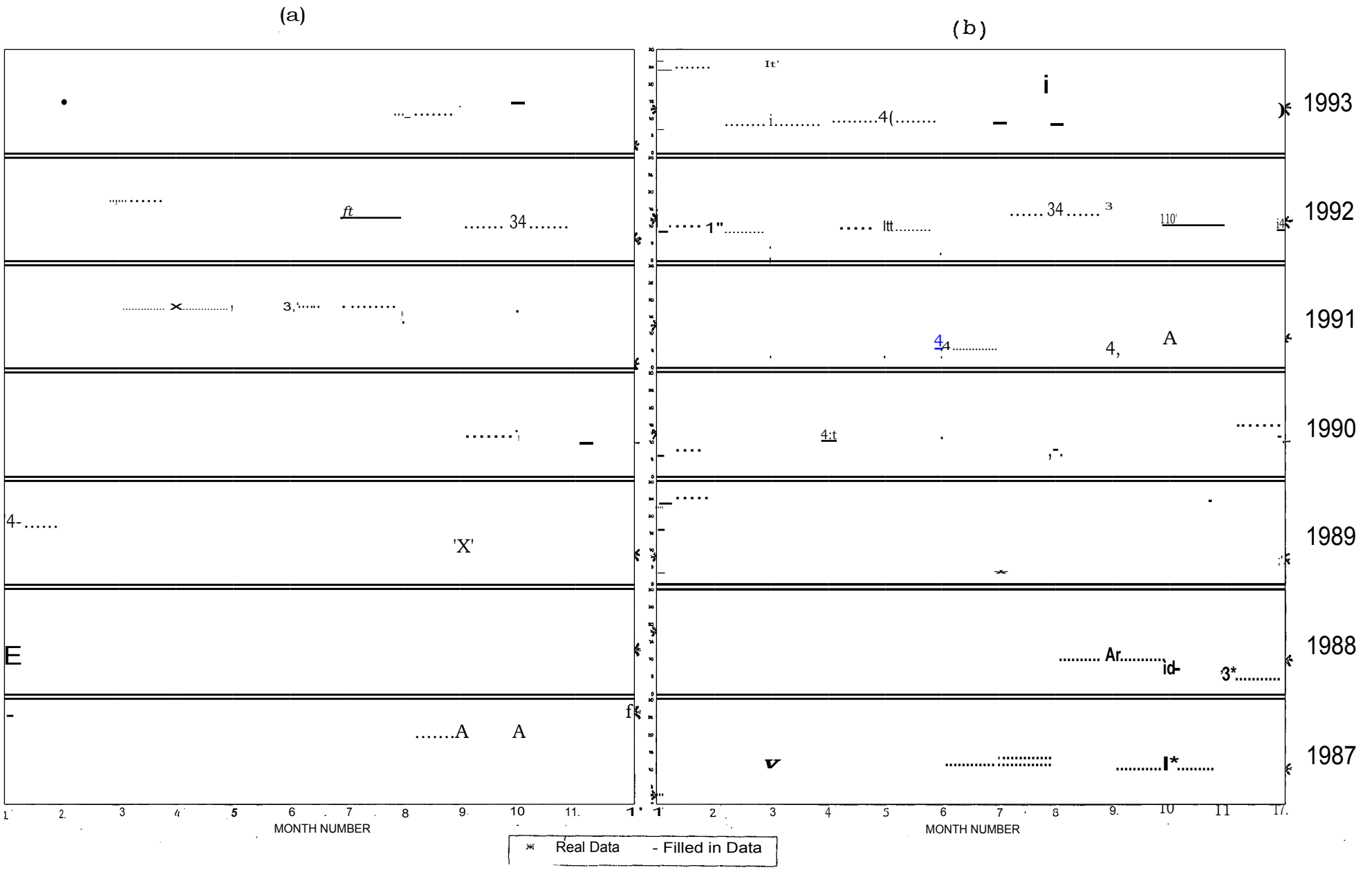

FIGURE 5.12 The monthly amplitudes of the (a) zonal (y_o = 5; vs = 5 ms / division) and (b) meridional (y_o = 0; vs = 5 ms^{-1} / division) components of the diurnal tide.

The monthly amplitudes of the diurnal tide for 1987 to 1993 are tabulated in Tables 5.5 (a) and (b) for the zonal and meridional components, respectively. The corresponding graphical presentations are shown in Fig 5. l 2 (a) and (b). My analysis will follow the scheme of Section 5.2.1 and I will compare the two tides as I go along.

Zonal amplitudes (Fig. 5.12 (a)) do not show clear seasonal behaviour but are generally larger (MIAs of -17 - 20 ms^{-1}) in mid-summer to mid-autumn with maximum amplitudes in March/April. Winter amplitudes are small (MIAs of <15 ms^{-}). Meridional amplitudes (Fig. 5.12 (b)) are more systematic. Generally, they have a maximum which is in March. The minima are, on average in winter. Meridional amplitudes are smaller than the zonal amplitudes as shown by AAAs of 10.8 ± 1.0 ms^{-1} compared to the 15.2 + 0.7 ms' of the zonal component.

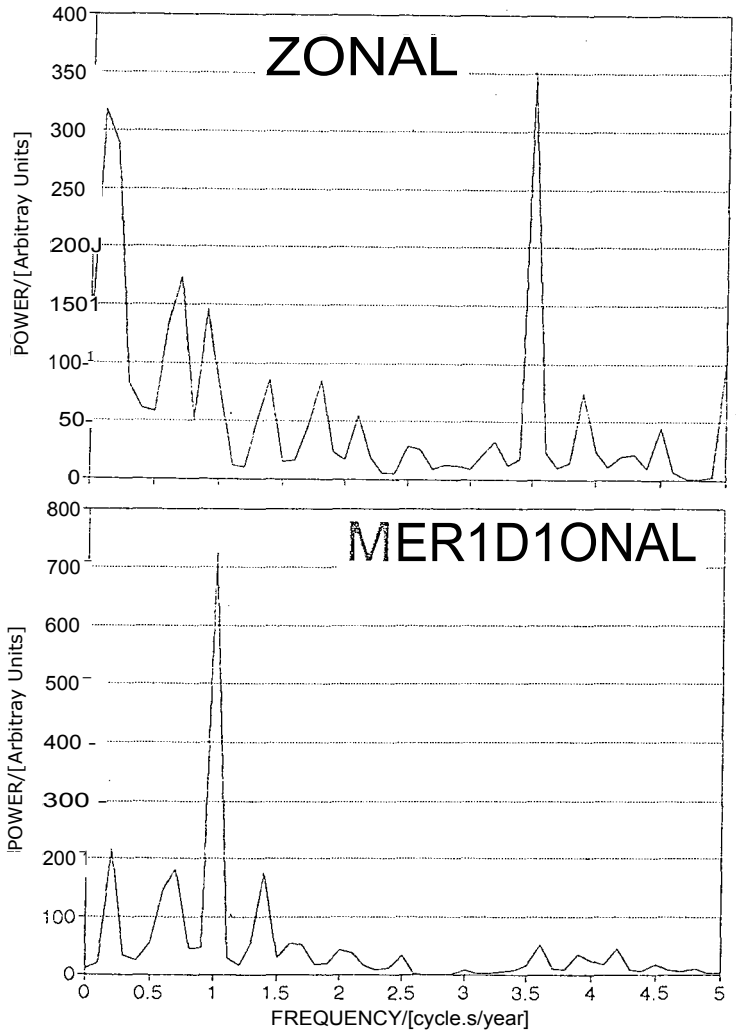

FIGURE 5.13. The seasonal spectra of the zonal and meridional diurnal tidal amplitudes.

Figure 5.13 shows the MEM spectrum of the diurnal monthly amplitude for the whole seven year (1987 - 1993) period. The meridional amplitudes have an annual periodicity while the zonal amplitudes have an unexpected frequency of three and a half cycles per year . Interannually, there is great variability as indicated by the deviation of the individual monthly amplitudes from the MIA which can be as large as 67% for some months (e.g. August for the meridional component). The meridional component is more variable compared to the zonal component.

5.3.2 PHASE

Table 5.6 (a) and (b) show the monthly zonal and meridional phases of the diurnal tide respectively with corresponding graphs shown in Fig. 5.14 (a) and (b). A number of annual and interannual patterns are observed and these are discussed below.

(a)

	YEAR									
MONTH	1987	1938	1989	1990	1991	1992	1993	MIA	UN(M1A	SD(MIA)
1	8.6	12.9	10.9	10.8	10.0	10.2	10.5	- 10.5	0.5	12.1
2	9.6	10.9	10.3	7.4	10.5			9.8	0.6	14.6
3	10.2	8.4	9.8	9.5	10.7		10.0	9.8	0.3	8.2
4	11.0	8.8		9.4	10.2	10.6	9.2	9.9	0.3	8.6
5	12.0	11.0		12.2	12.2	13.2	12.5	12.2	0.3	6.0
6	14.2	12.9	11.8	12.3	15.0	12.3	15.4	13.4	0.5	10.7
7	12.2	13.3	13.4	14.0		13.8		13.3	0.3	5.2
8	13.6	12.1	13.7		12.8	13.7		13.2	0.3	5.2
9	10.7	9.0	11.9		9.8	10.5		10.4	0.5	10.4
10	9.1	8.5			10.7	8.8		9.3	0.5	10.4
11	10.7	9.3			10.8	11.6		10.6	0.5	9.0
12	11.3	11.0	10.6		13.1	12.4	9.8	11.4	0.5	10.7
AA	11.1	10.7	11.5	10.8	11.5	11.7	11.2	11.2	0.2	3.4

(b)

	YEAR									
MONTH	1987	1983	1989	1990	1991	1992	1993)1	MIA	UN(MIA	SD(MIA)
1	13.6	19.9	19.7	19.7	19.5	18.4	19.9	18.7	0.9	12.3
2	14.3	16.8	16.3	15.1	17.6			16.0	0.6	8.3
3	15.5	14.2	16.0	17.3	13.1		17.8	16.5	0.6	9.1
4	127	14.5		17.4	16.0	17.7	16.5	15.3	0.3	120
5	15.6	11.7		11.9	15.8	14.6	15.9	14.3	0.3	13.7
6	16.7	14.4	13.4	2.9	15.8	14.0	17.3	14.3	1.1	19.5
7	15.8	15.8	11.5	15.7		15.4		14.3	0.3	126
3	15.6	11.3	17.7		13.8	16.2		14.9	1.1	16.4
9	13.9	12.5	14.0		14.1	15.3		14.0	0.5	7.3
10	14.7	17.8			16.6	16.6		16.4	0.7	8.0
11	15.1	19.5			14.1	19.3		17.0	1.4	16.3
12	17.9	20.0	20.6		14.8	18.4	18.0	13.3	0.3	11.3
AA	15.11	15.7	16.2	15.1	16.0	16.6	17.61	16.01	0.3	5.4

TABLE 5.6. The phases of the (a) zonal and (b) meridional components of the diurnal tide.

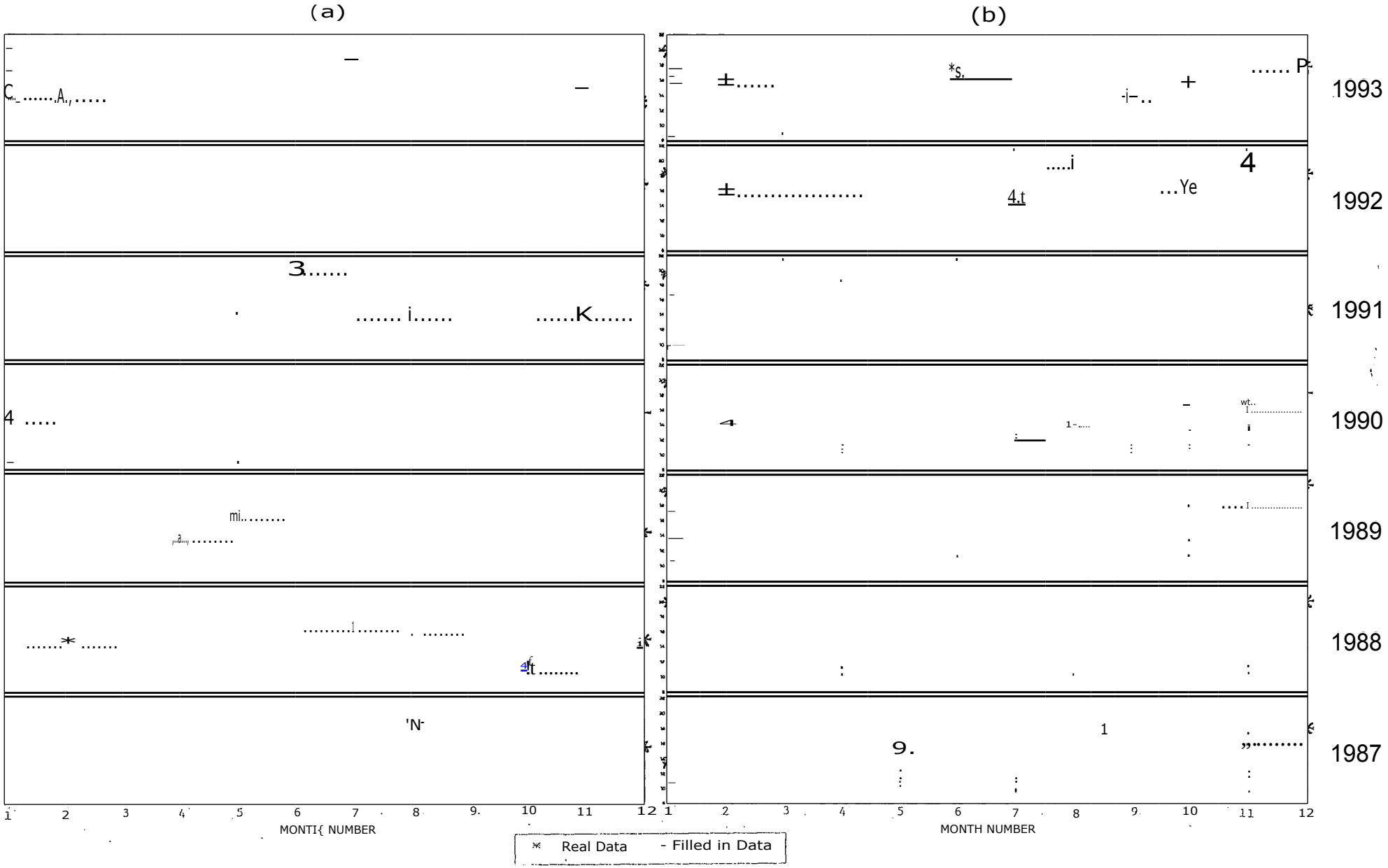

FIGURE 5.14 The monthly phases of the (a) zonal ($y_{„}$= 6; vs = 2 h /division) and (b) meridional (y_0 = 8; vs = 2 h/ division) components of the diurnal tide.

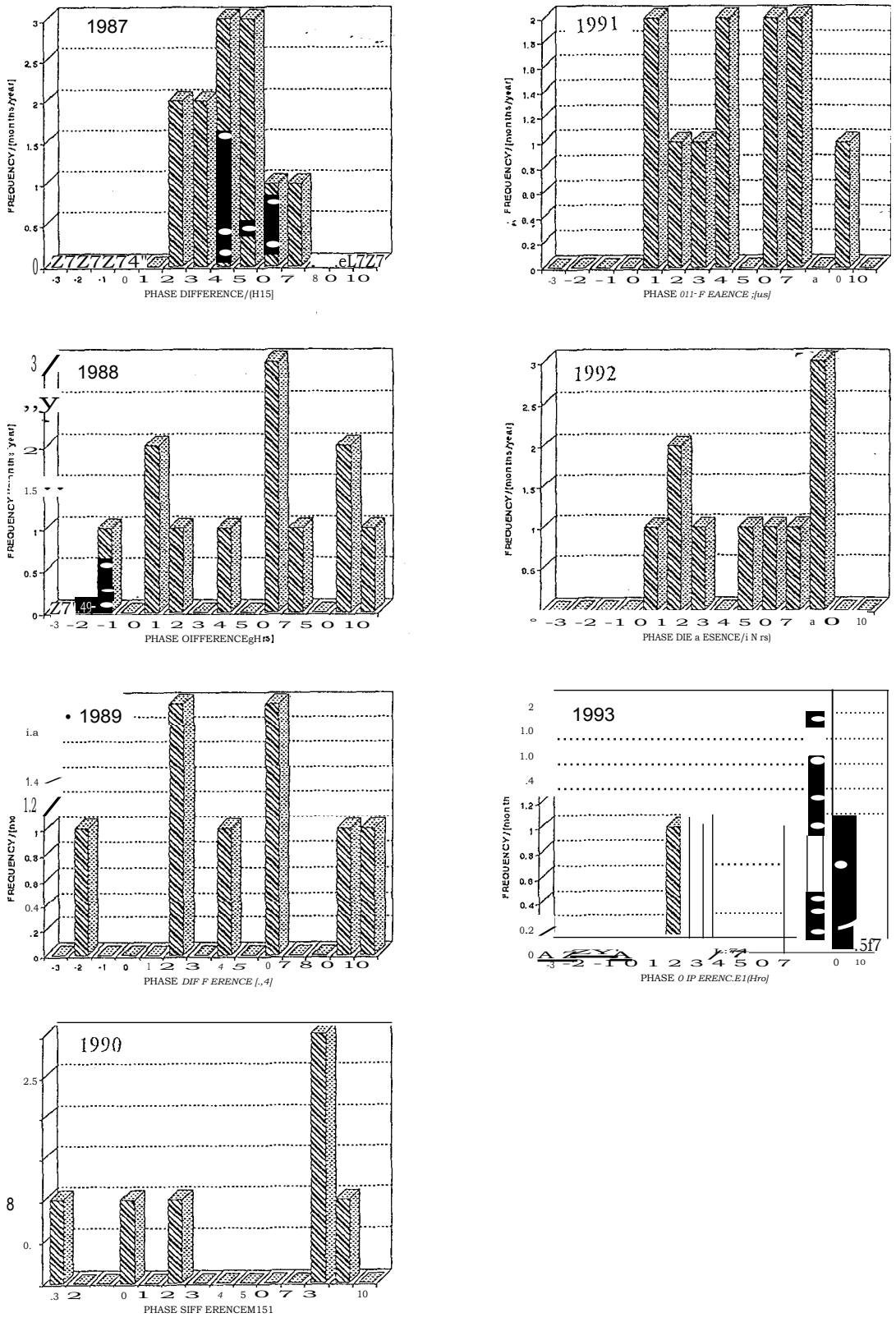

FIGURE 5.15 The annual frequency distribution of the phase differences of the diurnal tide.

The zonal phases have a pattern of phases of - 12.0 - 16.0 h in late autumn and winter. The annual average phases are - 11 -12 h and have an AAA of 11.2 ± 0.2 h. Meridional phases lack definition but generally the MIAs show a tendency of the summer and equinoctial phases to be 15 - 19 h and the winter phases to be - 14 - 15 h. The annual averages are - 15 - 18 h with an AAA of 16.0 ± 0.3 h. Zonal phases have a vely high degree of interannual consistency with small (< 15%) deviations from the MIA. Meridional phases, on the other hand, are more variable from year to year with standard deviations of up to -20%.

	YEAR								
IMONTH	1987	1933	1939	1990	1991	1992	1993	MIA	UN(M1A)
1	5.0	7.0	3.9	8.9	9.5	8.2	9.4	8.1	0.6
2	4.7	5.9	6.0	7.7	7.1			6.3	0.5
3	5.3	5.8	6.2	7.9	7.4		7.8	6.7	0.4
4	1.7	5.7		8.0	5.8	7.1	7.4	5.9	0.9
5	3.6	0.7		-0.3	3.7	1.3	3.4	2.1	0.7
6	2.5	1.5	1.6	-3.4	0.8	1.6	1.9	0.9	0.8
7	3.6	2.5	-1.9	1.7		1.6		1.5	0.9
8	2.0	-0.8	4.1		1.0	2.5		1.7	0.8
9	3.2	3.5	2.2		4.3	4.8		3.6	0.5
10	5.6	9.3			5.9	7.7		7.1	0.9
11	4.4	10.2			3.3	7.3		6.4	1.6
12	6.6	9.1	10.0		1.6	6.0	8.2	6.9	1.2
AA	4.0	5.0	4.6	4.4	4.6	4.9	6.4	4.3	0.3

TABLE 5.7. The phase difference of the diurnal tide. Positive for zonal leading.

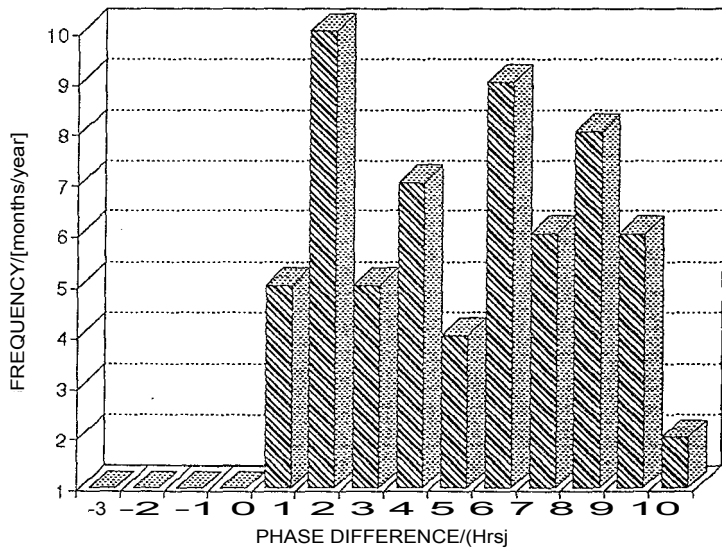

FIGURE 5.16 Frequency distribution of the phase differences of the diurnal components for the whole 7 year period. Positive for the zonal component leading.

Tables 5.7 and Fig. 5.15 show the annual frequency distribution of the phase differences between the zonal and the meridional tides for 1987 to 1993. Fig 5.16 is the same as Fig. 5.15 but for the

whole 7 year (1987 -- 1993) period.. Though there are years when the expected 6 h phase difference is most frequent, the 2 h phase difference (Table 5.7 and Fig. 5.15) is generally most frequent as shown by Fig. 5.16. The range of diurnal phase differences (-3 to 10 h) is larger than that of the semidiurnal tide, (Fig. 5.4 and 5.5) whith shows the greater variability of the f:)!Iiier tide. Another difference between the two is that while the few cases when the meridional component is leading are generally in summer for the semidiurnal tide, they are generally in winter for the diurnal tide. The annual average phase differences are - 4 - 6 h- with an AAA of 4.8 ± 0.3 h

5.3.3. OTHER GRAPHICAL REPRESENTATIONS

Diagrams corresponding to those of Section 5.2.3 (Fig. 5.6 - 5.10) are Fig.5.17 to 5.23. Fig. 5.17 shows the harmonic dials of the diurnal tide for 1987 and 1988. With the exception of the meridional parameters in 1987, tidal amplitudes and phases show significant seasonal dependence. However the seasonal zones are less consistent than those of the semidiurnal tide. The expected 6 h phase difference is not clearly defined, which is consistent with Fig. 5.15 (a) and (b) which show the dominance of 4 and 5 h phase differences in 1987 and a marginal dominance of the 6 h phase difference in 1988.

The monthly wind vector is shown on the polar plots of Fig. 5.18 and 5.19 for 1987 and 1988 respectively, with the main parameters listed in Table 5.8. These plots show great inconsistency between the two years in both amplitude and phase difference. There are a few months (e.g. October, December 1987; February, March, April 1988) for which the phase difference is close to the theoretical 6 h. For both years the rotation of the wind vector is anticlockwise except for August 1988 which is marginal since polarization is almost linear.

Table 5.8 gives the values of the maximum velocity vector, its time of occurrence and its direction. The maximum velocity vector for the diurnal tide has an AAA of 17.4 ± 0.5 ms' its times of occurrence have an AAA of 9.2 ± 0.5 h (and 21.2 ± 0.5 h). The maximum velocity vector, as with the semidiurnal tide (see Section 5.2.3), is primarily directed northeast (or equivalently southwest).

ZONAL MERIDIONAL

(10h 00b

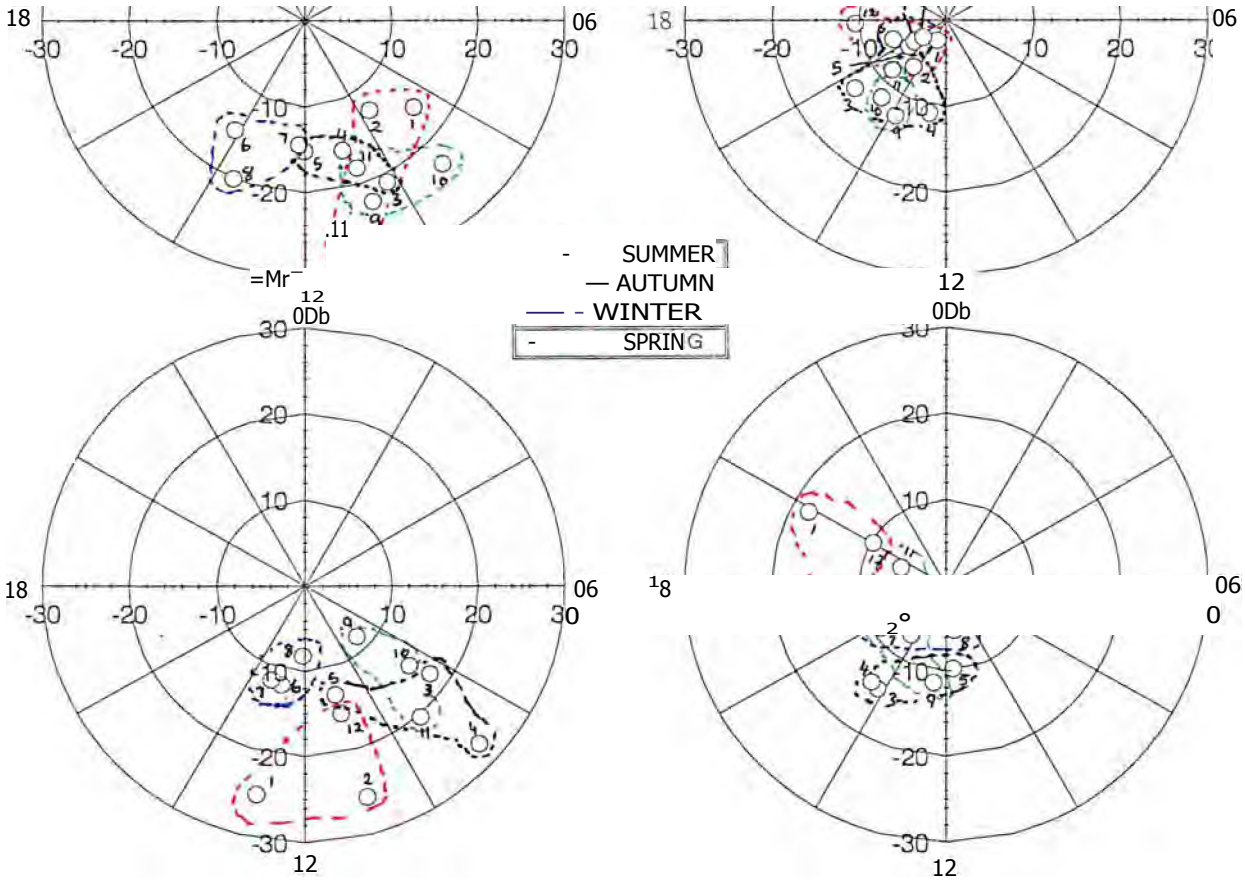

FIGURE 5.17 The harmonic dials of 1987 (top two) and 1988 (bottom two) for the diurnal tide. The numbers next to the points indicate the month numbers. Units on the axes are in m/s.

(a)

	YEAR									
MONTH	1987	1988	1989	1990	1991	1992	1993	MIA	UN(MIA)	SD(MIA)
1	16.0	25.9	21.5	20.0	16.7	17.5	18.3	19.4	1.3	17.6
2	13.0	25.7	14.7	10.2	23.7			17.4	3.1	39.1
3	21.3	17.7	25.5	22.9	26.2		28.4	23.7	1.6	16.3
4	18.7	27.5		20.1	18.7	20.0	22.0	21.2	1.4	15.7
5	15.5	16.4		10.2	18:0	19.4	15.4	15.8	1.3	19.8
6	15.9	13.6	13.8	9.1	18.7	16.7	11.8	14.2	1.2	22.6
7	14.7	14.0	13.6	14.7		23.1		16.0	1.8	24.9
8	20.3	9.7	14.9		12.8	23.6		16.3	2.5	34.8
9	24.3	12.9	16.5		8.9	16,0		15,7	2.5	36.0
10	23.1	16.3			11.2	16.8		16.8-	2.4	28.8
11	18.5	21.0			16.6	7.9		16.0	2.9	35.7
12	27.1	17.3	13.8		10.4	11.8	14.3	15.8	2.5	38.3
AA	19.0	18.2	16.8	15.3	16.5	17.3	18.4	17.4	0.5	7.3

(b)

	YEAR									
MONTH	1987	1988	1989	1990	1991	1992	1993	MIA	UN(MIA)	SD(MIA)
1	8.3	24.0	10.5	9.8	9.0	21.0	9.8	13.2		49.1
2	9.8	11.3	10.5	6.0	9.0			9.3		21.8
3	10.5	9.0	9.8	7.5	8.3		6.8	8.6		16.3
4	11.3	9,0		8.3	11.3	10.5	7.5	9.6		16,7
5	12.0	11.3		12.0	2.3	1.5	13.5	8.8		61.5
6	2.3	1.5	24.0	12.0	3.0	0.8	3.8	6.8		125.7
7	12.0	2.3	1.5	2:3		14.3		5.5		95.4
8	1.5	12.0	1.5		1.5	2.3		3.8		123.3
9	11.3	11.3	12.0		23.3	14.3		14.4		35.4
10	21.0	8.3			11.3	6.8		11.8		54.2
11	11.3	9.0			1.5	10.5		8.1		55.5
12	11.3	10.5	21.8		2.3	6.0	6.8	9.8		69.0
AA	10.2	9.9	.11.4`	8.3	7.5	8.8	8.0	9.2	0.5	15.4

(c)

	YEAR									
MONTH	1987	1988	1989	1990.	1991	1992	1993	MIA	UN(MIA)	SD (MI A)
1	1.5	160.7	164.0	147.3	137.3	147.8	142.0	128.6	21.5	44.2
2	10.7	3.1	1.4	145.6	148.1			61.8	34.8	125.8
3	8.9	9.6	178.1	135.2	133.0		113.3	96.3	28.9	73.4
4	, 33.1	4.0		149.0	18.1	171.2	143.4	86.5	30.9	87.6
5	11.4	36.3		47.7	47.5	33.8	35.5	35.4	5.4	37.5
6	19.2	30.0	24.7	21.3	16.0	42.1	26.7	25.7	3.3	33.6
7	9.7	36.1	15.2	18.4		39.9		23.8	6.0	56.0
8	8.0	32.5	8.1		34.8	35.0		23.7	6.4	60.3
9	23.6	57.6	26.2		34.9	65.8		41.6	8.5	45.8
10	2.7	158.7			8.1	137.0		76.6	41.4	108.0
11	13.8	165.7			70.5	151.3		100.3	35.6	71.0
12	176.4	153.1	148.6		56.4	85.1	110.5	121.7	18.6	37.5

TABLE 5.8 The (a) maximum velocity vector, (b) its time of occurrence and (c) its direction (anticlockwise relative to east) for the diurnal tide.

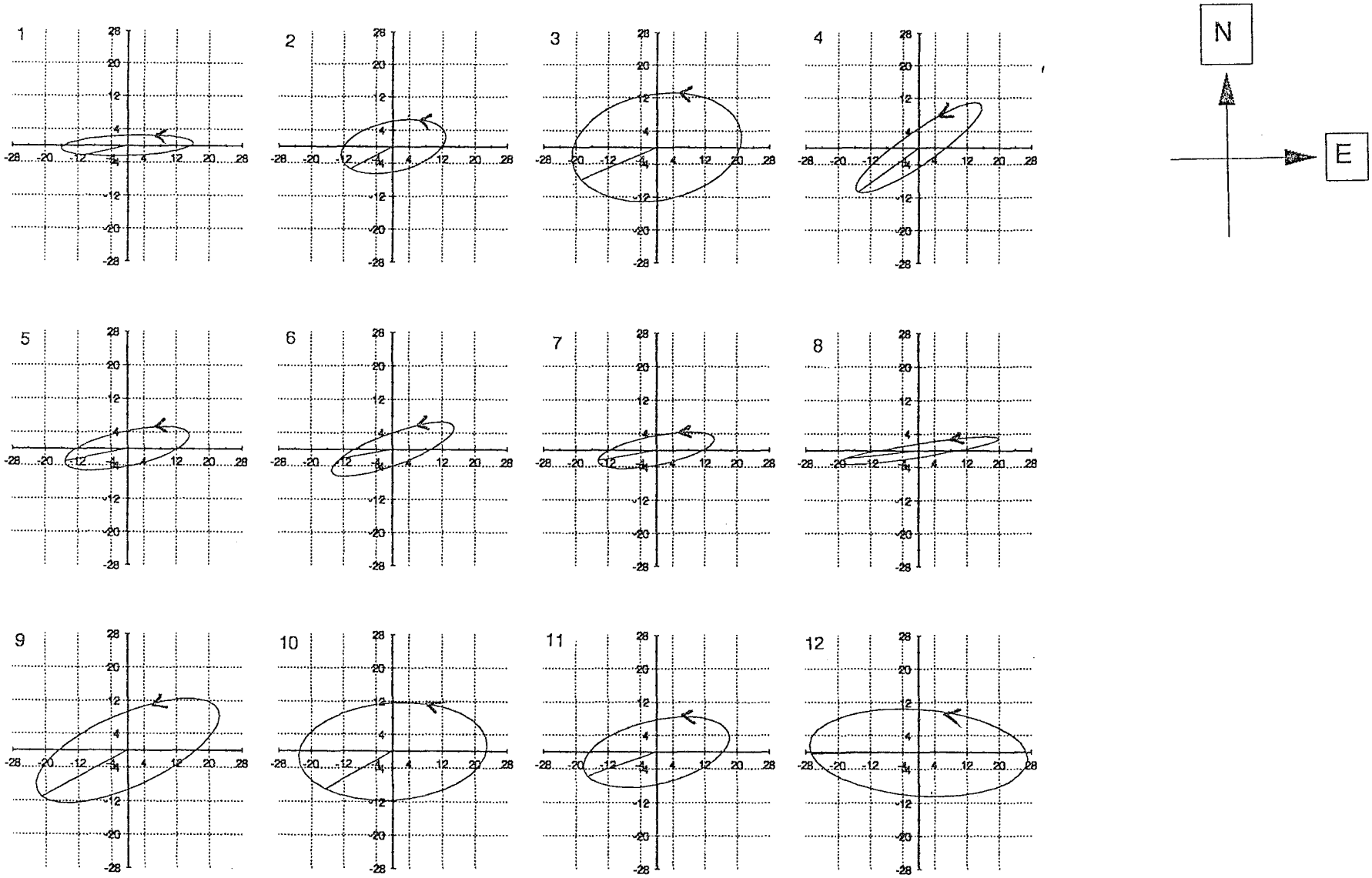

FIGURE 5.18 The monthly polar plots of the diurnal tide for 1987. The month number is written on the top left hand corner of the corresponding polar plot. Units for both axes are m/s.

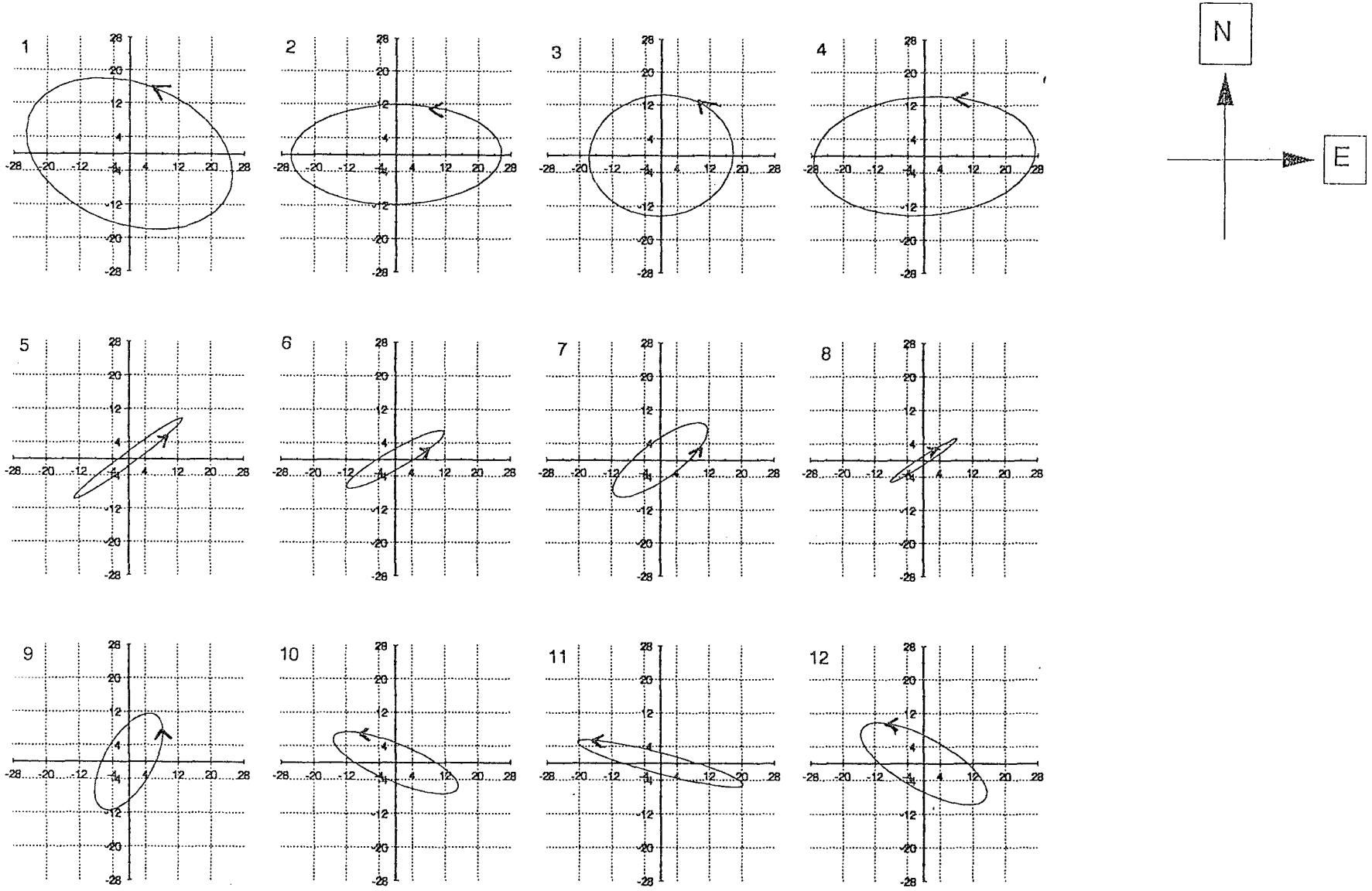

FIGURE 5.19 The monthly polar plots of the diurnal tide for 1988. The month number is written on the top left hand corner of the corresponding polar plot. Units for both axes are m/s.

Fig. 5.20 and Fig. 5.21 show the zonal and the meridional surface plots of the diurnal wind velocity components for 1987 and 1988. There are a number of noticeable features and these are discussed below:

There is a significant interannual variability in the behaviour of the diurnal tide which is in sharp contrast to the semidiurnal tidal behaviour (Figs. 5.9 and 5.10).

2. There are, however, a few common features between 1987 and 1988. Zonal amplitudes are larger in summer and the equinoxes with peaks centered in March and September/October in 1987 and April and November in 1988. In Section 5.2.4 we noticed a similar one month shift for the meridional component though in that case it involved secondary peaks. The meridional component has peaks in March/April and again in September/October. The maxima are approximately equal for both years. Winter velocities are small with peaks in June (1987) and July (1988). Again showing a month shift.

3. Both the zonal and the meridional components are negative around midnight which corresponds to westward and southward motion respectively. Zonal phase behaviour has annual consistency as shown by the peaks of the surface plots while the meridional phase behaviour is more variable especially in 1988 (Fig. 5.21., (B.1)).

A comparison of the surface plots for 1988 (Fig. 5.22 and 5.23) shows that the tides dominate the wind field in the meteor region. Fig. 5.22 shows the dominance of the diurnal tide in the zonal wind field which agrees with Tables 5.5 (a) and 5.1 (a). For the meridional wind (Fig. 5.23) there is no outright dominance by any of the tides which is also in agreement with the above mentioned tables. The corresponding comparison for 1987 shows similar trends.

5.3.4. COMPARISON AND DISCUSSION

The diurnal tide consists of both propagating and evanescent modes and, as mentioned earlier, the former is more dominant near the equator and the latter more dominant at high latitudes (CL; Poulter, 1980). At midlatitudes a mixture of evanescent and propagating modes generally exists resulting in this region having a complicated tidal structure due to interference effects (Forbes,

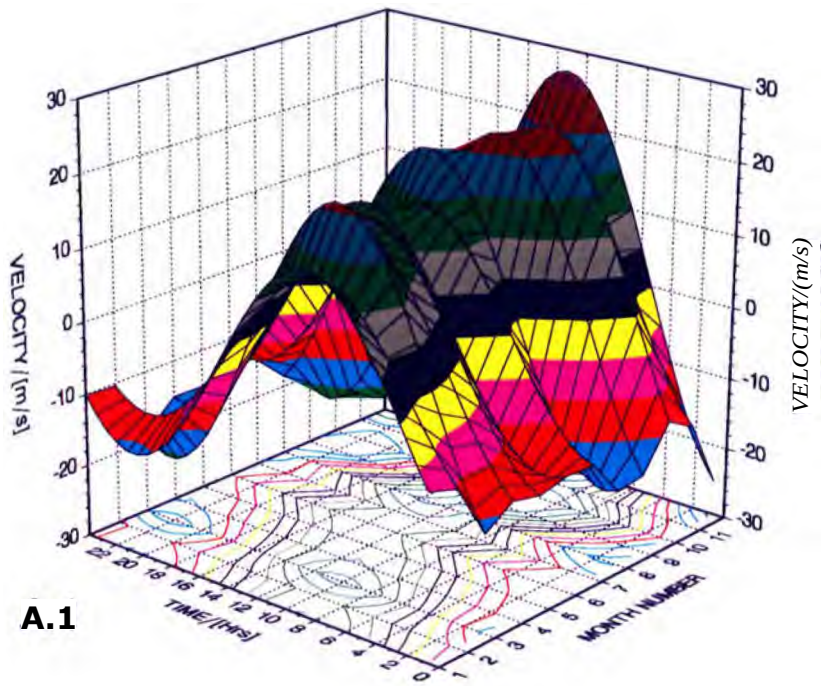

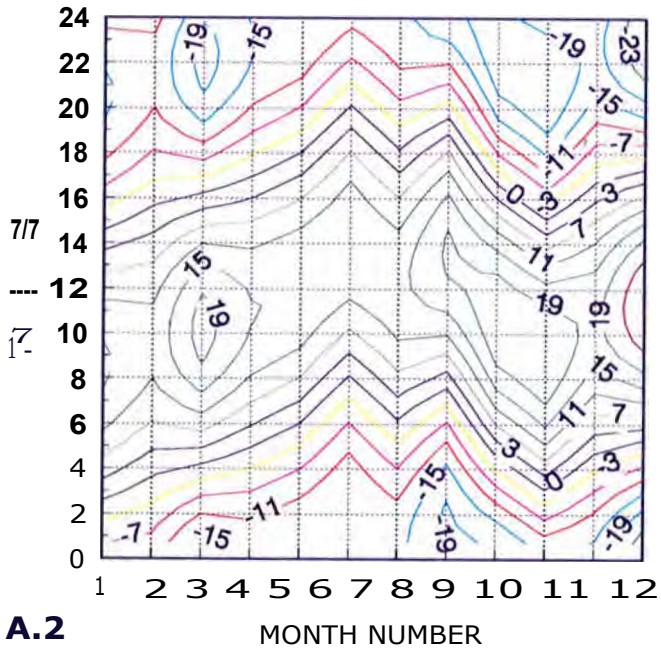

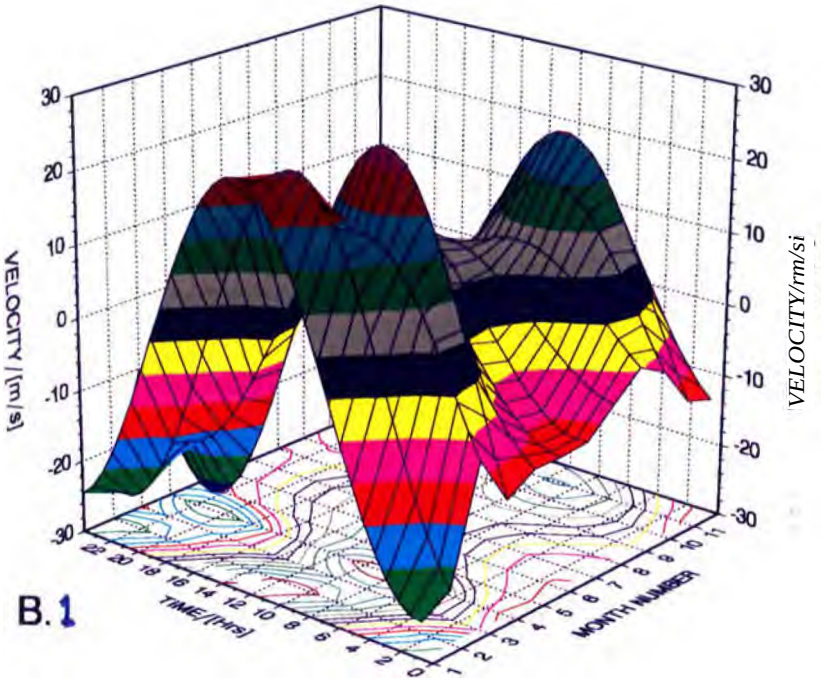

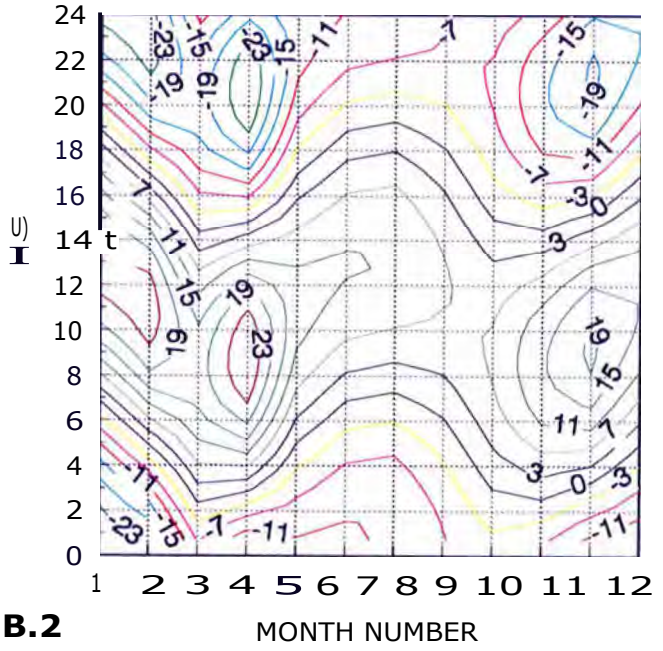

FIGURE 5.20
Surface plots ((A.1) and (B.1)) and corresponding contour plots ((A.2) and (B.2)) for the zonal component of the diurnal tide for 1987 (top two) and 1988 (bottom two).

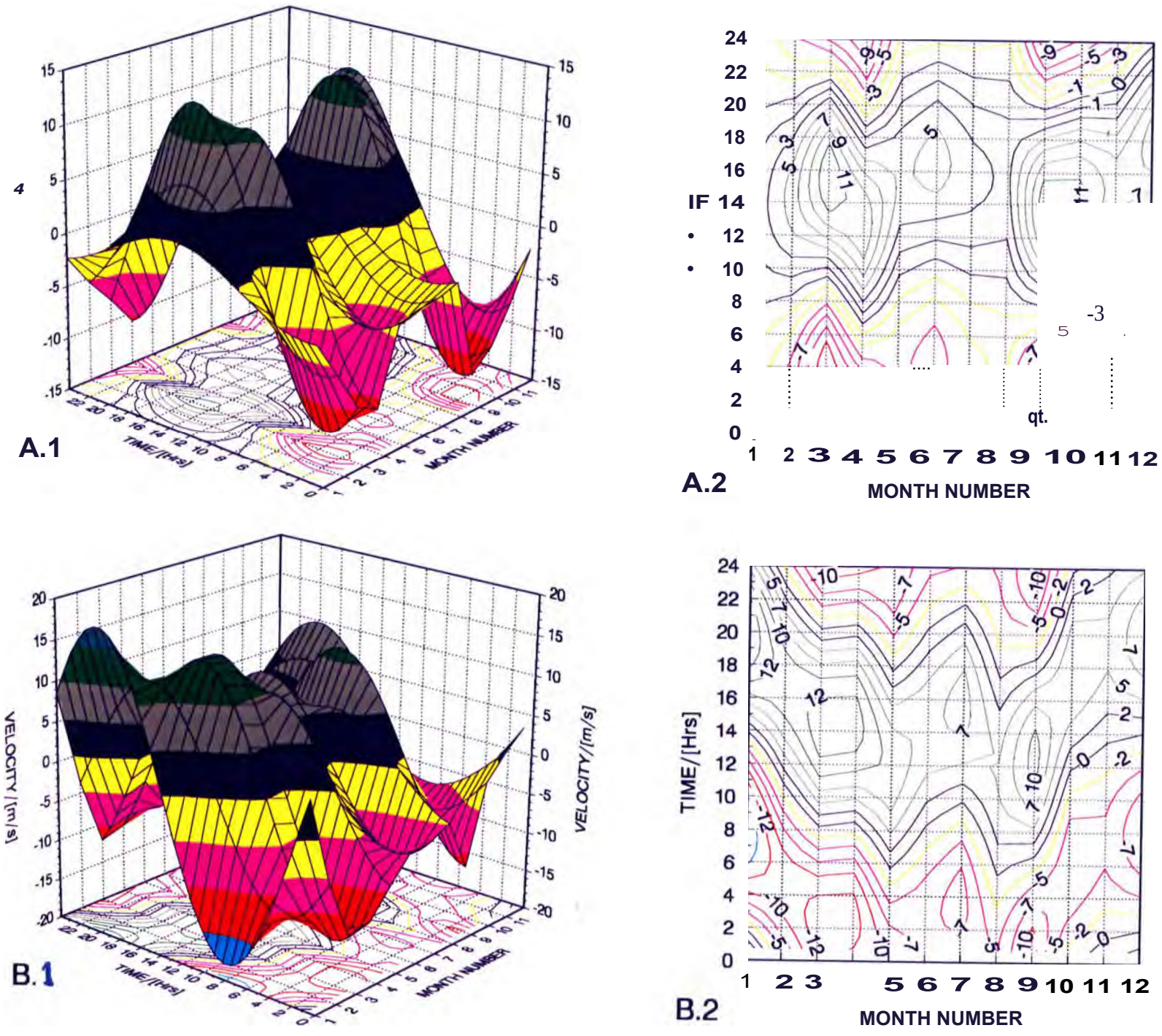

FIGURE 5.21 Surface plots ((A.1) and (13.1)) and corresponding contour plots ((A.2) and (B.2)) for the meridional component of the diurnal tide for 1987 (top two) and 1988 (bottom two).

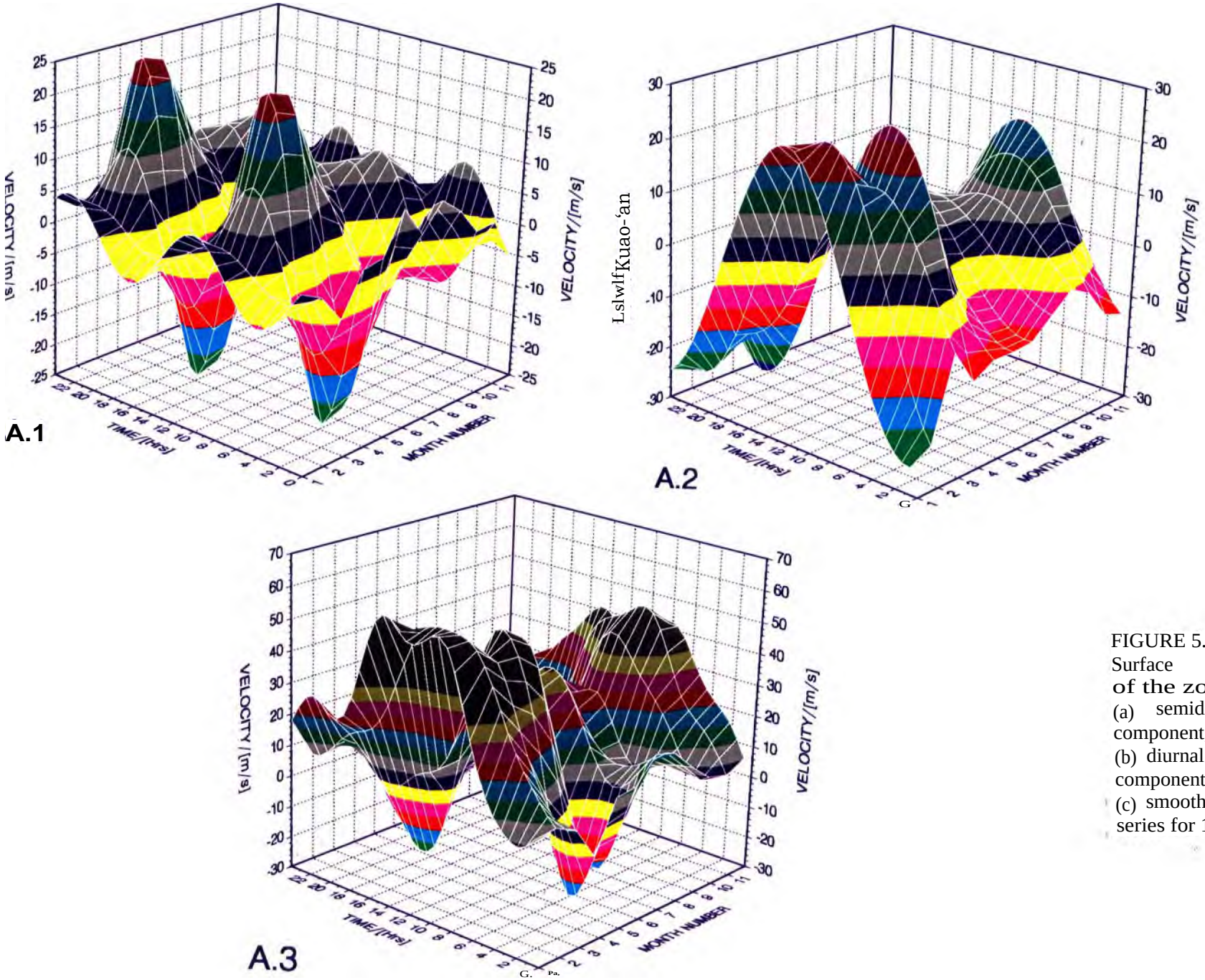

FIGURE 5.22 Surface plots of the zonal (a) semidiurnal component, (b) diurnal component and (c) smoothed time series for 1988.

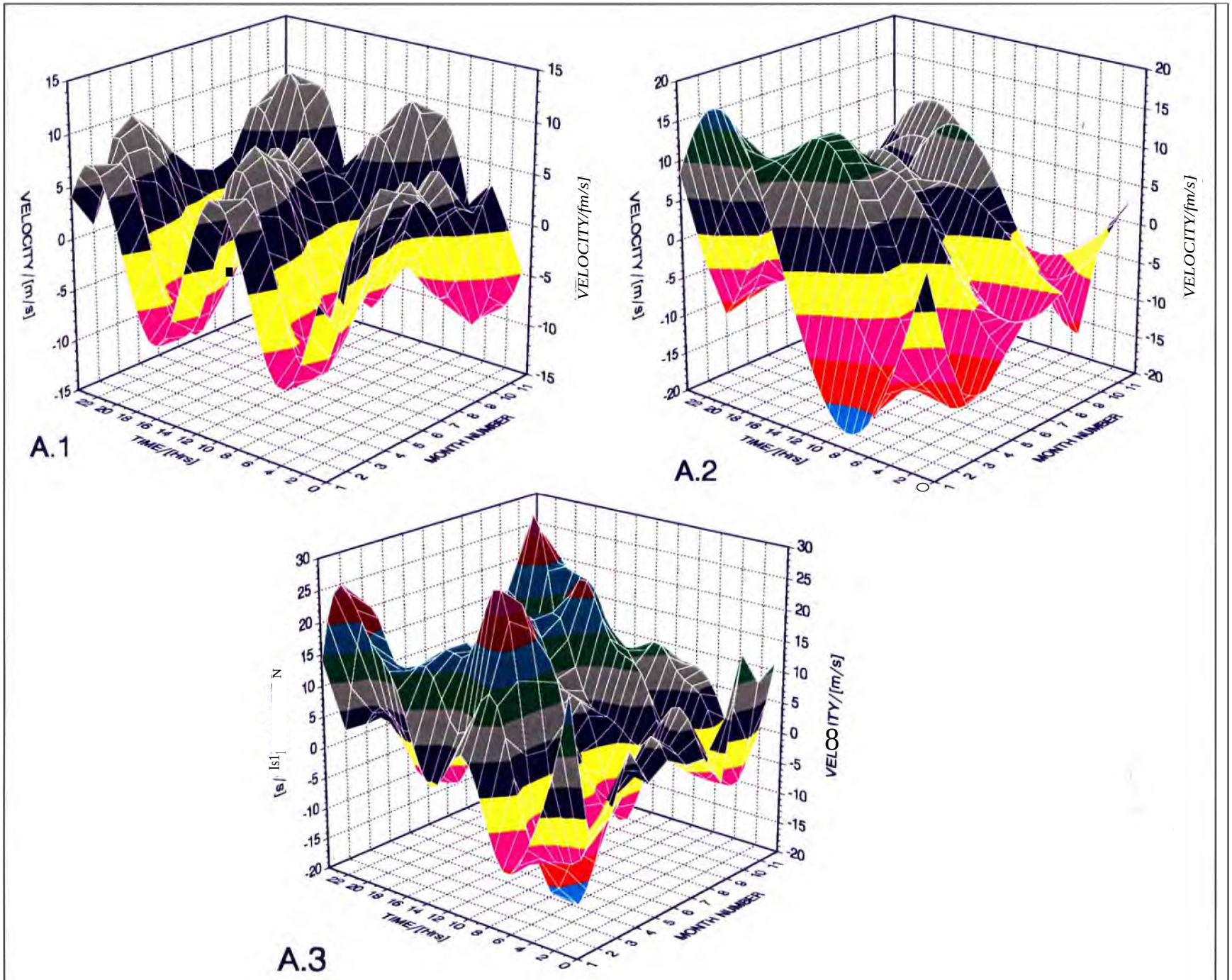

FIGURE 5.23
Surface plots of the meridional (a) semidiurnal component, (b) diurnal component and (c) smoothed time series for 1988.

1990). Consequently the diurnal tide is more latitude dependent than the semidiurnal tide so restricting comparable inter-station results to stations at similar latitudes.

A. AI IPLITUDE

The zonal and meridional amplitudes of the diurnal tide at GT are generally in good agreement with the trends observed at Adelaide (VTK). At both sites the amplitudes (EW and NS) reach their maxima in autumn. The diurnal tide, as mentioned in the theory, is more sensitive to damping but according to VTK the large equinoctial amplitudes imply less damping during these periods. There are two other possible factors that contribute to the equinoctial maxima:

(i) The zonal mean wind. A westward (eastward) zonal prevail wind increases (decreases) the amplitude of (1, 1) the tidal wind (V86). This is confirmed by the GT results; the equinoctial diurnal amplitude maxima (Fig. 5.12) generally coincide with equinoctial zonal prevailing wind minima (Fig. 4.10 (a)).

(ii) Enhanced water vapour excitation. The diurnal tide is primarily excited by insolation absorption by water vapour (Harris, 1993) and according to Groves (1982 b) the heating component J, $^{1-]}$ for water vapour is greater during equinoctial months than the solstitial ones.

The smaller diurnal amplitudes observed at GT during the solstices compared to the equinoxes are similar to observations made at Adelaide (VTK). Winter amplitudes are generally smaller (MIA of -7 ms^{-1} (NS) and -14 ms (EW)) compared to summer amplitudes (MIA of -11 ms^{-1} (NS) and 16 $ms^{-'}$ (EW)). This can be explained by the "distortion" of the velocity structure of the (1,1) mode (V86; FH). This distortion results in seasonal asymmetry with the summer peak being -40% larger than the winter peak (FH) as shown in Fig. 5.24. It is interesting to note that the small winter diurnal amplitudes (Fig. 5.12) generally coincide with the maximum of the zonal prevailing wind (Fig. 4.10 (a)) which is consistent with (i) above.

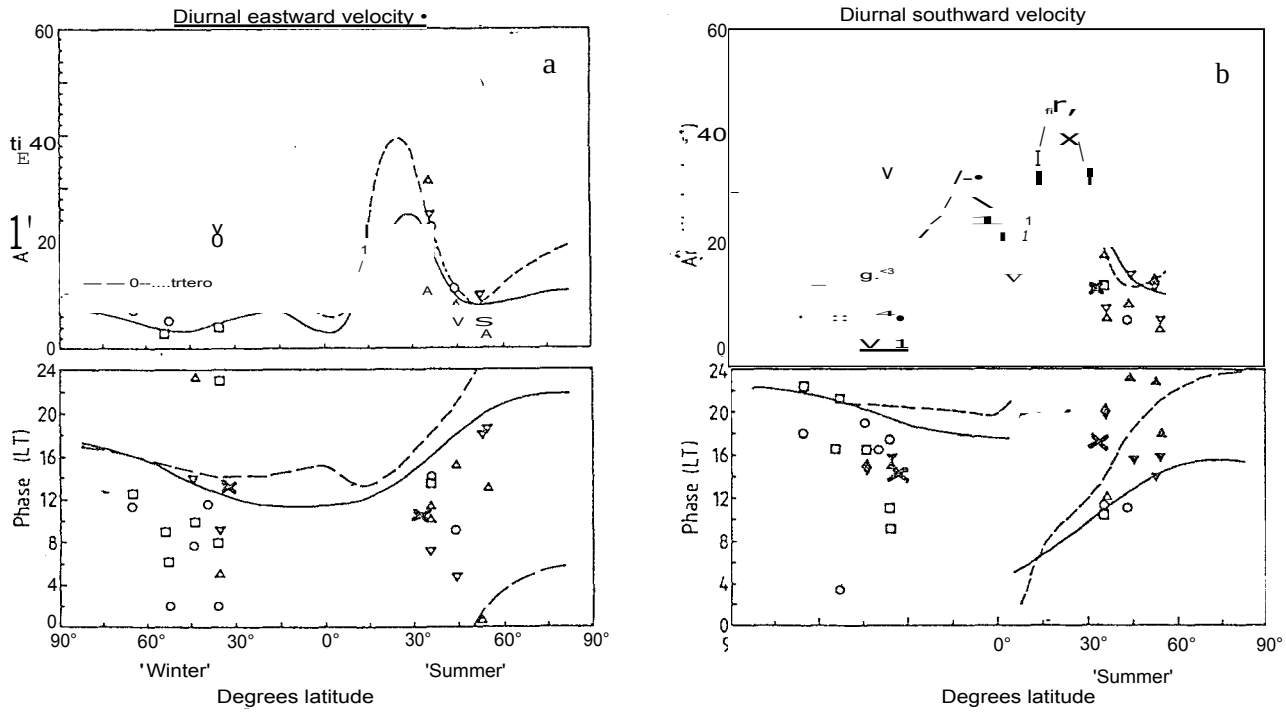

FIGURE 5.24. The models of the amplitude (top) and phase (bottom) for (a) the zonal component and (b) the meridional component for dissipation models A (dashed lines) and B (solid lines). The points indicated with objects represent results from various observers (after FH). The crosses represent the solstice averages of the MIA at GT.

Fig. 5.24 shows FH's models for the diurnal tide for two dissipative models A and B (see FH for details). I have represented the solstice averages of the MIA at GT with crosses. The GT results are in good agreement with the model amplitude, not only in seasonal sense but also in absolute terms, except for the meridional summer amplitude which is -ms 15 ms '(-58%) smaller than the model amplitudes. There are a number of possible causes for this discrepancy: (i) the interference between the propagating and evanescent modes which are found at midlatitudes (Forbes, 1990); (ii) the sensitivity of the diurnal tide to local solar variation due to its mixed composition of evanescent and propagating modes (Poulter, 1980); and (iii) dissipation.

Compared to the semidiurnal tide, the diurnal amplitudes show greater interannual variability as shown by the standard deviations of - 16 - 59% (EW) and - 21 - 67% (NS) compared to - 18 - 52% (EW) and - 12 - 43% (NS) for the semidiurnal tide. Comparison of the AAAs of the tides indicates that the diurnal amplitudes are - 16 - 20% larger than the semidiurnal amplitudes. This is generally consistent with observations made at Adelaide and Kyoto (VTK), but contrasts with

high latitude observations (e.g. Phillips and Vincent, 1987) where the semidiurnal tide is stronger than the diurnal tide because diurnal modes decay with increasing latitude (Avery *et al.,* 1989; CL).

B. PHASE

The diurnal tidal phases have less consistent interannual behaviour. In contrast to observations made at Adelaide and Kyoto (VTK), the zonal phases have a more defined annual pattern than the meridional phases. The zonal phase tends to be delayed when progressing from summer to winter, while meridional phases lack definition. Comparing the GT phases viith FH's models (Fig. 5.24) shows large discrepancies, especially with the meridional phases. The discrepancies with the models are both in seasonal relative teims and in absolute terms. These discrepancies may be due to similar causes as those mentioned for amplitudes above. The most probable phase difference between the zonal and the meridional components is 2 h, but the AAA (Table 5.7) is much nearer the expected value of 6 h. VTK results show phase differences of 10 h (December) to 7 h (June and equinox).

C. TIDAL VELOCITY VECTOR

The averages of the maximum velocities of the rotating wind vectors are -17 ms (Table 5.8) and 12.14 ms^{-1} at GT and Yambol (42.5°N, 26.6°E), respectively. This is to be expected because diurnal mode decays with increasing latitude. The times of the maximum velocity are 9.2 ± 0.5 h (and 21.2 ± 0.5 h) (Table 5.8) and 11.2 h for the two sites, respectively. This is consistent with their being on almost the same longitude (26.5°E and 26.6°E, respectively). While at GT the rotation is predominantly anticlockwise, at Yambol it is predominantly clockwise in winter and equinoxes, and clockwise in summer. At both sites the direction of the maximum velocity is predominantly northeast (or southwest) which shows no symmetry about the equator.

5.4 LONGITUDINAL TIDAL VARIABILITY

5.4.1 AMPLITUDE

a

	YEAR							
MONTH	1987	1988	1989	1990	1991	1992	1993	MIA
1	5.1	5.1	11.2	10.0	4.3	7.2	5.6	6.9
2	15.0	2.5	10.0	7.8	8.5			8.8
12	6.6	8.0	5.5	6.3	2.6	3.8	7.0	5.7
AA	8.9	5.2	8.9	8.0	5.2	5.5	6.3	6.9

b

	YEAR							
MONTH	1987	1988	1989	1990	1991	1992	1993	MIA
1	6.4	7.5	13.6	12.8	8.6	9.9	10.7	9.9
2	13.8	7.9	9.5	6.3	13.2			10.1
12	4.7	6.6	7.4	9.0	4.0	11.0	10.6	7.6
AA	8.3	7.3	10.1	9.4	8.6	10.5	10.6	9.3

TABLE 5.9. The amplitudes of the (a) zonal and (b) meridional components of the semidiurnal tide at GT.

a

	YEAR							
MONTH	1987	1988	1989	1990	1991	1992	1993	MIA
1	12.6	8.7	16.6	13.4	5.3	9.1	13.2	11.3
2		10.6	13.1	10.3		6.0		10.0
12	5.6	11.7	12.0	4.4	9.7	7.1	7.4	8.2
AA	9.1	10.3	13.9	9.4	7.5	7.4	10.3	9.7

b

	YEAR							
MONTH	1987	1988	1989	1990	1991	1992	1993	MIA
1	11.5	9.0	10.9	11.2	7.9	12.9	10.5	10.5
2		11.1	9.7	8.8		5.8		8.8
12	5.6	9.5	9.4	10.8	10.7	6.3	9.9	8.9
AA	8.6	9.9	10.0	10.3	9.3	8.3	10.2	9.5

TABLE 5.10 The amplitudes of the (a) zonal and (b) meridional components of the semidiurnal tide at Adelaide

Tables 5.9 to 5.10 show the semidiurnal amplitudes for the summer months at GT and Adelaide. The Adelaide data were obtained in an exchange arrangement between the University of Adelaide and Rhodes University, and have been averaged over a 20 km height range centered on 95 km to match as closely as possible the assumed height distribution at Grahamstown. These two sites are almost on the same latitude (-34°S) so that latitude dependent effects are eliminated. In

this section we are going to use a *SZli77777er Average* (SA) an equivalent of an AA but for *summer* instead of *annual* averages, and accordingly ASA will replace the AAA. Meridional amplitudes for the semidiurnal tide are comparable between the two sites with SAs of - 7 - 11 ms "and ASAs of 9.3 ms^{-1} (GT) and 9.5 ms"' (Adelaide). The zonal amplitudes are smaller (SAs of - - 9 ms at GT compared to Adelaide (SAs of - 7 - 14 ms") with ASAs of 6.9 ms" and 9.7 ms" respectively. Whereas at Adelaide the zonal and the meridional components are comparable, at GT the meridional is stronger. Zonal seasonal averages are small at both centres (< 6 ms 'at GT, < 8 ms" at Adelaide) in 1991 and 1992. This might suggest a correlated behaviour, but this should be treated cautiously because there are data missing for February 1992 for GT and 1991 for Adelaide.

a

	YEAR							
MONTH	1987	1988	1O8O	1990	1991	1992	1993	MIA
1	15.9	25.4	20.7	17.4	11.5	14.6	14.3	17.1
2	14.1	26.2	14.5	9.4	22.1			17.3
12	27.1	16.2	11.9	8.1	5.6	10.7	6.5	12.3
AA	19.0	22.6	15.7	11.6	13.1	12.7	10.4	15.0

b

	YEAR							
MONTH	1987	1988	1989	1990	1991	1992	1993	MIA
1	2.9	17.1	5.3	8.1	6.1	8.4	10.2	8.4
2	5.3	12.6	4.4	6.9	15.7			9.0
12	5.0	6.5	5.7	9.6	8.4	10.4	6.0	7.4
AA .	4.4	12.1	5.4	8.2	10.0	• 9.4	8.1	8.2

TABLE 5.11 The amplitudes of the (a) zonal and (b) meridional components of the diurnal tide at GT.

a

	YEAR							
MONTH	1987	1988	1989	1990	1991	1992	1993	MIA
1	15.9	24.4	10.1	12.2	4.8	3.8	10.5	11.7
2		16.8	11.0	28.7		19.1		18.9
12	15.6	13.0	17.8	5.7	6.6	11.0	6.6	10.9
AA	15.8	18.1	13.0	15.5	5.7	11.3	8.5	12.6

b

	YEAR							
MONTH	1987	1988	1989	1990	1991	1992	1993	MIA
1	10.2	18.9	11.1	8.5	7.8	7.8	12.9	11.0
2		14.0	8.1	23.2		14.7		15.0
12	11.2	15.9	12.7	7.2	10.4	8.9	18.6	12.1
AA	10.7	16.2	10.6	13.0	9.1	10.5	15.7	12.3

TABLE 5.12 The amplitudes of the (a) zonal and (b) meridional components of the diurnal tide at Adelaide

The diurnal amplitudes (Table 5.11 and 5.12) at Adelaide are slightly larger than the semidiurnal amplitudes as shown by the ASAs of -12 ms" and -10 ms for the diurnal and semidiurnal tide respectively. AT GT this is only true for the zonal component whereas the meridional components are almost equal (-9 ms"). The zonal summer averages of - 12 - 23 ms and ASA of 15.0 ms at GT are larger than the corresponding values of 6 - 18 ms^{-1} and 12.6 ms at Adelaide. The opposite is true for the meridional component as shown by the ASAs of 8.2 ms' and 12.3 ms for GT and Adelaide respectively. At both sites the zonal and meridional components have the largest summer averages in 1988 and generally January has the largest amplitude in that year, again suggesting a correlated SH behaviour.

5.4.2 PHASE

a

YEAR								
MONTH	1987	1988	1989	1990	1991	1992	1993	MIA
1	7.8	10.8	5.5	7.0	7.4	8.0	7.3	7.8
2	10.6	0.6	7.7	7.1	9.8			9.0
12	11.1	5.8	7.1	6.6	5.9	7.1	7.7	7.3
AA	9.8	8.7	7.1	6.9	7.7	7.5	7.5	7.9

b

YEAR								
MONTH	1987	1988	1989	1990	1991	1992	1993	MIA
1	10.2	10.2	8.8	9.6	10.7	10.2	9.5	9.9.
2	0.8	9.1	10.3	11.3	11.0			8.5
12	11.5	8.6	8.8	8.6	8.0	8.5	9.3	9.0
AA	7.5	9.3	9.3	9.8	9.9	9.4	9.4	9.2

TABLE 5.13 The phases of the (a) zonal and (b) meridional components of the semidiurnal tide at GT.

a

YEAR								
MONTH	1987	1988	1989	1990	1991	1992	1993	MIA
1	8.7	7.4	7.3	7.2	7.4	7.4	7.4	7.3
2		7.2	7.0	7.5		6.5		7.1
12	7.4	7.5	6.9	7.0	6.9	7.3	9.6	7.5
AA	7.0	7.4	7.1	7.3	7.1	7.0	8.5	7.3

b

YEAR								
MONTH	1987	1988	1989	1990	1991	1992	1993	MIA
1	10.0	10.6	10.5	10.9	10.7	9.9	11.0	10.5
2		10.2	10.7	11.6		10.4		10.7
12	11.3	11.1	10.4	10.3	10.5	10.9	0.6	9.3
AA	10.6	10.7	10.5	10.9	10.6	10.4	5.8	9.9

TABLE 5.14 The phases of the (a) zonal and (b) meridional components of the semidiurnal tide at Adelaide

The zonal phases for the semidiurnal tide (Table 5.13 and 5.14) have summer averages of - 7 - 10 h at GT and - 7 - 9 h at Adelaide, with ASAs of 7.9 h and 7.3 h respectively. Therefore GT has phases that are -0.6 h later than the Adelaide phases in local time. The meridional phases have summer averages of - 7 - 10 h at GT and -10 h at Adelaide, with corresponding ASAs of 9.2 h and 9.9 h. In this instance Adelaide has phases that are -0.7 h later than those at GT. The semidiurnal tidal phases at the two centres are thus in close agreement (within 1 h).

	YEAR							
MONTH	1987	1988	1989	1990	1991	1992	1993	MIA
1	8.7	12.8	11.7	12.2	11.8	11.3	11.5	11.4
2	9.1	11.0	10.6	7.9	10.5			9.8
12	11.6	12.1	11.6	12.5	11.5	12.4	12.6	12.0
AA	9.8	12.0	11.3	10.9	11.3	11.9	12.01	11.3

	YEAR							
MONTH	1987	1988	1989	1990	1991	1992	1993	MIA
1	9.0	20.2	20.7	21.6	22.7	18.8	20.6	19.1
2	10.8	16.9	15.5	13.0	17.6			14.8
12	18.2	22.0	22.5	22.6	14.5	18,5	18.4	19.5
AA	12.7	19.7	19.6	19.1	18.3	18.7	19.5	18.2

TABLE 5.15 The phases of the (a) zonal and (b) meridional components of the diurnal tide at GT.

	YEAR							
MONTH	1987	1988	1989	1990	1991	1992	1993	MIA
1	13.5	14.2	16.2	12.6	14.1	12.6	14.2	13.9
2		13.3	12.6	12.4		12.8		12.8
12	12.6	14,2	14.1	15.0	14.9	13.6	18.1	14.6
AA	13.1	13.9	14.3	13.4	14.5	13.0	16.2	14.0

	YEAR							
MONTH	1987	1988	1989	1990	1991	1992	1993	MIA
1	23.8	22.9	23.3	23.0	24.4	23.5	21.9	23.2
2		22.0	22.2	20.9		19.7		21,2
12	21.9	23.6	23.7	23.8	23.6	22.4	25.6	23.5
AA	22.9	22.9	23.1	22.5	24.0	21.9	23.7	23.0

TABLE 5.16 The phases of the (a) zonal and (b) meridional components of the diurnal tide at Adelaide.

For the diurnal tide, the zonal phases (Table 5.15 and 5.16) have summer averages of 10 - 12 hat GT and - 13 - 16 hat Adelaide, with ASAs of 11.3 h and 14.0 h respectively. The meridional phases at Adelaide are around midnight ('- 22 - 1 h). This results in misleading

summer averages in cases where some of the months have phases that are just after midnight, so resulting in a small average (e.g. 1991 and 1993). To solve this I added 24 h to the relevant phases in the computation of the ASA which, as a result, has a value of 23.0 h. The GT phases on the other hand, do not have a similar problem since they are - 13 - 20 h and have an ASA of 18.2 h. The phase difference between GT and Adelaide is therefore -3 h and -5 h for the zonal and meridional phases respectively, with Adelaide having later phases.

However, for the diurnal tide the propagating non-migrating modes have $s > 1$ and hence are slower than the Sun. This implies that for the diurnal tide, GT is expected to have later phases than Adelaide hence, I have delayed the phases at GT by 24 h. Consequently the phase difference between GT and Adelaide becomes -21 h and -19 h for the zonal and meridional components respectively.

5.4.3 COMPARISON AND DISCUSSION.

	ZONAL WAVENUMBER	PHASE VELOCITY	PHASE DIFFERENCE
SEMIDIURNAL TIDE	0	**	**
	1	30.0	-3.7
	3	10.0	3.7
	4	7,5	7.5
DIURNAL TIDE	0	**	**
	2	7.5	7.5
	3	5.0	14.9
	4	3.8	22.4

TABLE 5.17 Phase velocity and phase difference between GT and Adelaide (longitude difference 112'). ** signifies evanescent. Positive phase difference indicates later phase at GT.

SS estimated that the differences in amplitude due to longitudinal variability of the semidiurnal tide can be as high as -10 ms'. The difference in amplitude between GT and Adelaide is <5 ms'" which is consistent with SS's estimate. Table 5.17 shows the theoretical phase difference between GT and Adelaide. Positive values represent later phases at GT than at Adelaide. For the semidiurnal tide, I found small phase differences, suggesting that this tide is dominated by migrating modes in agreement with SS (see Fig 2.1). On the other hand, diurnal tide has phase

differences of - 19 - 21 h, taking GT to be having later phases as discussed earlier. According to Table 5.17 this suggests a strong composition of non-migratory modes with $s = 4$. Unfortunately no simulation similar to that of SS for the semidilimal tide (Fig 2.2) has been carried- out for the diurnal tide to allow for a detailed discussion.

5.5 DAY-TO-DAY TIDAL VARIABILITY

5.5.1 RESULTS

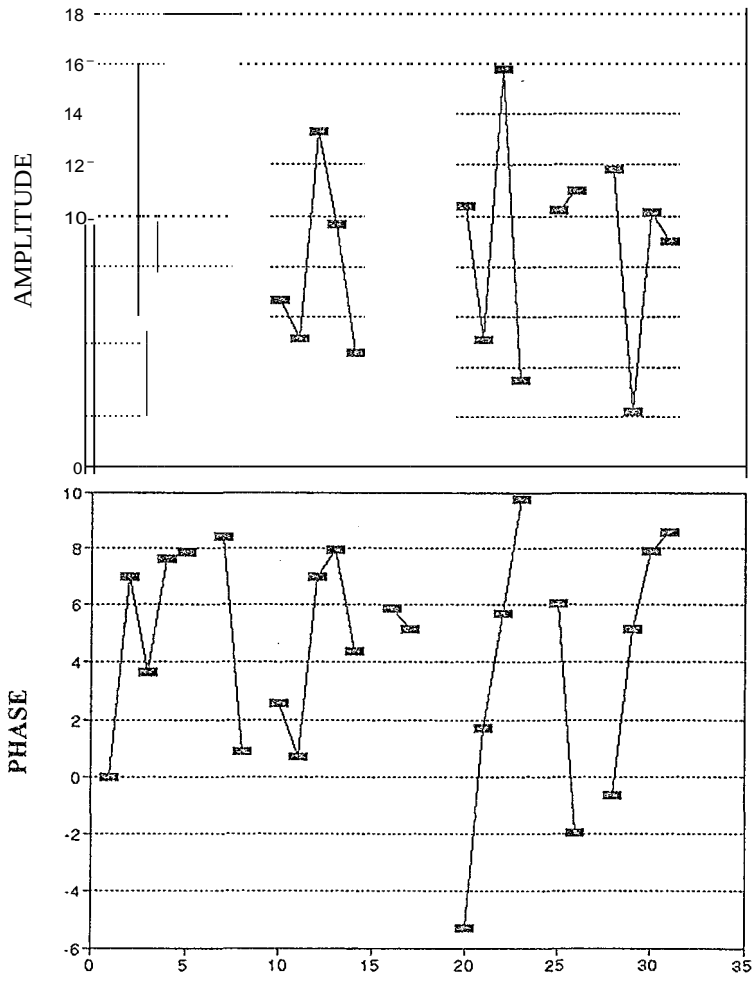

FIGURE 5.25. The daily amplitudes (top), and phases (bottom), of the zonal semidiurnal tide for 1 - 31 January, 1987.

Fig. 5.25 (a) and (b) show examples of daily 'tidal' amplitudes and phases respectively. Though the term 'tide' will be used in this section, it should be noted that this is simply for convenience, because a tide is a global oscillation of a meteorological variable (e.g. temperature, pressure) and is spatially coherent (Section 1.3). For the rest of this section inverted commas will not be used for 'tide', but the telin will be used with the abm'ie Understanding.

YEAR	MONTHS	SEMIDIURNAL	DIURNAL
1987	Jan. - March	0.08	0.35
	April - June	0.28	0.21
	July - Sept.	0.13	0.17
	Oct. - Dec.	0.23	0.40
1988	Jan. March	0.16	0.12
	April - June	0.08	0.39
	July - Sept.	-0.16	0.34
	Oct. - Dec.	-0.04	-0.20

TABLE 5.18. The correlation coefficients of tidal amplitudes.

The daily amplitudes and phases of tides show great day-to-day variability as shown by Fig 5.25. Though the variability does not immediately show any systematic pattern, it is not (purely) random as shown by Figs.5.26 and 5.27. These figures show time series filtered with pass bands of width 0.5 c/day centered on the frequencies of the semidiurnal (Figs.5.26) and diurnal (Figs. 5.27) tides. The amplitude modulation is generally oscillatory, especially for the semidiurnal tide. These modulations are highly variable and are generally uncorrelated between the zonal and meridional components for both tides. This is also to be seen from examination of the appropriate correlation coefficients (from now on CC). Table 5.18 shows CC for zero shift obtained from equation 3.2 5. The CCs indicate the degree of correlation between the zonal and meridional component of the tide in the corresponding column, for three months intervals. The CCs are at most 0.4, indicating poor correlation between the amplitude modulations of zonal and the

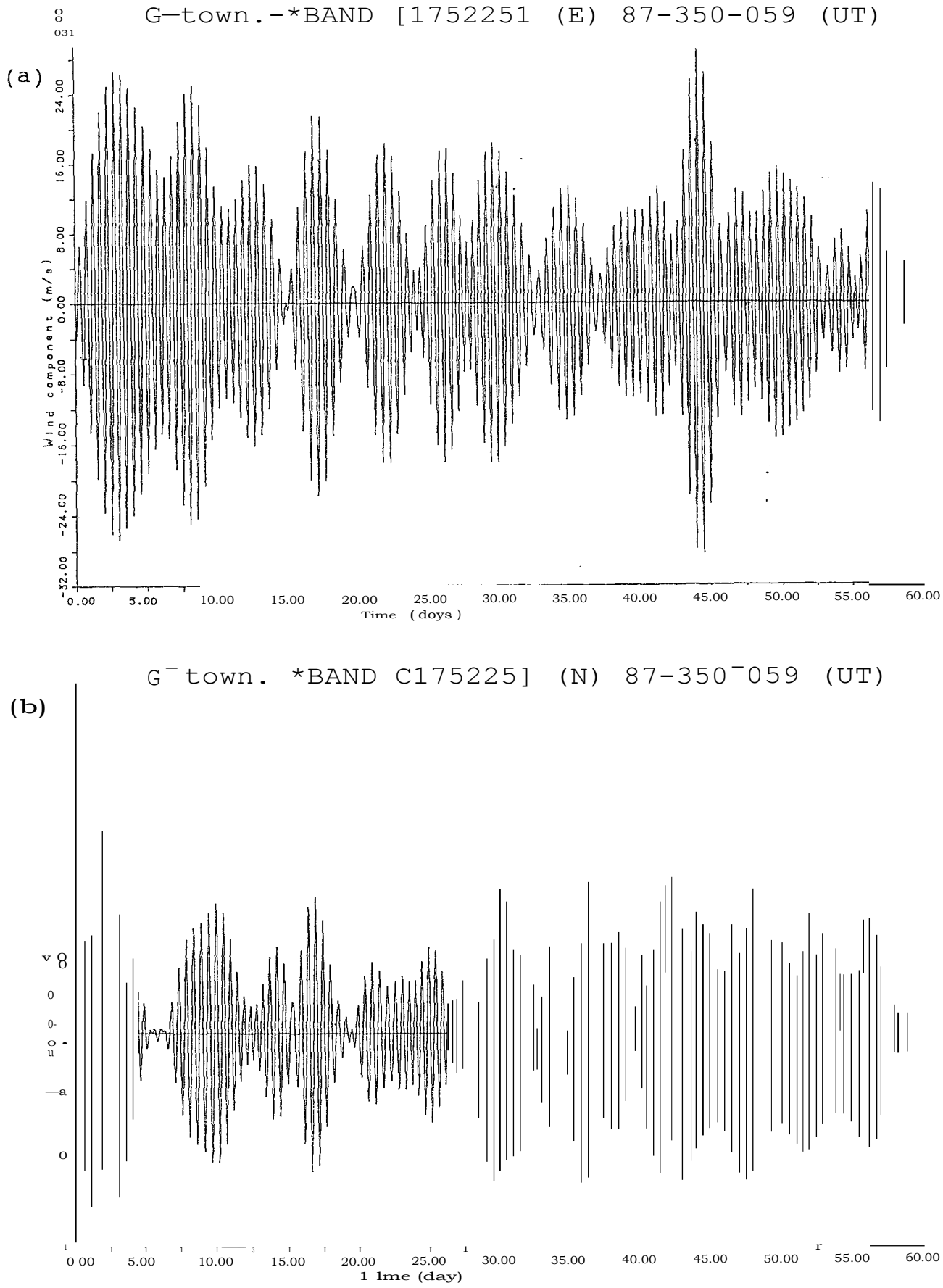

FIGURE 5.26 A filtered time series of the (a) zonal and (b) meridional components for a frequency filter centred on the semidiurnal frequency.

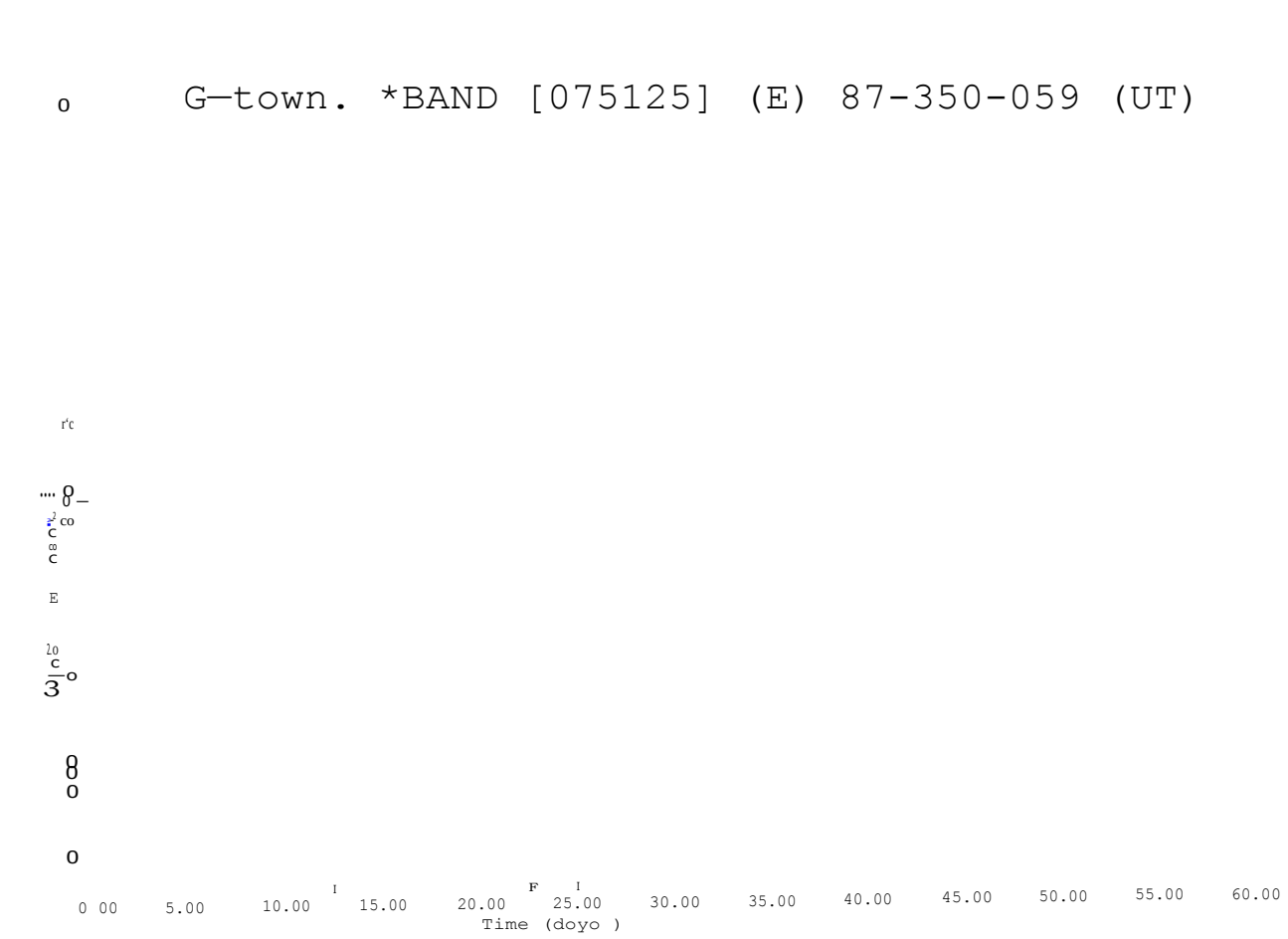

(b)

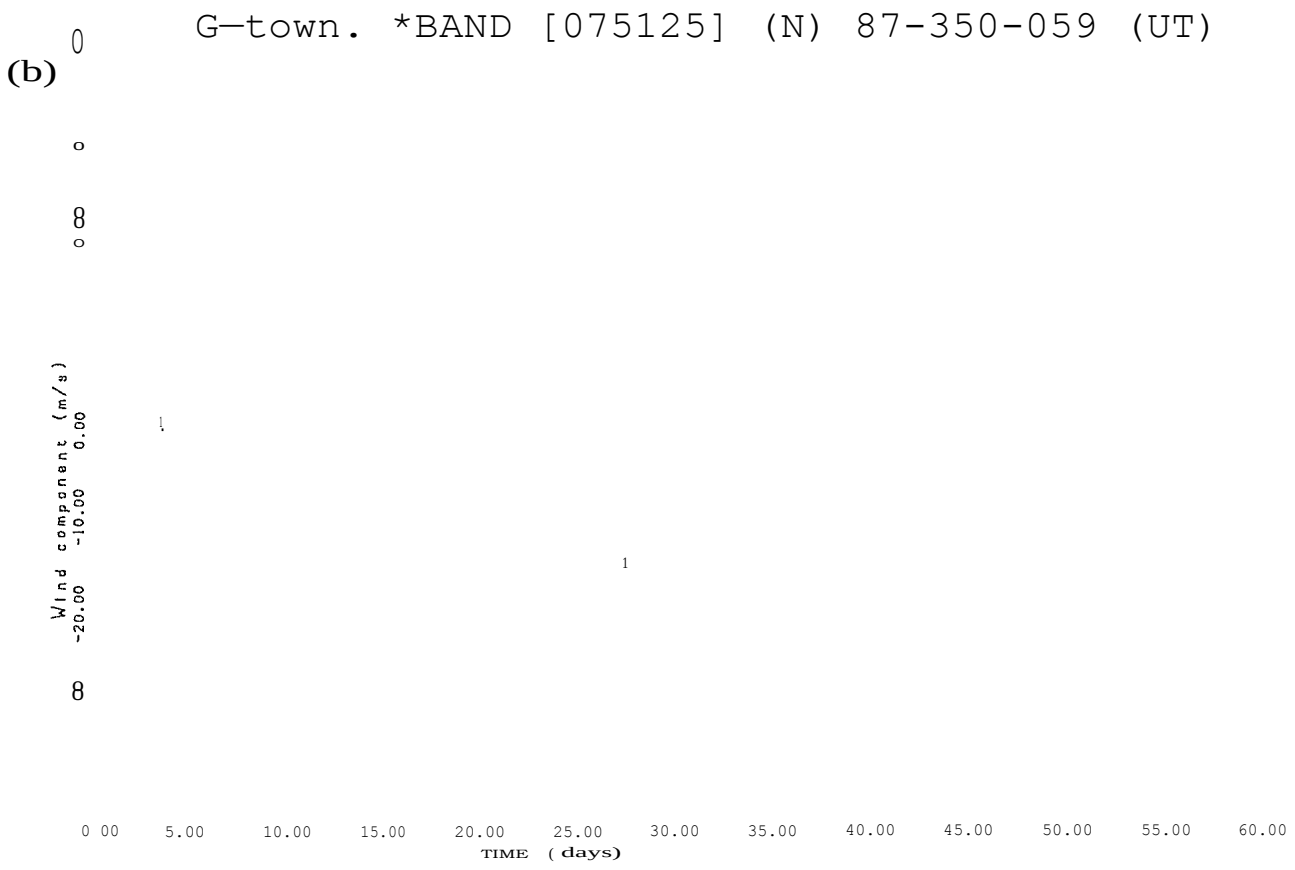

FIGURE 5.27 A filtered time series of the (a) zonal and (b) meridional components for a frequency filter centred on the diurnal frequency.

meridional components. The diurnal tide shows more correlation than the semidiurnal tide. The modulations sometimes (eg. Fig.526 (a)) have a typical periodicity of a few days.

5.5.2 COMPARISON AND DISCUSSION

My results show substantial day-to-day tidal variability, which agrees with observations made at other sites (eg. Phillips and Briggs, 1991). If the variations were a real feature, it would be expected that there be some correlation between the variation of the zonal and meridional amplitudes. This is not the case for GT results as shown by the CC of up to 0.4 , which is somewhat less than the value of 0.6 at Adelaide, as found by Phillips and Briggs. The lack of correlation at GT might be due to averaging over a 20 km height range. This suggestion is supported by Williams and Virdi (1989) who found a correlation of 71% at 110 km but almost no correlation (-3%) 10 km higher than that. Such behaviour is consistent with what has already been mentioned (Section 5.2.4) and it can only be emphasized here that tides consist of modes which are both height and latitude dependant. These respond differently to the possible sources of tidal variability discussed in Section 2.2.7. Therefore integrating over a large height range is bound to affect any possible correlation.

CHAPTER 6

SUMMARY

6.1 THE THESIS

In this thesis I have studied the behaviour of the atmosphere dynamics in the meteor region above Grahamstown (33°19'S, 26°30/E) based on observations made between 1987 and 1993 inclusive. In Chapter 2 I have reviewed the theory of upper atmospheric dynamics, in particular tidal dynamics. I have basically used three mathematical procedures, namely, harmonic analysis, maximum entropy method (MEM) and linear correlation, in my analysis of the data obtained from the GT meteor radar.

The results obtained in this thesis are generally consistent with observations made at different sites and with theoretical models. There are several important features observed at GT. The spectra of the winds above GT are dominated by tidal (24- and 12-h) solar harmonic components. Occasionally there are 48-, 16- and 8-h components. The 6-h component is very weak at GT. The spectra are generally dominated by the semidiurnal hainionic in autumn and winter, and by the diurnal hai monic in spring and summer.

The prevailing winds are primarily zonal with an AAA of 16.9 ± 1.7 ms" compared to < 10 ms for the meridional flow. Except for October 1987, the zonal prevailing wind is eastward. Meridional flow is primarily equatorward but also has a significant poleward flow especially in winter. The zonal flow has a semiannual periodicity, while the meridional flow has strong annual periodicity. The prevailing wind vector is predominantly directed northeast, but has great interannual variability in terms of magnitude.

In agreement with what has been pointed out by other authors (e.g. Cevolani *et al.,* 1983) tidal amplitudes above GT are comparable and sometimes even exceed the magnitude of the prevailing wind. The diurnal tide is slightly stronger than the semidiurnal tide. This is shown by the AAAs of 15.2 ± 0.7 ms' (EW) and 10.8 ± 1.0 ms' (NS) for the diurnal amplitudes as against 12.2 ± 0.9 ms' (EW) and 9.1 ± 0.2 ms^{-1} (NS) for the semidiurnal tide. The meridional component is

generally weaker than the zonal component. On average, both the zonal and meridional amplitudes tend to be largest in autumn for both tides, while their meridional amplitudes are generally smallest in winter. The semidiurnal phases have AAAs of 9.7 ± 0.2 h (EW) and 11.7 ± 0.1 h (NS), yielding a phase difference of -2 h (`expected value 3 h). The phase bimodality of the semidiurnal tide reported by other authors (e.g VTK) is not defined at GT though there is a tendency for the phases to be delayed by - 1 - 3 h during the equinoxes and winter. Diurnal phases have AAAs of 11.2 ± 0.2 h and 16.0 ± 0.3 h for the zonal and meridional components respectively. This gives a phase difference of -5 h (expected value 6 h).

The tidal wind vectors are generally elliptically polarized and rotate anticlockwise as expected for the SH. The maximum velocity is predominantly northeast for both tides and occurs at -6 h (-12 h) (semidiurnal) and -9 h (-21 h) (diurnal) which are in reasonable agreement with the respective values of 6.03 h and 11.2 h at Yambol which is almost on the same longitude as GT. The magnitude of the semidiurnal vectors is in reasonable agreement at the two sites, whereas Yambol has smaller diurnal magnitudes. This is consistent with the fact that the diurnal tide is more latitude dependent than the semidiurnal tide (Poulter, 1980) and its modes decay with increasing latitude (Avery *et al,* 1989).

I also studied the longitudinal and day-to-day variability of tides. GT and Adelaide are geographically at -34°S which eliminates latitude dependent effects. The tidal amplitudes at both sites are comparable with the difference being < 5 ms^{-1}. The semidiurnal phases at both sites are approximately equal which suggests that the semidiurnal tide is dominated by migrating modes. For the diurnal tide, GT has phases which are - 20 - 21 h later than at Adelaide, suggesting a presence of non-migrating modes with s = 4. As with observations made at other places e.g. Adelaide (Phillips and Briggs, 1991), tides at GT have great day-to-day variability. For both tides the zonal and meridional amplitude variations are not as well correlated as the corresponding variations observed by Phillips and Briggs at Adelaide. This discrepancy might be due to integrating over 20 km height range. On the other hand, inspection of suitably filtered time series suggests that amplitudes are not random, but are on average oscillatory, especially for the semidiurnal tide.

6.2 FUTURE RESEARCH

First it should be noted that the results given above have been hampered by lack of height resolution. Some of the discrepancies observed between GT and other sites cannot be ascribed to local effects because we are sometimes comparing observations with different height ranges. Due to mode superposition and the associated interference effects, such results are not necessarily expected to agree. Therefore for future research at GT the radar has to be upgraded to have height resolution not only to identify local effects and minimize errors but also to open the scope for possible future research. Height resolution would allow for the study of the tidal vertical structure and therefore the possible characterization of the modal structure of tides above GT.

A specific area of research that can be looked into is the longitudinal variability of tides. With GT and Adelaide so suitable positioned at -34°S, there is an avenue for such a study which, as yet, has never been done extensively. The results reported in this thesis on longitudinal tidal variability are not conclusive especially since they only involve summer months. Much work has been done in studying the hemispheric asymmetries between the geographically conjugate sites at Adelaide (35°S, l38°E) and Kyoto (35N, l36°E) (e.g. VTK). A similar study can also be done between GT (33.3°S, 26.5°E) and Yambol (42.5°N, 26.6(E) which are almost geographically conjugate. This can provide a quadrangular comparison which can help in .the better understanding of longitudinal and hemispheric (latitudinal) tidal behaviour.

APPENDIX A

TABLES

(a)

MONTH)	YEAR 1987	1988	1989	1990	1991	1992	1993	MIA	UN(M •	SD(MIA
1	1.0	5.7	1.8	1.9	2.4	1.3	1.4	2.2	0.6	73.6
2	4.2	1.8	3.3	1.5	3.7			2.9	0.5	41.4
3	3.1	3.6	3.7	0.9	2.5		3.3	2.3	0.4	36.4
4	4.5	3.0		8.7	3.6	1.2	1.3	3.7	1.1	74.4
5	1.2	3.1		11.3	8.0	1.5	2.4	4.6	1.7	89.7
6	3.5	4.5	6.2	5.6	2.4	.2.1	1.6	3.7	0.7	43.8
7	2.5	2.8	4.4	8.5		3.0		4.2	1.1	58.4
8	2.1	0.9	5.7		6.8	• 4.0		3.9	1.1	63.0
9	4.0	1.7	2.8		3.2	3.3		3.0	0.4	28.0
10	1.9	0.5			4.4	3.4		2.5	0.9	68.4
11	1.7	2.2			1.4	1.8		1.8	0.2	18.4
12	3.3	2.0	1.8		3.1	1.4	0.8	2.1	0.4	45.9
AA	2.7 I	2.6	3.7	5.5	3.3	2.3	1.8	3.2	0.5	38.4

(b)

tiMie	YEAR 1987	1988 I	1989	1990	1991	1992	1993	MIA	UN(MIAI	SD(MIA
1		1.5	4.3	6.2			4.0	4.5	0.7	38.9
2		1.0	3.1	7.4				- 4.5	1.3	63.8
3	M b 9	4.3	6.2	5.2	cn 4 Jn		3.7	5.7	0.6	26.7
4		6.9		9.1		4,	3.9	5.9	0.8	34.5
5		2.6		5.2			3.0	2.9	0.6	48.9
6		1.0	2.0	3.4		9 g	0.8	1.6	0.4	62.2
7		2.1	3.9	4.5		9		2.9	0.7	.54.0
8		1.8	3.4			C21		3.4	0.6	40.7
9		0.8	2.0		00	c00.1g)		1.5	0.3	42.9
10		3.9						3.6	1.1	58.6
11		6.1			S") vPs			3.7	0.9	47.7
12	80	2.6	5.5			-t-	5.8	3.7	0.8	51.2
AA	3.9	2.9	3.8I	5.9	4.3	2.1	3.5	3.8I	0.4	31.2

TABLE 1. The amplitude of the (a) zonal and (b) meridional component of the 8h oscillation.

(a)

MONTI-lI	YEAR 1987	1988	1989 I	1990	1991	1992	1993	MIA	UN(MIA	SD(MIA
1	2.2	3.8	3.4	2.7	3.0	1.2	1.0	2.5	0.41	43.4
2	2.0	1.3	0.3	2.8	3.0			2.1	0.4	41.2
3	1.1	2.8	3.5	2.4	0.2		1.6	1.9	0.5	63.0
4	2.7	3.2		1.1	1.9	3.0	2.6	2.4	0.3	32.4
5	1.3	0.4		3.1	1.6	2.5	1.1	1.6	0.4	59.8
6	2.6	1.7	3.0	3.0	2.2	1.4	1.9	2.3	0.2	28.4
7	1.2	0.4	2.5	3.5		2.2		2.0	0.5	60.1
8	3.6	0.7	1.5		1.4	1.4		1.7	0.5	64.1
9	4.0	2.0	3.5		2.2	1.9		2.7	0.4	35.5
10	0.9	2.6			1.5	1.3		1.6	0.4	45.7
11	3.3	3.8			3,4	1.7		3.0	0.5	29.5
12	2.2	3.4	1.8		1.8	0.9	1.4	1.9	0.3	43.9
AA	2.3	2.2	2.5	2.7	2.0	1.8	1.6	2.1	0.2	18.0

(b)

MONTH]	YEAR 1987	1988	1939	1990	1991	1992	1993	MIA	UN(MIA	SD(MIA
1	1.2	2.5	4.6	5.0	1.8	0.8	2.5	2.6	0.6	61.8
2	4.0	3.6	2.1	5.8	2.9			3.7	0.6	38.3
3	2.1	3.7	1.7	6.0	6.7		3.3	3.9	- 0.8	51.7
4	5.1	2.7		6.0	7.6	27	2.5	4.4	0.9	48.0
5	2.3	2.4		4.6	9.2	4.9	5.4	4.3	1.0	52.6
6	4.3	3.2	3.2	4.5	6.5	3.1	0.5	3.6	0.7	50.4
7	1.3	2.8	2.4	3.4		0.8		2.1	0.5	42.9
8	3.2	2.6	2.1		4.4	2.7		3.0	0.4	28.9
9	2.2	2.7	6.1		1.9	1.5		2.9	0.8	64.6
10	2.3	3.3			0.7	1.8		2.0	0.5	53.9
11	3.5	4.6			1.1	0.3		2.5	0.9	74.0
12	3.0	1.8	0.3		3.7	1.1	1.7	20	0.5	55.0
AA	2.91	3.0]	2.9	5.0	4.2I	2.0	2.1	3.2	0.4I	31.8

TABLE 2. The amplitude of the (a) zonal and (b) meridional component of the 6h oscillation.

APPENDIX B

FIGURES

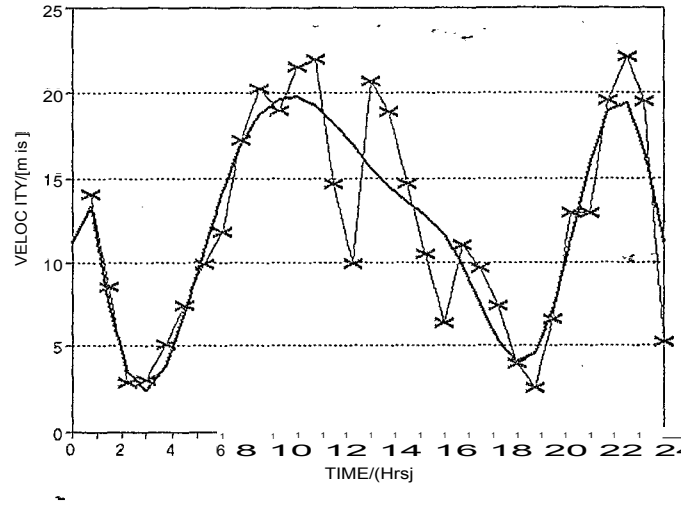

1(a) JANUARY

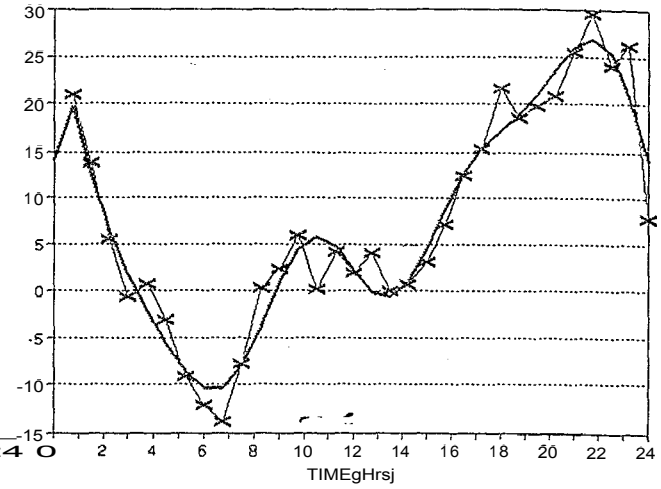

1(b) JANUARY

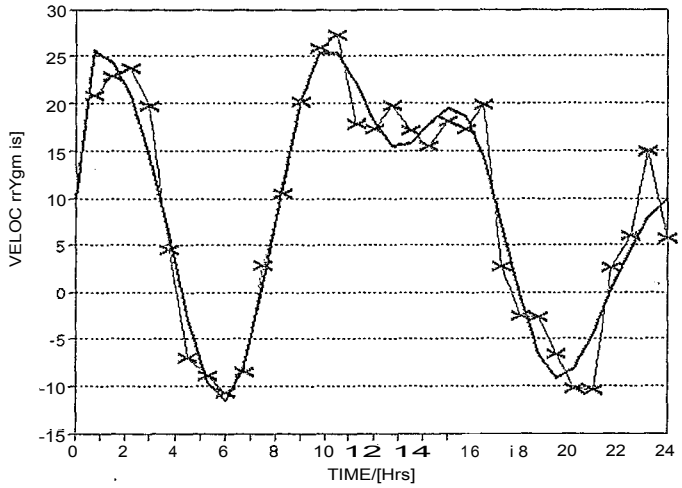

2(a) FEBRUARY

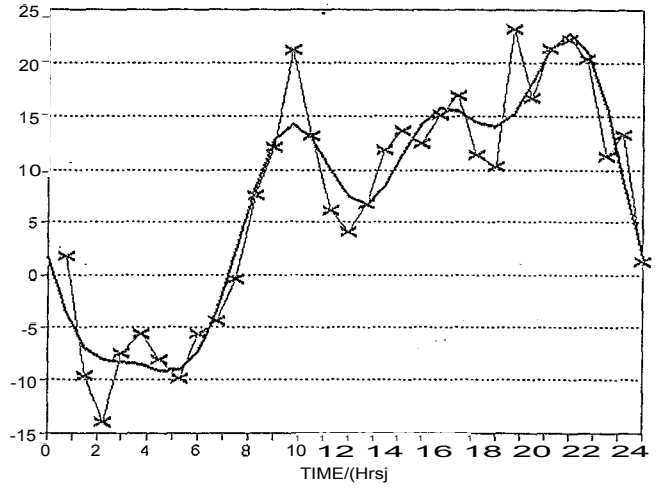

2(b) FEBRUARY

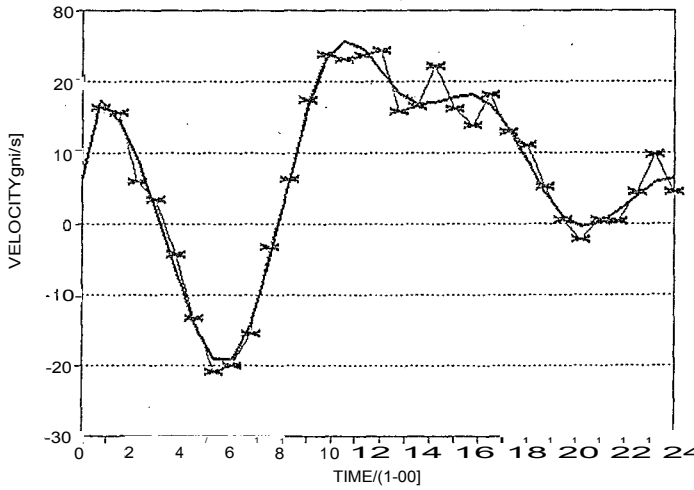

3(a) MARCH

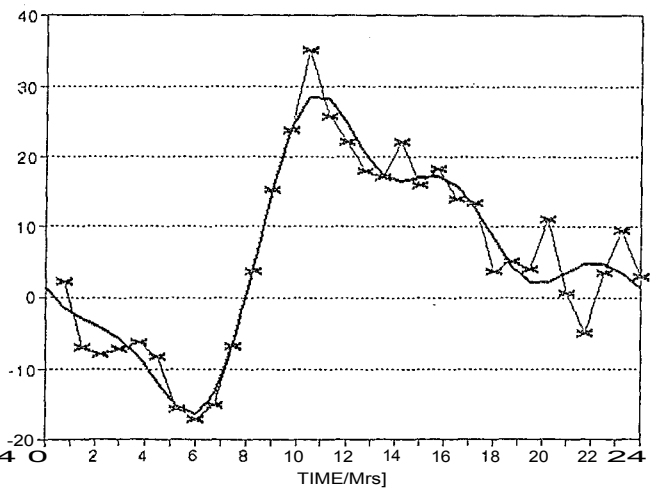

3(b) MARCH

FIGURE 1. The meridional time series for 1987 (left) and 1988 (right).

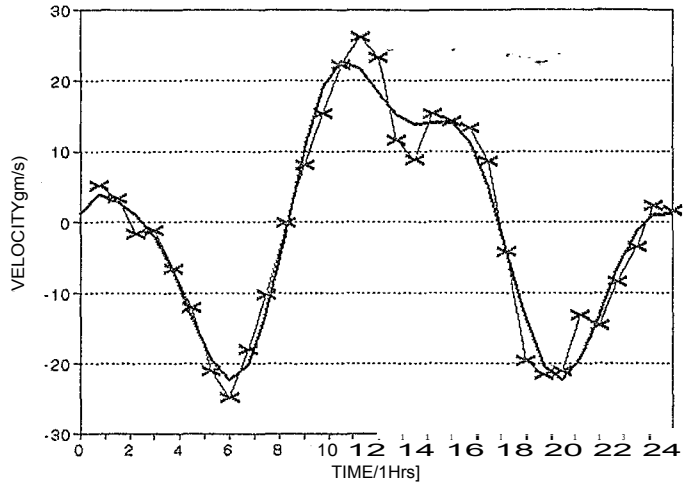

4(a) APRIL

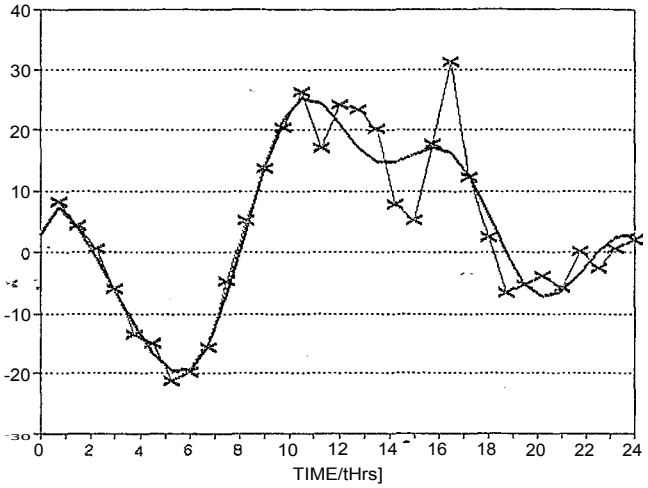

4(b) APRIL

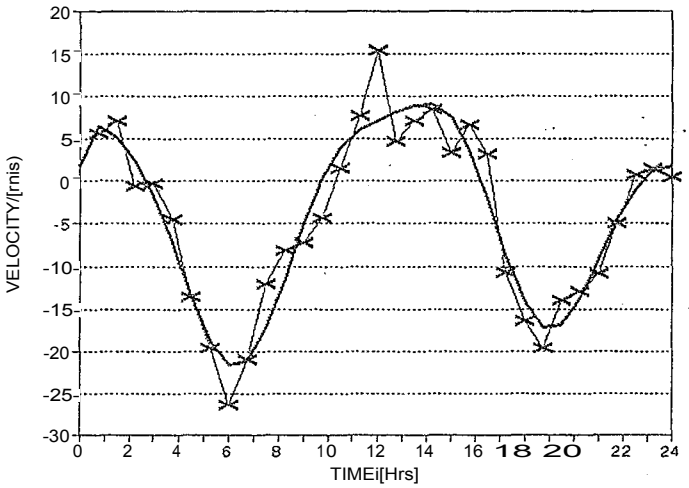

5(a) MAY

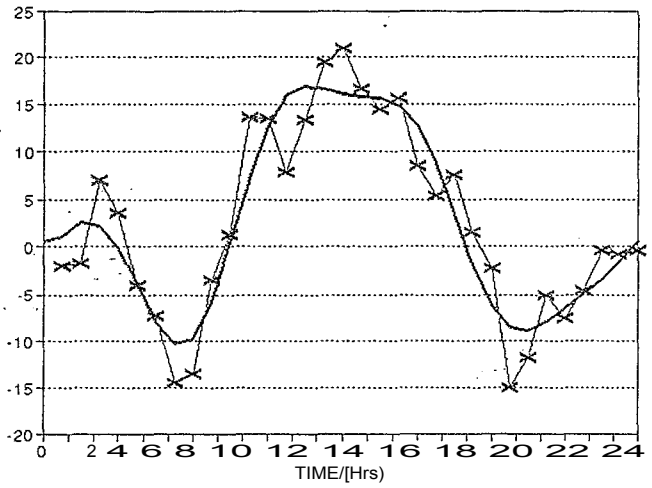

5(b) MAY

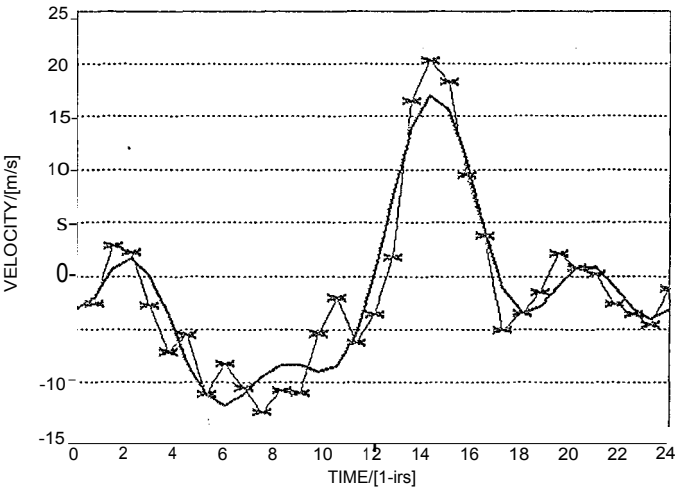

6(a) JUNE

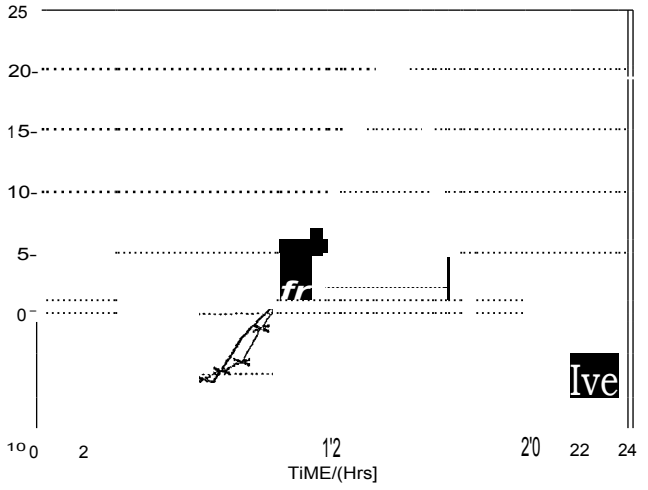

6(b) JUNE

FIGURE 1. (Continue)

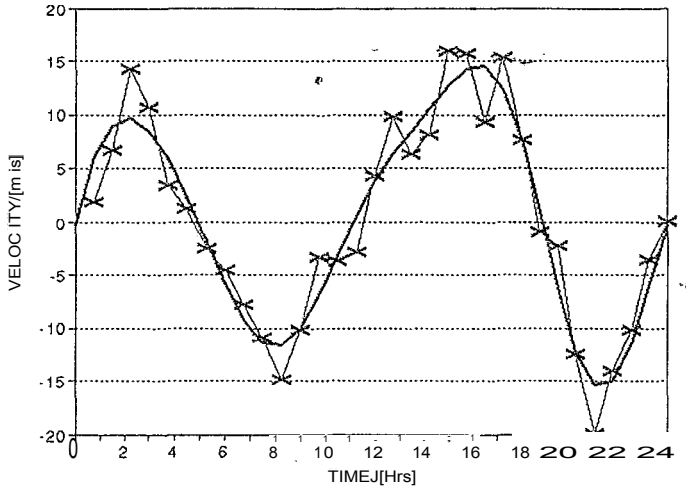

7(a) JULY

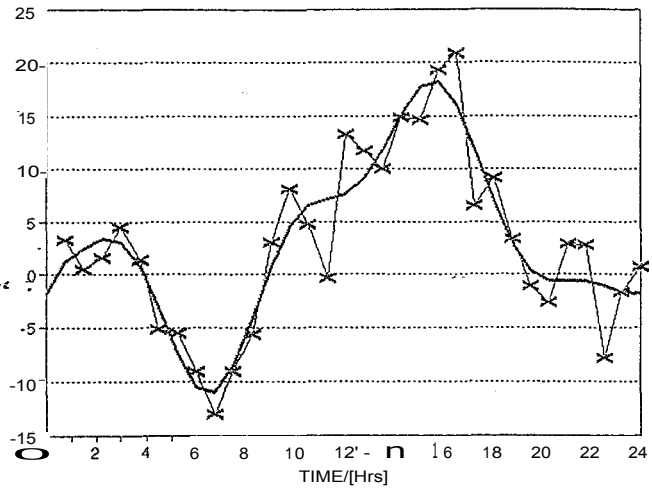

7(b) JULY

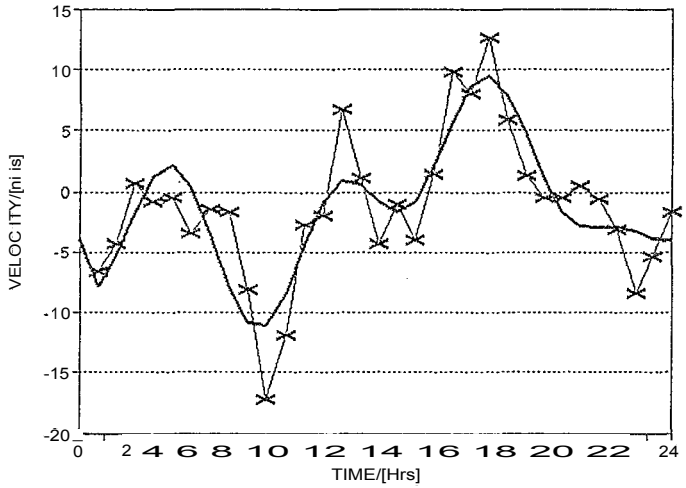

8(a) AUGUST

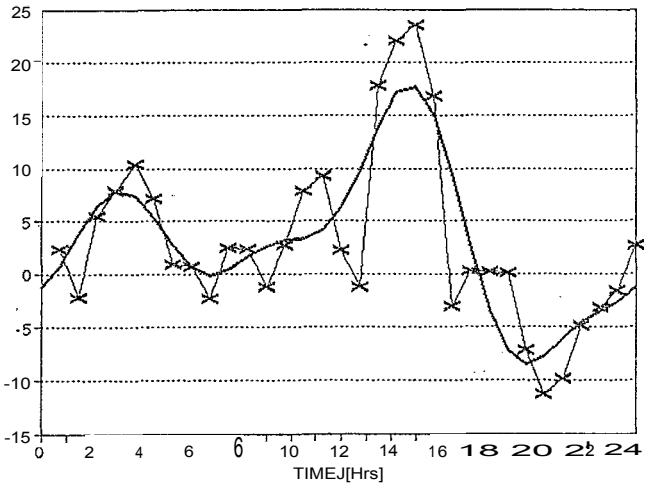

8(b) AUGUST

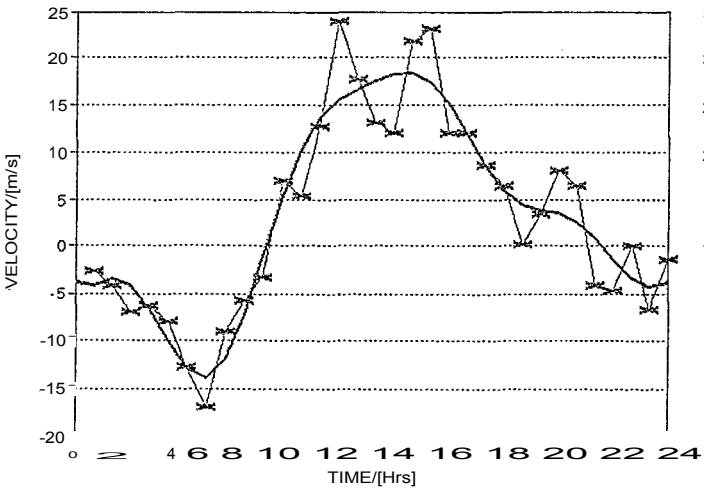

9(a) SEPTEMBER

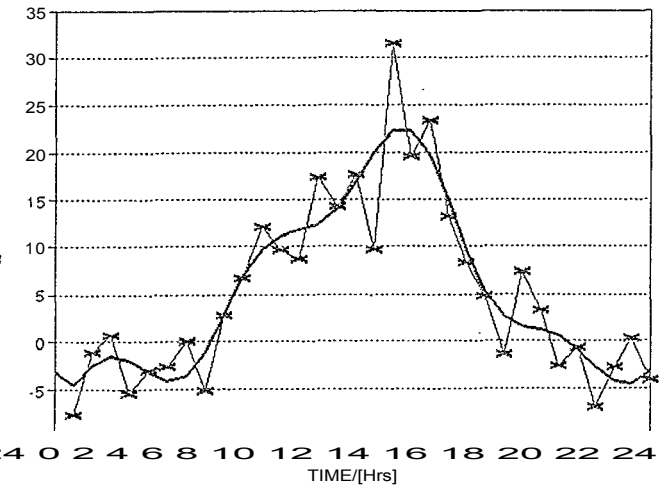

9(b) SEPTEMBER

FIGURE 1. (Continue)

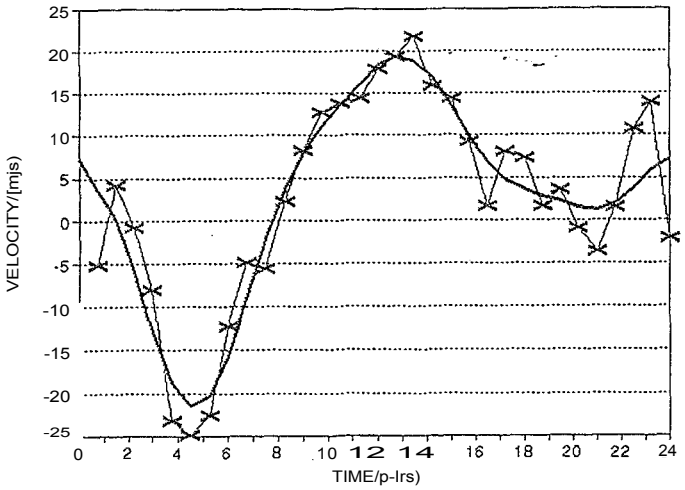

10(a) OCTOBER

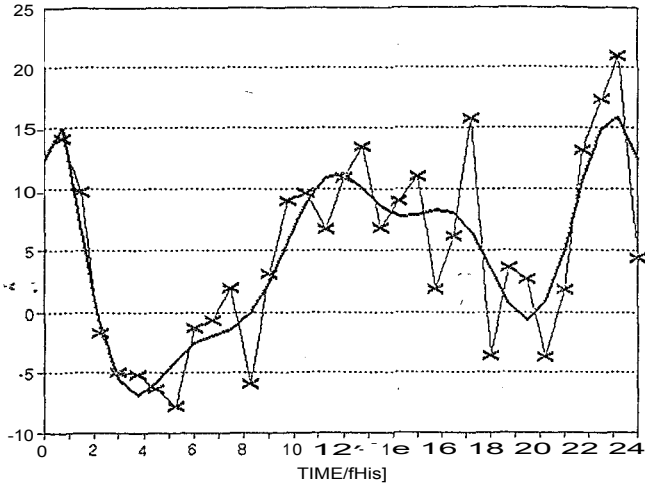

10(b) OCTOBER

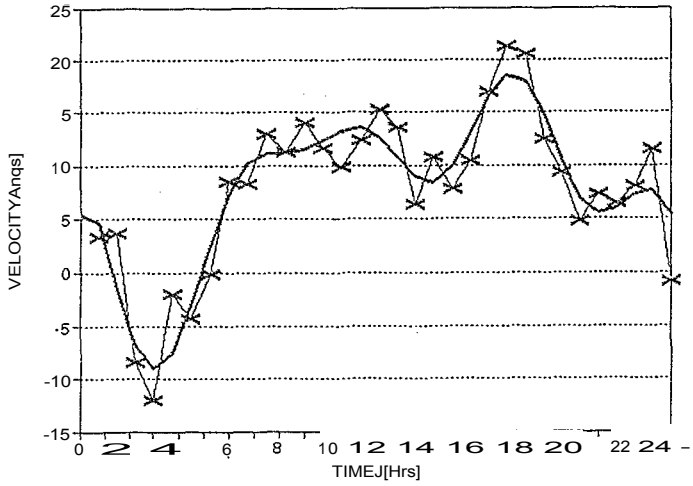

11(a) NOVEMBER

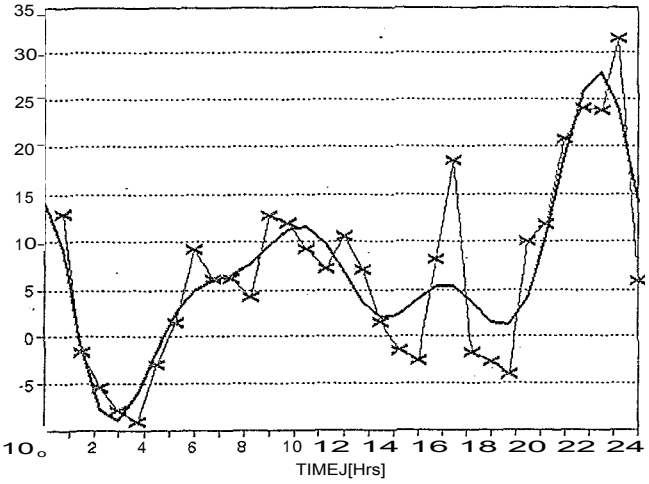

11(b) NOVEMBER

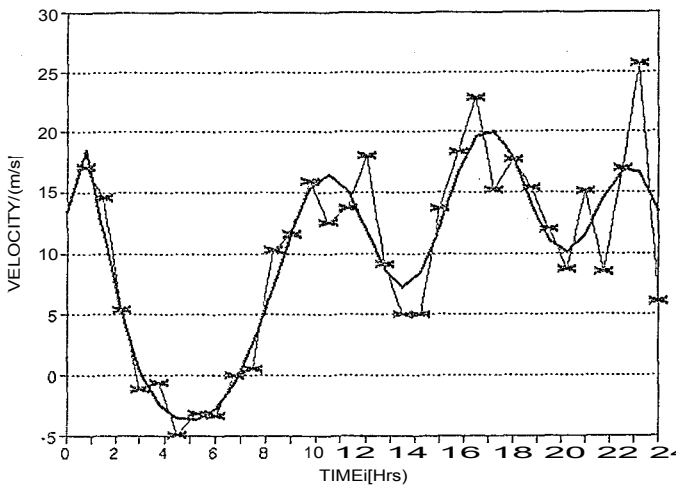

12(a) DECEMBER

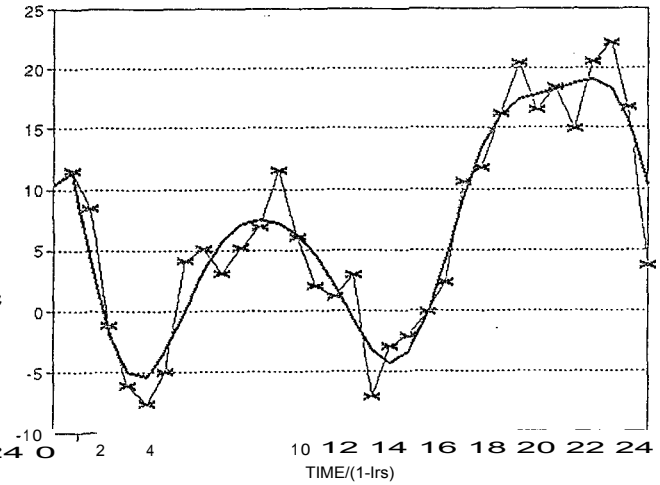

12(b) DECEMBER

FIGURE 1. (Continue)

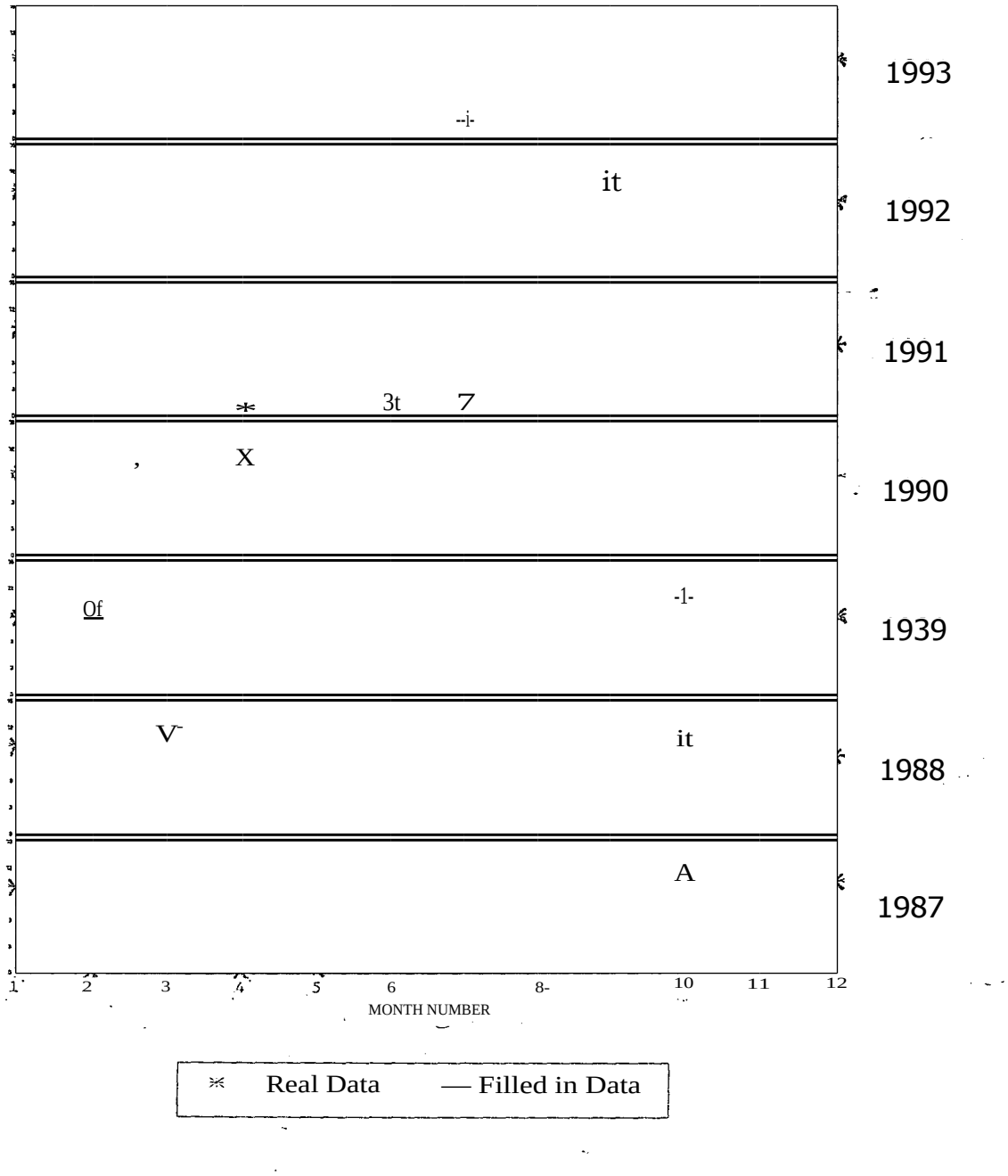

FIGURE 2. The meridional phase of the semidiurnal tide showing a 'false phase bimodality'. y_o = 0 and vs = 3 h/division.

IBLIOGRAPHY

Aso, T., Nonovama, T., and Kato, S. (1981), 'Numerical simulation of semidiurnal atmospheric tides', *Journal of Geophysical Research* 86, I 1388.

Avery, S. K., Vincent, R. A., Phillips, A., Manson, A., and Fraser, G. J._ 1989), 'High-latitude tidal behaviour in the mesosphere and lower thermosphere, *Journal of Atmospheric and Terrestrial Physics* 51, 595.

Beer, T. (1976), *The Aerospace Environment,* Wykeham Publications (London) Ltd., London and Winchester.

Bernard. R. (1981), 'Variability of the semi-diurnal tide in the upper mesosphere', Journal *ofAtmospheric and Terrestrial Physics* 43, 663.

Canziani, P. O. (1994), 'On tidal variability and the existence of planetary wave-like oscillations in the upper thermosphere - I. Observations of tidal variability', *Journal of Atmospheric and Terrestrial Physics* 56. 901.

Cevolani, G., Kingsley, S. P. and Muller, H. G. (1983), 'Three-station meteor wind observations in Northern Europe during summer 1980', *Journal of Atmospheric and Terrestrial Physics* 45, 275.

Chapman, S. and Lindzen, R. (1970), *Atmospheric Tides,* D. Reidel Publishing Company, Dordrecht, Holland.

Childers, D. G. (1978), *Modern Spectrum Analysis,* Institute of Electrical and Electronic Engineers, (IEEE), John Wiley and Sons, Inc., New York, 1.

Dartt, D., Nastrom, G. and Belmont, A. (1983), 'Seasonal and solar cycle wind variations, 80-100 km', *Journal of Atmospheric and Terrestrial Physics* 45, 707.

Fellous, .1. L., Bernard, R., Glass, M., Massebeuf, M., and Spizzichino, A. (1975), 'A study of the variation of atmospheric tides in meteor zones', *Journal of Atmospheric and Terrestrial Physics 37,* 151 1.

Fellous, J. L., Spizzichino, A., Glass, M. and Massebeuf, M. (1974)', Vertical propagation of Tides at meteor heights', *Journal of Atmospheric and Terrestrial Physics* 36, 385.

Flattery, T. W.: *Hough Functions,* Technical Report, No. 21, Department of Geophysical Sciences, University of Chicago, 1967.

Forbes, J. M. (1982a), 'Atmospheric Tides 1. Model description and results for the solar Diurnal component', *Journal of Geophysical Research* 87, 5222.

Forbes, J. M. (1982b), 'Atmospheric Tides 2. The solar aid lunar semidiurnal components', *Journal of Geophysical Research* 87, 5241-.

Forbes, J. M. (1984), 'Middle atmosphere tides', *Jovrnal of Atmospheric and Terrestrial Physics* 46, 1049.

Forbes, J. M. (1986a), 'ATMAP Workshop, University Club, Kyoto University, December 5, 1984,' *Handbook of the Middle Atmosphere Program (MAP)* 21, 14.

Forbes, J. M. (1986b), 'Proceedings of the workshop on atmospheric tides, Prague Czechoslovakia, August 14, 1985', *Handbook of the Middle Atmosphere Program (MAP)* 21, 56.

Forbes, J. M. (1990), 'Atmospheric tides between 80 km and 120 km', *Adv. Space. Res.* 10, (12) 127.

Forbes, J. M. and Garreth, H. B. (1978), 'Thermal excitation of atmospheric tides due to Insolation absorbtion by 0_3 and H_2O', *Geophysical Research letters* 5, 1013.

Forbes, J. M. and Hagan, M. E. (1988), 'Diurnal propagation with mean winds and dissipation', *Planetary and Space Science* 36, 579.

Forbes, J. M. and Vial, F. (1989), 'Monthly simulations of the solar semidiurnal tide in the Mesosphere and lower thermosphere', *Journal of Atmospheric and Terrestrial Physics* 51, 649.

Fraser, G. J., Vincent, R. A., Manson, A. H., Meek, C. E., Clark, R. R. (1989), 'Inter-annual variability of tides in the mesosphere and lower thermosphere', *Journal of Atmospheric and Terrestrial Physics* 51, 555.

Glass, M. and Spizzichino, A. (1974), 'Waves in the lower thermosphere: recent experimental investigations', *Journal ofAtmo.spheric and Terrestrial Physics* 36, 1825.

Goody, R. M., and Walker, J. C. G. (1972), *Atmospheres,* Foundations of Earth Science Series, Prentice-Hall Inc., Englewood Cliffs, New Jersey.

Groves, G. V. (1982a), Hough components of ozone heating, *Journal of Atmospheric and Terrestrial Physics* 44, 111.

Groves, G. V. (1982b), Hough components of water vapour heating, *Journal of Atmospheric and Terrestrial Physics* 44. 281.

Harris, T. (1993), 'Large-scale dynamics of the upper mesosphere and lower thermosphere', PhD thesis, University of Adelaide, Adelaide, Australia.

Hines, C. 0. (1972), 'Motions in the ionospheric D and E regions', *Phil. Trans. P. Soc. Lund.* 271, 457.

Houghton, J. T. (1977), *The Physics of Atmospheres,* Cambridge University Press, Cambridge, - London.

lribarne, J. V. and Cho, H.-R. (1980), *Atmospheric Physics,* D. Reidel Publishing Company, Dordrecht, Holland.

Knudsen, J. G. and Katz, D. L. (1958), *Fluid Dynamics and Heat Transfer,* McGraw-Hill Book Company, Inc., New York.

Lindzen, R. S. and Hong, S.-S. (1974), 'Effects of mean wind and horizontal temperature Gradients on solar and lunar semidiurnal tides in the atmosphere', *Journal of Atmospheric Science* 31, 1421.

Manson, A. H. and Meek, C. E. (1984), 'Winds and Tidal oscillations in the upper middle atmosphere at Saskatoon (52°N, 107°W, L=4.3) during the year June 1982 - May 1983', *Planet. Space Sci.* 32, 1087.

Manson, A. H., Meek, C. E., Fellous, J. L and Massebeuf, M. (1987), 'Wind oscillations (-6h - 6 days) in the upper middle atmosphere at Monpazier (France 45°N, 1°E) and Saskatoon (Canada, 52°N, 107°W) in 1979-1980', *Journal of Atmospheric and Terrestrial Physics* 49, 1059.

Manson, A. H., Meek, C. E., Gregory, J. B. and Chakrabarty, D. K. (1982), 'Fluctuations in Tidal (24-, 12-h) characteristics and oscillations (8-h - 5-d) in the mesosphere and lower thermosphere (70-110 km): Saskatoon (52°N, 107°W), 1979-1981, *Planetary and Space Science* 30, 1283.

Manson, A. H., Meek, C. E., Teitelbaum, H., Vial, F., Schminder, R., Kerschner, D., Smith, M. J., Fraser, G. J. and Clark, R. R. (1989), 'Climatologies of semidiurnal and diurnal tides in the middle atmosphere (70-110 km) at middle latitudes (40-55°), Journal *of Atmospheric and Terrestrial Physics* 51, 579.

Odishaw, H. (1964), *Sun, Upper Atmosphere, and Space,* Research in Geophysics, Massachusetts Institute of technology, Cambridge.

Pancheva, D. and Mukhtarov P1. (1994), 'Variability of Mesospheric Dynamics observed at Yambol (42.5°N, 26.6°E) by Meteor Radar', *Journal of Atmospheric and Terrestrial Physics* 56, 1271.

Phillips, A. and Briggs, B. H. (1991), 'The day-to-day variability of upper atmosphere tidal Winds and dynamo currents', *Journal of Atmospheric and Terrestrial Physics* 53, 39.

Phillips, A. and Vincent, R. A. (1987), 'Winds in the middle atmosphere at Mawson, Antarctica: II Tides', *Australian National Antarctic Research Expedition Research Notes* 48, 93.

Poole, L. M. G. (1988), 'The GrahamstovVn all-sky meteor radar', *Journal of Atmospheric and Terrestrial Physics* 50, 585.

Poole, L. M. G. (1990), 'The characteristics of the mesospheric two-day wave as observed at Grahamstown (33.3°S, 26.5°E), *Journal of Atmospheric and Terrestrial Physics* 52, 259.

Poulter, E. M. (1980), 'Winter motions in the southern hemisphere meteor region', *Journal ofAtmospheric and Terrestrial Physics* 42, 661.

Press, W.H., Flannery, B. P., Teukolsky, S. A. and Vetterling, W. T. (1986), *Numerical Recipes,* Cambridge University Press, Cambridge.

Rees, M. H. (1989), *Physics and Chemistry of the Upper Atmosphere,* Cambridge University Press, Cambridge.

Sibert, M. (1961), *Atmospheric Tides,* Advances in Geophysics, Vol. 7, Academic press, New York, 105.

Sivkov, A. M. and Shved, G. M. (1994), 'Influence of latitudinal and longitudinal variations of ozone and water vapour on the solar semidiurnal tide', *Journal of Atmospheric and Terrestrial Physics* 55, 815.

Stubbs, T. J. (1976), 'Mean and periodical components of ionospheric tides in the D-Region at 35°S during 1972', *Journal of Atmospheric and Terrestrial Physics* 38, 979.

Teitelbaum, H., Vial, F., Manson, A. H., Giraldez, R. and Massebeuf, M. (1989), 'Non-linear interaction between the diurnal and semidiurnal tides: terdiurnal and diurnal secondary waves', *Journal of Atmospheric and Terrestrial Physics* **51,** 627.

Tsuda, T., Nakamura, T. and Kato, S. (1987); 'Mean winds observed by the Kyoto meteor Radar in 1983-1985, *Journal of Atmospheric and Terrestrial Physics* **49,** 461.

Vial,,F. (1986), 'Numerical simulation of atmospheric tides for solstice conditions', *Journal of Geophysical research* **91,** 8955.

Vial, F. (1989), 'Tides in the middle atmosphere', *Journal of Atmospheric and Terrestrial Physics* **51, 3.**

Vial, F., Forbes, J. M. and Miyahara, S. (1991), 'Some transient aspects of tidal propagation', *Journal of Geophysical Research ,* **96,** 1215.

Vial, F. and Teitelbaum, H. (1984), 'Some consequences of turbulent dissipation on diurnal thermal tide', *Planetary and Space Science* **32,** 1559.

Vincent, R. A., Tsuda and Kato, S. (1988), 'A comparative study of mesopheric solar tides observed at Adelaide and Kyoto', *Journal of Geophysical Research* **93,** 699.

Walterscheid, R. L. (1981), 'Inertio-gravity waves induced accelerations of mean flow having an imposed periodic component: implication for tidal observations in the meteor region', *Journal of Geophysical Research* **86,** 9698.

Wilkes, M. V. (1949), *Oscillations of the Earth's Atmosphere,* Syndics of Cambridge Uniyersity Press, Cambridge.

Williams P. J. S. and T. S. Virdi (1989), 'EISCAT Observations of tidal modes in the lower thermosphere', *Journal of Atmospheric and Terrestrial Physics* **51,** 569.

Worthing, A. G. and Geffiier, J. (1943), *Treatment of Experimental Data,* John Wiley and Sons, Inc., New York.